A 2-D coupled surface and sub-surface flow model for river flow simulation with piedmont zone

A thesis submitted

in partial fulfilment of the requirements for the award of the

degree of

DOCTOR OF PHILOSOPHY

By

Sudarshan Patowary

DEPARTMENT OF CIVIL ENGINEERING

INDIAN INSTITUTE OF TECHNOLOGY GUWAHATI

GUWAHATI-781039, ASSAM, INDIA

May, 2018

Prof. A. K. Sarma
B.P.Chaliha Chair Professor
For Water Resources

Indian Institute of Technology Guwahati,
Guwahati-781 039

Phones: 0361- 2582409 (O)
0361-2584449 (O)
0361- 2584409 (R)
0361- 2690953 (R)
9435732225 (m)
Fax: 0361- 2582440
E-mail: aks@iitg.ernet.in

DEPARTMENT OF CIVIL ENGINEERING

Certificate

It is certified that the work contained in the thesis entitled "***A 2-D coupled surface and sub-surface flow model for river flow simulation with piedmont zone***" by Sudarshan Patowary, Roll Number 11610413, a student in the Department of Civil Engineering, Indian Institute of Technology Guwahati for the award of the degree of Doctor of Philosophy has been carried out under my supervision and that this work has not been submitted elsewhere for a degree.

Arup Kumar Sarma

Declaration of Authorship

I, Sudarshan Patowary, declare that this thesis titled "**A 2-D coupled surface and sub-surface flow model for river flow simulation with piedmont zone**" and the work presented in it has been carried out by me under the supervision of Proof. Arup Kumar Sarma, Department of Civil Engineering, Indian Institute of Technology Guwahati. This work has not been submitted anywhere for award of any degree.

Sudarshan Patowary
Department of Civil Engineering
Indian Institute of Technology, Guwahati

Acknowledgements

I would like to place on record my deep sense of gratitude and sincere thanks to my thesis supervisors Dr. Arup Kumar Sarma, Professor, Department of Civil Engineering, Indian Institute of Technology Guwahati for his invaluable guidance and full hand cooperation throughout the all aspects of this research work. I also admire his patient explanation of the concepts and basic principles.

I would also like to put on record my heartfelt thanks and reverence to the chairman of the Doctoral Committee, Dr. Sudip Talukdar, Professor, Department of Civil Engineering, Indian Institute of Technology Guwahati, for his valuable suggestions and help at various stages of this research work. I am indebted to Dr. Rajib Bhattacharjya, Professor, Department of Civil Engineering, Indian Institute of Technology Guwahati and Dr. Pinakeswar Mahanta, Professor, Department of Mechanical Engineering, Indian Institute of Technology Guwahati, for their keen interest, valuable suggestions and guidance provided to complete this work as members of the Doctoral Committee. I would like to give my sincere thanks to Dr. R. G. Niswonger to provide me field data of Trout creek river.

My sincere thanks are also due to all the Faculty members of Water Resources Engineering and Management, Indian Institute of Technology Guwahati for their keen interest and suggestions. I express my sincere thanks to the staff members of the Civil Engineering Department, Indian.

Institute of Technology Guwahati for their kind cooperation during my work. It is virtually impossible to name all my friends and well-wishers with whom I shared many happy moments during my stay at Indian Institute of Technology Guwahati, but I would be failing in my duty, if do not take the names of Dr. Hriday Moni Kalita, Dr. Ratan Sarma, Debraj Biswash, Shyamal deka, Jayashree Hazarika, Sagarika Patowary, Raktim Choudhury. My sincere thanks to Mr. P. K. Sarma for his helping hand in field study.

I would also like to offer my love, admiration and respect to my parents and other family members for their love, blessings and moral support

Finally, to the Almighty God who has seen me this far.

Abstract

The interaction between surface and groundwater flow in a non-prismatic river has been a topic of interest among researchers since last three decades. The interaction between the surface and the groundwater is a complex phenomenon the quantification of which needs several considerations such as variations of topographical, geological, and geographical conditions. The existence of a piedmont zone (highly permeable river bed) in the foothill location of a river is one of such critical characteristic that can significantly influence the flow conditions in a river. Existence of piedmont zone in the river bed changes the downstream flow scenario significantly. Downstream flow situation assessed by routing of upstream hydrograph may yield erroneous flow assessment, if the existence of such piedmont zone is ignored and therefore, it is a matter of concern for water resources planning and flood management. Moreover, most of the researchers, to reduce complexity, carried out hydrodynamic studies neglecting the infiltration zone in the river bed.

Geological investigation (Goswami et.al 1996, Sukla and Bora 2003 and Goswami and Yhokha 2010) have revealed that piedmont zones exist at several locations in the foothills of Himalaya, through which a significant amount of river water may infiltrate into the ground and water infiltrated through the piedmont zone moves as groundwater and joins the mainstream at downstream. Therefore, for reliable flow forecasting in a Himalayan river passing through a piedmont zone, consideration of surface and ground water interaction in the modelling process is quite important.

To overcome above difficulties, a two dimensional coupled surface-subsurface flow model is developed, where surface and subsurface flow are linked via exchange of flux between two systems. Saint-Venant equation is the most common equation to describe free surface flow. In this study free surface flow considering piedmont zone in the computational domain is described by the Saint- Venant equation coupled with Green-Ampt. infiltration equation. The water infiltrated through the recharge zone moves as unsaturated flow and joins the mainstream at downstream. This process is modelled by the two dimensional Richards equation.

The two dimensional shallow water equation and Richards equation are nonlinear equation which is not amiable to solve analytically without simplification. Again

simplification makes the results erroneous. With the advent of high speed computer, the researchers have widely used different numerical schemes e.g. finite difference, finite volume and finite element methods for solution of these nonlinear equations. In this study Beam and Warming implicit scheme is used to solve free surface flow equation with Green-Ampt. infiltration equation and Alternate Direction Implicit scheme is used for Richards equation, as Beam and Warming scheme is developed only for hyperbolic system of equation. The developed models are validated with the field data and experimental data and found that there is a good agreement between the results.

Results obtained by the application of the model in a hypothetical river show that piedmont zone has significant effect on downstream surface elevation, depth hydrograph and discharge hydrograph. Because of piedmont zone peak depth and discharge attenuate by 5% and 7% respectively. Again water infiltrated through the piedmont zone, starts to contribute to main stream after 72 hour and because of this contribution the flow volume increases by 3.62%. Sensitivity analysis of hydraulic conductivity and capillary fringe show that for 100 % variation of hydraulic conductivity taking K=0.0005 m/s as central value, percentage change in peak depth and peak discharge is ±7% and ±4.2% respectively. Again water table rise is very sensitive to capillary fringe α. Smaller the size of capillary fringe more is the water table rise.

To evaluate the field applicability of the proposed model, it is applied to a tributary of Brahmaputra River where such piedmont zone is reported (Goswami et al.1996). Double ring infiltration test was performed on the field to determine infiltration characteristics of the river. While application of the model in hypothetical cases has given opportunity to get insight in to the process, its application in a real field has ascertained robustness of the model and has given better idea about need of filed data for obtaining reliable result from such model application.

Table of content

List of figure

List of Table

List of Notation

A	Jacobian of E in 2-D Beam and Warming scheme
aa	Parameter used in IDF curve
AA	Area of watershed
Av	Artificial viscosity
A_p	Area of watershed
B	Jacobian of S in 1-D Beam and Warming scheme
bb	Parameter used in IDF curve
BB	Jacobian of F in 2-D Beam and Warming scheme
C	Celerity
CC	Run off Coefficient
CT	Regulating coefficient for artificial viscosity
C_p	Run off coefficient
$C(\psi)$	Specific moisture moisture capacity
D	Diagonal matrix of Eigen value of P
$D(\theta)$	Unsaturated diffusivity
E	Vector of Beam and Warning scheme
F	Vector of Beam and Warming scheme
F_c	Cumulative infiltration rate
F^*	Cumulative infiltration obtain from Richards equation

f	Infiltration rate
f^*	Infiltration rate obtain from Richards equation
g	Acceleration due to gravity
h	Water surface depth for unsteady free surface elevation
$h(t)$	Water surface height with respect to time
I	Identity matrix
I_p	Intensity of rainfall
k_s	Saturated hydraulic conductivity
$k(\psi)$	Unsaturated hydraulic conductivity
L_c	Length of the longest flow channel
m_{lx}	Momentum loss in X-direction
m_{ly}	Momentum loss in Y-direction
N	Manning's roughness coefficient
n	Pore size distribution
P	Jacobian of E in 1-D Beam and Warming scheme
Q	Jacobian of S in 2-D Beam and Warming scheme
Q_p	Maximum flood hydrograph
R	Hydraulic radius
S	Vector of Beam and Warming scheme
S_c	Slope of the longest flow channel

S_e	Effective saturation
s_{0_x}	Bed slope in X- direction
s_{0_y}	Bed slope in Y- direction
s_{f_x}	Friction slope in X- direction
s_{f_y}	Friction slope in Y- direction
t	Time coordinate
T_c	Time of concentration
t_p	Basin lag time
t_r	Effective rainfall
U	Vector of Beam and Warning scheme
u	Velocity in X- direction for unsteady free surface elevation
v	Velocity in Y- direction for unsteady free surface elevation
x	Horizontal space coordinate
y	Lateral space coordinate
z	Vertical space coordinate
$Z(t)$	Depth of saturated zone
α	Capillary fringe size
γ	Parameter leading to variety of finite difference scheme
Δt	Time interval

Δx	Longitudinal grid interval
Δy	Transverse grid interval
Δz	Vertical grid interval
η	porosity
θ	Moisture content
θ_o	Initial water content
θ_r	Residual water content
θ_s	Saturated water content
ψ	Suction head
$\psi(t)$	Time dependent effective suction head
μ	Parameter leading to variety of finite difference scheme

Chapter 1

Introduction

1.1 Purpose of the study

Flow forecasting at a downstream location through hydrodynamic routing of flow hydrograph of an upstream section, though is a common practice, may yield erroneous result because of ignoring surface and ground water interaction, particularly when a river passes through the highly permeable piedmont zone. The existence of piedmont zone in a river bed is one of the critical parameters from many that can significantly influence the river flow scenario. Geological studies (Goswami et.al 1996, Sukla and Bora 2003 and Goswami and Yhokha 2010) have revealed existence of piedmont zones at several locations in the foothills of Himalaya, through which a significant amount of river water may infiltrate into the ground. Therefore, for reliable flow forecasting in a Himalayan river passing through a piedmont zone, consideration of surface and ground water interaction in the modelling process is quite important. The interaction between the surface and the groundwater is a complex phenomenon the quantification of which needs several considerations such as variations of topographical, geological, and geographical conditions. Therefore, to reduce complexity, most of the researchers carried out hydrodynamic studies neglecting the infiltration zone in the river bed. Downstream flow situation assessed by routing of upstream hydrograph may yield higher flow depth if the existence of such piedmont zone is ignored and therefore, it is also a matter of concern for water resources planning and flood management. Interaction between surface and groundwater flow in a river has been a topic of interest among researchers since last three decades owing to its significance in flood forecasting, watershed modelling, water-balance study and water resources management in general.

A dynamic model of unsteady two-dimensional flow is often based on Shallow water equation, which is known as Saint-Venant equation. Because of its non-linear hyperbolic form, analytical solution of this partial differential equation is very much challenging and therefore, recourse is generally made to numerical solution. With the

development of the efficient numerical algorithm and the advent of high-speed digital computer, the solution of nonlinear equations is now becoming easier. Again, water infiltrated through the piedmont zone existing in the river bed, moves as the groundwater and may join the mainstream at a far downstream location. Therefore, it is necessary to include influence of piedmont zone while modelling unsteady flow in a channel having such geological formation. To simulate the process, a model is developed where equation of shallow water wave is coupled with infiltration equation and groundwater movement equation to route flood in a river having a piedmont zone in the foothill. The surface and subsurface models are linked via an exchange of flux between the two systems.

The main aim of the project is to develop a new two-dimensional mathematical model with the following specific objectives:

- To study unsteady flow behaviour in a river channel having a piedmont zone
- To study the effect of important soil parameters on different primitive flow variable of practical significance along with their sensitivity analysis.
- To study the ground water movement considering the water infiltrated from the piedmont zone.
- To develop a coupled surface sub- surface flow model for flow forecasting at a downstream section.

1.2 Organisation of the thesis

The entire work has been divided into several phases and is presented in different chapters as given below.

In chapter 2, a brief review of the past works done on solution of the unsteady free surface flow equations along with infiltration model and groundwater model is discussed. Shallow water equation and groundwater equation are highly nonlinear equations which are not amiable to solve analytically. Therefore, in this chapter, a brief literature review of the different numerical technics for the solution of above equations is presented.

Chapter 3 encompasses the detailed discussion of the governing equations for developing the two- dimensional coupled surface water groundwater model. This chapter mainly focuses on the shallow water equation, Green- Ampt infiltration equation and Richards equation. Transformed form of Richards equation is also discussed in this chapter.

Solutions of governing equations are discussed in chapter 4. The governing equations are highly nonlinear in nature which are impossible to solve analytically without having some simplification. Therefore, for solution of these governing equations, numerical methods are used.

Chapter 5 introduces the development of model including its validation with some field data and already existing model.

Details of the application of the developed model are deliberated in chapter 6. Effect of depth hydrograph, discharge hydrograph and elevation are discussed in this chapter. A sensitivity analysis of different flow parameter with hydraulic conductivity are also carried out in this chapter.

Chapter 7 discussed the conclusion and future work of the projects.

Chapter 2

Literature Review

2.1 Introduction

Model study of unsteady river flow is generally carried out without giving due consideration to some of the important factors like existence of a piedmont zone in a river bed which influences the flow scenario at downstream significantly. Movement of this infiltrated water is also an important parameter to study, as this may also join the downstream flow after elapse of some time. Previously, different researchers developed a numbers of surface water, groundwater coupled model to study the surface water groundwater interaction. Researchers are also paying interest to study the flow of river, different characteristic of river, sedimentation of river etc. However, most of the investigators are neglecting the existence of the piedmont zone in the computational domain which plays an important role in the downstream flow scenario and groundwater movement. So, in this study, an effort is being made to develop a hydrodynamic flood routing model capable of handling the effect of a recharge zone existing in the river bed. Coupled model between surface and ground water are linked via an exchange of flux between the two systems. Therefore, to get the right direction for developing an unsteady flow model considering the groundwater recharge zone, we need to study past research works regarding unsteady flow model, infiltration model and groundwater model. Review of past research work has therefore been grouped into following three parts:

1) Review of work for unsteady flow model and its solution

2) Review of infiltration model

3) Review of groundwater model and its solution.

2.2 Previous works on unsteady free surface flow model

Three basic fundamental laws- conservation of mass, momentum and energy can represent the free surface unsteady flow. As two flow variables, such as flow depth and flow velocity or flow depth and discharge are sufficient to define the flow condition

two governing equations are sufficient to represent the unsteady flow, either mass momentum couple or mass energy couple of conservation law is used depending on the physical situation. Saint- Venant in 1871(Chaudhry 2008) derived the governing equations for unsteady flow, which is a set of conservation of mass and momentum equations. These equations, also called shallow water wave equations, are a set of non-linear hyperbolic partial differential equations. Since these equations are very complex and difficult to solve analytically without large number of approximations, they are generally solved using numerical techniques. Starting from characteristics equation different numerical methods e.g. finite difference method, finite volume method and finite element method etc. were used by different researchers which are discussed below. Stoker in 1957, Chow in 1959 and Henderson in 1966 in their books derived the equation of motion by different procedures.

Ritter (1892) was the pioneer to solve the Saint- Venant equation analytically. He solved the Saint- Venant equation on a frictionless horizontal channel for simulation of dam break flow (Saikia 2007). Ritter gave explicit expressions for water depth and velocity of flow from a dam site.

Depth of flow "h" and velocity of flow "v" at time "*t*" at a distance x form dam site are represented by Ritter equation as:

$$h=\frac{1}{9g}(2\sqrt{gh_o}-\frac{x}{t})^2 \qquad 2.1$$

$$v=\frac{2}{3}(\frac{x}{t}+\sqrt{gh_o}) \qquad 2.2$$

where h_o is depth at dam site.

But this classical solution of Ritter fails to describe accurately the physical flow as the friction at the wave tip is not negligible.

The Characteristic method is a graphical procedure which is first developed by Monge in 1789 (Chaudhry 2008) for the integration of partial differential equation. In this method, partial differential equations are first reduced to some algebraic equations and then solved from some initial data.

Massau in 1889 and Craya in 1946 used the Characteristic method for analysing surges in open channels and after that Isaacson et al. (1954) further utilised this method for routing hydrograph in a real field. They used one- dimensional unsteady free surface flow equation and assuming the constant slope and width of the river they routed hydrographs through Ohio river and its confluences with Mississippi river in USA.

An attempt was made by Dressler (1952) for the solution of the combined Saint Venant equations along with Chezy resistance equation using the method of characteristics for simulation of flood wave due to the breaking of a dam in a horizontal rectangular channel.

The non-dimensional form of the equation

$$\frac{\partial UN}{\partial TN} + U\frac{\partial UN}{\partial XN} + 2C\frac{\partial CN}{\partial XN} + R\left(\frac{UN}{CN}\right)^2 = 0 \qquad 2.3$$

$$CN\frac{\partial UN}{\partial XN} + 2\frac{\partial CN}{\partial TN} + 2U\frac{\partial CN}{\partial XN} = 0 \qquad 2.4$$

$$\text{Where } XN = \frac{x}{h_o},\ TN = t\left(\sqrt{\frac{g}{h_o}}\right),\ UN = \frac{v}{\sqrt{gh_o}},\quad CN = \frac{c}{\sqrt{gh_o}} \qquad 2.5$$

Gunaratnam and Perkins (1970), Price (1974) and Trikha (1977) modified the method of characteristics to overcome the Courant's instability and makes the method of characteristic much more efficient while retaining much of its original simplicity and accuracy. But their modified scheme did not deal with the Koren instability which has to consider before using a very large Δt specially for that case where Froude number is very less. This Koren instability criterion is related to energy loss term. To overcome this difficulty Huang and Charles (1985) treated the energy slope term with semi- implicit ways and concluded that for the solution of Saint- Venant equation with the help of Characteristics method energy slope term should be treated more implicitly for the stability of the scheme.

Sarma and Das (2003) have developed a new characteristic-based analytical solution of flood for the situation where flood water, being released through an opening in the river dike, moves over a valley.

The flow depth "h" and flow velocity "v" at time "t" at a distance "x" form the dike, are represented as:

$$h = \frac{1}{9g}\left[3\sqrt{gh_o} - \frac{x}{t}\right]^2 \qquad 2.7$$

$$v = \frac{2}{3}\left[\frac{x}{t} + \frac{3}{4}\sqrt{gh_o}\right] \qquad 2.8$$

Though the Characteristics methods used by various researchers for the solution of shallow water equation, it has some disadvantages likes when some bores or shocks are present in the flow, the method of characteristics fails. To overcome these difficulties researchers have used finite difference methods extensively. Finite difference methods are two types' explicit finite difference method and implicit finite difference method.

The original finite difference method is very unstable. French (1985) used this scheme for the solution of shallow water equation. But in this scheme friction losses were increased by a large amount to make the scheme and therefore accuracy of this scheme is questionable.

Lax (1954) made a slight variation of the above unstable scheme. After that Houghton and Kasahara (1967) used this scheme for development of one- dimensional mathematical model. They had used this scheme for the solution of Shallow water equation over a ridge. They found that the approach velocity is inversely proportional to the ridge height. Sharp and Moore (1976) used Lax diffusive scheme for solution of Saint- Venant equation.

Miller and Chaudhry (1989) applied Lax diffusive scheme for the solution of 1D Saint Venant equations in both conservation and non-conservation form in a bend channel flow. To account for the super elevation of the water surface in the bend portion they used a formula based on absolute velocity of the wave, radius of curvature of the channel centreline and acceleration due to gravity. Comparison of results with experimental data showed that conservative form can produce better results.

Chaudhry (1987) applied this scheme in typical hydraulic problem and found that this scheme is one of the simplest to program and yield satisfactory results. More recently

Navarro and Villanueva (1999), Macchione and Morelli (2003), Saikia and Sarma (2006), Akbari and Firoozi (2010), Soleymani and Delphi (2012) used this scheme for solution of unsteady free surface flow.

Alexandre Preissmann (1961) when he was a hydraulic engineer at SOGREAH developed a finite difference implicit scheme for the solution of Saint- Venant equation. This scheme is second order accurate in both time and space. Preissmann scheme has become the standard method for one-dimensional numerical modelling in the field of hydraulic engineering. After development of this scheme in 1960s various researchers e.g. Liggett and Cunge (1975) and Cunge et al. (1980) applied this scheme in river hydraulics. It has the advantages that a variable spatial grid may be used, step wavefronts may be properly simulated by varying the weighting coefficient and the scheme yield exact solution of linearized form of governing equations for a particular value of Δx and Δt.

Fennema and Chaudhry (1986) compared three second order accurate finite difference scheme (MacCormack, Lambda, and Gabutti) for the analysis of unsteady free surface flow having shocks or bore. They had presented the details of these schemes their shock-capturing capabilities, stability restrictions, boundary conditions and use of artificial viscosity to dampen the numerical oscillations near the shock. They observed that Preissmann implicit scheme takes four to eight times the CPU time taken by these explicit schemes which are even easy to program.

Dennis and Peter (1987) examined the stability and convergence characteristics of four-point finite difference scheme due to Preissmann. They had considered the effect of weighting factor due to time and space. To avoid numerically induced oscillation they recommended that computational grid is refined so that local bed Courant number is greater than unity and the local bed spatial resolution is of order 10 or higher. A non-uniform grid is recommended to reduce computational time and storage.

Bellos and Sakkas (1987) employed the explicit predictor- corrector scheme to solve the Saint Venant equations in conservation form to compute the flood wave resulting from the total and instantaneous collapse of a dam in a broad rectangular channel. They compared the experimental and computational results in terms of wave front advance and stage hydrographs and observed a good agreement between these.

Explicit finite difference scheme has stability problem and to overcome this, implicit finite difference scheme was introduced in open channel flow. Fennema and Chaudhry (1989) first used Beam and Warming scheme for the solution of the 2D unsteady free surface flow equations which was developed by Beam and Warming (1976) for the settlement of the 2D Euler equation. This Alternate Direction Implicit (ADI) finite difference scheme is non- iterative and is second order accurate in time. Using this implicit scheme, they simulated the bore formed due to the partial breaching of the dam and obtained excellent results.

Miller and Chaudhry (1989) made a comparison between conservation and non-conservation form of Saint- Venant equation using Lax Diffusive scheme. They found that the conservation form of Saint-Venant equation predicts the height and celerity of the wave better than the non-conservation form.

Paul and Caroline (1990) did a comprehensive study on the stability analysis of Preissmann four- point scheme applied to the Saint-Venant equation including the friction term. They mentioned that linearized numerical schemes are stable when weighted towards new time level and when the magnitude of the Vedernikov number is less than one. Vedernikov number links the stability of the calculation to the hydrodynamic stability of the flow.

Fennema and Chaudhry in (1990) solved the 2D Saint Venant's equation using Mac-Cormack and Gabutti explicit finite-difference methods for the simulation of open channel flow. These schemes are second-order accurate in both space and time. In both methods, an artificial viscosity was added to smooth the high- frequency oscillation in the computed flow depth. These schemes were applied to analyse two common hydraulic flow problems—partial dam breach and passage of a flood wave through a channel contraction. They had compared the results obtained by these schemes with the Beam and Warming scheme and found satisfactory agreement among these schemes. The Mac-Cormack scheme failed for ht/hr ratio less than 0.25, the Gabutti scheme for this ratio less than 0.2 and Beam and Warming scheme for this ratio less than 0.001.

Bellos et al. (1991) examined the 2D flood waves resulting from the instantaneous break of dams. The governing equations were transformed into an equivalent square grid to overcome the difficulties associated with the determination of flow characteristics near

the boundary. They adopted MacCormack predictor- corrector scheme for the integration of the governing equations. They compared the computed results with experimental data and observed good conformity between them.

Lui et al. (1992) derived a finite difference computation method for solving operation type problem in open channel flow. The method was explicit and numerically stable. It was applied to Saint-Venant equation, discretized by Pressmann scheme. The computation results were compared with the results obtained using the double-sweep method, and there was good agreement between the two methods. This computation method was called a backward-operation method since it is for solving operation-type problems, and the computation was performed backwards both in space and time.

Bhallamudi and Chaudhry (1992) solved the 2D depth averaged unsteady free surface flow equations in a transformed coordinate system by using the predictor- corrector scheme to analyse flows in channel expansions and contractions. The unsteady flow model was used to obtain steady flow solutions by treating the time variable as an iteration parameter and letting the solution converge to the steady state. They compared the computed and measured results and observed that in cases where the assumption of hydrostatic pressure distribution is valid it could produce excellent results.

Rashid and Chaudhry (1995) developed a 1D hydrodynamic model for the simulation of unsteady flow in an open channel with flood plain. The governing Saint Venant equations were solved using the Preissmann four-point implicit finite-difference scheme. The suitability of two procedures for approximating the channel cross-section was investigated: (1) the flow velocity over the flood plains is negligible, the flood plain acts as storage only, (2) the entire channel section contributes to momentum flux. Although comparisons between the computed and experimental results were satisfactory in both cases, Approximation (1) gives better results than Approximation (2).

Molls and Chaudhry (1995) developed a depth-averaged model using a boundary- fitted coordinates, including effective stresses. They used Beam and Warming implicit scheme for the solution of the governing equation. The effective stresses are modelled by incorporating a constant eddy-viscosity turbulence model to approximate the turbulent Reynolds stresses. They found that in most cases effective stresses do not have a significant effect on converged solution. They used this model to different problems e.g.

hydraulic jump, flow in channel contraction, flow near a spur dyke, dam-break solution. For each case, they compared the results with the experimental data and found that the results between the computed and experimental results were satisfactory.

Szymkiewicz (1996) developed an implicit four-point scheme to study the inverse linear flow routing. He analysed the stability and accuracy of the numerical solution of the inverse problem for the Saint-Venant equation. According to him, the inverse flow routing requires different values of parameters (θ and Ψ) then the general preismann scheme (where $\theta \geq 1/2$ and $\Psi = 1/2$). Fourier analysis can explain this problem and carry out for a linear hyperbolic system. From this analysis, he had concluded that the four-point implicit scheme applied to inverse flow routing is unconditionally stable if $\theta \leq 1/2$ and $\Psi \geq 1/2$.

Jin and Fread (1997) developed characteristics based, upwind explicit numerical scheme for 1-D unsteady flow model. This new method was compared with an implicit scheme and shown that this scheme provided improved versatility and accuracy in some situation such as large dam- break waves and other unsteady flows with near critical mixed flow regimes.

Rahman and Chaudhry (1998) used a partial differential equation based on the conservative principle of grid arc lengths for clustering grids in one-dimensional along with the Saint- Venant equations to numerically simulate the flow. They used MacCormack explicit predictor- corrector scheme for numerical solution of the governing equation. Both the subcritical and the supercritical flows under extreme boundary conditions were solved by this method and found that for a specified number of grid points, compare to uniformly distributed grids this provided better quality solutions.

Delis et al. (2001) developed a one-dimensional open channel model using implicit scheme. They used Total Variation Diminishing (TVD) scheme for solving the Saint-Venant equation. They compared results obtained by the TVD scheme with the approximate Riemann solver introduced by Roe.

Preissmann scheme is widely used for the solution of Saint- Venant equation. For this model Maurizio (2002) investigated the stability, dissipation and dispersion by looking

at the truncation error. They had examined the variations of the space and time weighting coefficients, the Courant number, the Froude number, and the frictional resistance term. They presented a complete analysis of Preissmann general schemes which have been applied to the Saint-Venant's equations, without approximations.

Mousseau et al. (2002) presented an implicit nonlinearly consistent solution technique for the two-dimensional shallow water equations. They showed that the scheme is unconditionally stable. This scheme is an approximate method, and it is performed well than the traditional semi-implicit method.

Chaga and Souza (2005) developed a numerical model to study the flood propagation in a natural river. They used Saint-Venant equation as the governing equation. For development of the model they made some simplification e.g. flow is one dimensional, the vertical pressure distribution is hydrostatics, the water is considered as incompressible and homogeneous. The one dimensional form of shallow water equation is as follows

$$\frac{\partial Q}{\partial x}+\frac{\partial A}{\partial t}=0$$

$$\frac{\partial Q}{\partial t}+\frac{\partial (Q^2/A)}{\partial x}+gA(\frac{\partial y}{\partial x}-S_0)+gAS_f=0$$

They had done the sensitivity analysis of hydraulic parameters and found that these parameters play a significant role in the propagation of flood.

Alhan and Madina (2007) used MacCormac explicit scheme for the solution of the kinematic and diffusive equations. They developed a numerical model using previously mentioned equations for overland and open channel flow. They had validated the results with the analytical solution and found perfect agreement between them.

Siviglia et al. (2008) developed a morphodynamic model by coupling Saint- Venant equation with Exner equation. They proposed a quasi-conservative formulation of the differential system to reduce errors. MacCormack predictor corrector scheme was used for solution of the governing equations. They applied this model in different cases e.g. dam break flow for inviscid shallow water equations with available analytic solution,

experimental mobile bed case and natural mobile bed case and good results were observed.

Singh et al. (2011) developed a 2D model for simulation of dam break flow. They discretized the spatial derivatives using a well-balanced explicit central- upwind conservative scheme. They found that the model gives good results over a complex topography if the Courant number is less than 0.25. The model is validated with three benchmark test cases. A good agreement between analytical solutions and computed results is observed.

Bellos and Hrissanthou (2011) developed a 1-D unsteady flow model to study the dam break flood wave. They had used Saint- Venant equation as the governing equation and Lax- Wendroff and MacCormack scheme for the solution of the governing equation. They comparison between simulation data and experimental data, showed a high degree of convergence.

Kalita and Sarma (2012) made a comparison between two finite difference methods for solution of Saint- Venant equation. They made a conclusion that both the scheme lead to same results but with the help of Beam and warming scheme one can go for much larger time step.

Kalita et al. (2014) used Beam and warming scheme for solution of the free surface flow equation. Beam and Warming is an implicit scheme but non iterative because of which one can go for large time step and requires less computational time than other implicit scheme. They had used conservation form of governing equation as follows

$$U_t + E_x + F_y + S = 0$$

where

$$U = \begin{pmatrix} h \\ uh \\ vh \end{pmatrix} \quad E = \begin{pmatrix} uh \\ u^2h + \frac{1}{2}gh^2 \\ uvh \end{pmatrix} \quad F = \begin{pmatrix} vh \\ vuh \\ v^2h + \frac{1}{2}gh^2 \end{pmatrix} \quad S = \begin{pmatrix} q \\ -gh\left(s_{0_x} - s_{f_x}\right) \\ -gh\left(s_{0_y} - s_{f_y}\right) \end{pmatrix}$$

$$s_{f_x} = \frac{N^2 u\sqrt{u^2+v^2}}{h^{4/3}} \qquad s_{f_y} = \frac{N^2 v\sqrt{u^2+v^2}}{h^{4/3}}$$

Where h is the water depth, u is the velocity in x direction and v is the velocity in y direction s_{0_x} is the bed slope in x direction s_{0_y} bed slope in y direction, s_{f_x} and s_{f_y} frictional slope in x and y direction respectively.

For the complex flow domain, finite element methods were used. The underlying consistency and generality of the finite element method are attractive because separate computational algorithms for subcritical and supercritical flow are not required, and algorithm extension to the two-dimensional depth-averaged flow equations are straight forward.

Katopodes (1984) developed a 2D numerical model using Saint-Venant equation as the governing equation and solved the same by dissipative Galerkin scheme. The classical Galerkin- based finite element method formulation produces inferior results when applied to discontinuous channel flow. They found that the introduction of dissipation improved the phase error in the finite element simulation. The resulting model was second-order accurate on the time step. The method based on discontinuous weighting functions that produce "upwind" effects but at the same time maintain the accuracy of a central difference scheme. The performance of the method was verified with various test problems.

Akanbi and Katopodes (1988) developed a model for flood wave propagation on a dry bed. The governing equations are transformed to an equivalent system valid on a deforming coordinate system and are solved by a dissipative finite element technique. The accuracy and stability of the model are examined by comparing the model results with observed data from an experimental field test.

To overcome the failure of Dissipative Galerkin (DG) scheme in the field where sufficient shocks are observed, Hicks and Steffler (1992) developed a new characteristics dissipative Galerkin (CDG) scheme. This method possesses shock-handling capability without requiring any parameter variation. Spatial discretization of this system of equations was achieved through the use of linear interpolation functions to approximate the behaviour of the solution over each element. They used a linear stability analysis to

compare the phase and amplitude accuracy of the CDG scheme to that of the DG scheme and it was observed that this scheme gives very high phase accuracy for a Courant number 0.5 or less than it.

Khan (2000) used Petrov-Galerkin finite element scheme to solve Saint- Venant equation for dam break flow. They compared the results with the analytical solution for a dam break over the frictionless horizontal bed, show that the model possesses excellent phase accuracy, for both positive and negative waves, and can predict the discharge distribution accurately. He performed two more test, one for a smooth horizontal bed; and the other consisting of two cases, for sloping channel with smooth and rough bed. The computed water surface profiles agree well with the measured data in each instance.

Schwanenberg and Harms (2004) developed a model using Runge- Kutta discontinuous Galerkin finite-element method for the solution of two- dimensional depth- averaged shallow water equation. By doing a simple treatment of boundary conditions and source terms the scheme can handle complicated boundary with high-order accuracy. Because of explicit time integration with the use of orthogonal shape functions, the method is computationally as efficient as finite-volume schemes. To confirm the accuracy of the scheme they did several steady transcritical and transient flows. The results show perfect agreement with analytical solutions.

Chen et al. (2007) developed a numerical model using a modified form of the Saint-Venant equation, in which effects of inclination and non prismaticity are incorporated into an approximate term to ensure implementation of the conservative formulation. They proposed a modified version of Galerkin finite element scheme for the solution of the modified form of the Saint- Venant equation. The proposed model showed good results when applied for steady flow in a diverging channel with a hydraulic jump, dam break flow in a converging- diverging channel and unsteady flow in Oldman river in southern Alberta.

Ghostine et al. (2010) used Runge-Kutta discontinuous Galerkin method (RKDG) with a slope limiter for the solution of the two-dimensional Saint Venant equations. They studied the robustness and the stability of the scheme. The study was mainly involved with the prediction of the water depths, the location of the right and oblique hydraulic jumps in the crossing, and especially the distribution of the flow discharges in the

downstream branches. They compared the RKDG method with second order finite-volume method and shown the advantages of this method. Comparison with the experimental data showed the method accurately predicts the hydraulic jump location, water depths and the discharge distribution.

More recently, Rossell and Ting (2013) extended the finite element model for evaluation of contraction scour on the areas near the James River bridges near Mitchell in USA. From the study, they observed that unique hydraulic condition creates at the bridge site because of three main factor namely channel meandering, the no-flow boundary condition and the dense trees along the left bank. They also found that the predicted scour depth was very sensitive to the critical shear stress and slope of the curve of erosion rate versus shear stress.

The finite volume methods have been widely employed to solve 2-D depth-averaged equations. They conserve mass and momentum to each cell and fluxes can be evaluated at the cell faces by solving Reimann problem. Finite volume schemes can be applied to irregular flow domain, and at the same time, they are as easy to implement as finite difference scheme. The main advantages of this scheme are its simplicity and ease of implementation. It can also handle sharp gradient in the water surface profile if they are present.

Zhao et al. (1994) developed a two-dimensional unsteady flow model based on finite volume method with a combination of unstructured triangular and quadrilateral grid in a river- basin system. The advantages of this scheme are that it calculated the mass and momentum flux across each side of the element as a Reimann solver. This feature enables this model to deal with the wetting and drying process of floodplain and wetland studies, a dam breaking phenomena involving discontinuous flow, supercritical flow, subcritical flow and other cases.

Mingham and Causon (1998) developed a high-resolution time-marching method for solving the two-dimensional shallow water equations. This method used a cell- centred formulation rather using a space- staggered approach. They applied this method to several dam break problems including 1D dam break, circular dam break, oblique bore formation and partial dam break cases and excellent quality results were observed.

Bradford and Katopodes (2001) developed a finite volume based model for two-dimensional unsteady flow which is applied to simulate the advance and infiltration of an irrigation wave in two-dimensional basins of complex topography. The fluxes were computed with Roe's approximate Riemann solver, and the monotone upstream scheme for conservation laws was used in conjunction with predictor-corrector time-stepping to provide a second-order accurate solution. The proposed model was compared with various experimental data for 1D and 2D problems involving rough, impermeable, and permeable beds, including a poorly levelled basin and excellent results, were observed.

Ying et al. (2004) proposed an upwind- conservative scheme with a weighted average water-surface-gradient approach to computing open channel flows. The scheme was based on control volume. The inter cell flux was computed by the one-sided upwind method. The water surface gradient was evaluated by the weighted average of both upwind and downwind gradients. The scheme was tested with various examples, including dam-break problems, hydraulic jump, partial dam-break problem, overtopping flow, a steady flow over a bump with a hydraulic jump and a dam-break flood case in a natural river valley. They compared the numerical results with an exact solution or experimental data and found that the proposed scheme is capable of accurately reproducing subcritical, supercritical and transcritical flows. This scheme does not require artificial viscosity or front tracking technique to capture steep gradients or discontinuities in the solution.

Wu (2004) developed a depth-averaged two-dimensional (2D) numerical model for unsteady flow and nonuniform sediment transport in open channels using finite volume method. To consider the effects of the gravity on the sediment transport capacity and the bed-load movement direction in channels with steep slopes they proposed an empirical equation. The proposed model was applied to various cases like channel aggregation, channel degradation, basin erosion and the East Fork River in Western United States and fine results were observed.

Zarrati et al. (2005) developed a 2-D depth averaged numerical model for the nonorthogonal curvilinear coordinate system. The model can be handled a complex mesh arrangement. They had applied this model to three meandering channels with the same specification of natural river and found the results are satisfactory.

Blade et al. (2008) developed a numerical method based on Roe TVD finite volume scheme for the solution of the Saint- Venant equation. The benefits of this scheme are that it can be applied to irregular boundaries and preserves the correct steady flow when stationary boundary conditions are used. Results obtained were compared with experimental results, and real resemblances were observed.

Lai (2010) developed an unstructured hybrid mesh numerical method to simulate unsteady flow in open channel flow using finite volume method. The main advantages of this method are that it can be applied to arbitrary shape mesh cell and in depth averaged equation mass conservation is satisfied both locally and globally. The method applies to both steady and unsteady flows and covers the entire flow range: subcritical, transcritical, and supercritical. The model results were validated with natural river and found satisfactory agreement.

Kuiry et al. (2010) used finite volume method for the solution of Saint- Venant equation. Diffusive wave equation represented the flow exchange between the one-dimensional river cells and the adjacent floodplain cells or that between adjoining floodplain cells. The accuracy of this model is compared with respect a two-dimensional 2-D finite volume model on hypothetical river-floodplain domains.

Zhang et al. (2013) developed a coupled surface water solute transport model for basin fertigation where advection upstream splitting method and central finite-volume scheme with dissipation characteristic were employed to discretize the spatial derivatives of physical flux, spatial derivatives of advection matrix, diffusion vector, and water-level slope vector. The model results were validated with the field experiment and found that the model exhibits outstanding performance for calculating water flow and solute transport under full-time, first-half, and second- half fertilizer-application experiments.

More recently Stecca et al. (2016) developed a 1-D Saint-Venant-Hirano model for mixed-sediment morphodynamics. The Explicit finite volume upwind method was used for the solution of the principal part of the model. They verified their accuracy of the scheme and did three case studies namely empirically assess the balancedness of vertical mass fluxes under degradation, the convergence to the analytical linearised solution for the propagation of infinitesimal-amplitude waves and Ribberink's E8-E9 flume experiment.

2.2.1 Concluding remark on free surface flow model

Review of literature has established that different investigator at different time solved the unsteady flow in open channel by using different approaches e.g. finite difference methods, finite element methods and finite volume method. From the literature, it has been noticed that finite difference method can be classified into three categories namely characteristic method, explicit method and implicit method. Though the Explicit finite difference schemes are easy to implement and required less computer time, the schemes have to satisfy some criterion in case of stability. Advantages of implicit finite difference schemes are that these schemes are very stable and allow large time step but these schemes are difficult to implement and required more computer time than explicit finite difference scheme. Most of the implicit schemes are iterative in nature and therefore require more computational time. Researchers have mostly used finite element methods for complex geometry. Finite element methods though more complex as compared to finite difference method, do not provide much additional advantages in solving Saint-Venant equation. Finite volume schemes can be applied to irregular flow domain, and at the same time they are as easy to implement as finite difference schemes. The main advantages of this scheme are its simplicity and ease of implementation. It can also handle sharp gradient in the water surface profile if they are present. Out of all these numerical schemes, Beam and Warming scheme has been extensively used by the researchers. The main advantages of this scheme are that it is implicit scheme but non-iterative in nature which reduces the computational time. So in this study governing equation of unsteady flow is solved by Bean and Warming finite difference scheme.

2.3 Previous work on infiltration and ground water model

Infiltration model in the unsaturated region and to study the flow movement of infiltrated water in that region is a significant problem in several branches in hydrology. Researchers have developed the different numerical model to study the infiltration processes and ground water movement.

2.3.1 Previous works on Green-Ampt. infiltration model

Green, W.H. and G. Ampt. (1911) developed an equation for infiltration in soil physics. After their name this equation popularly known as Green-Ampt.. infiltration equation. This equation originally developed to study infiltration into uniform soil. After that

Childs and Bybordi (1969) and Bybordi (1973) applied this equation to measure infiltration into layered soil profile with hydraulic conductivity decreases from the surface. Further Hachum and Alfaro (1980) modified the Green-Ampt. equation for vertical infiltration into a nonuniform soil profile by using a harmonic mean of effective hydraulic conductivities of wetted soil layers.

Chu (1978), Smiles et al. (1981), Dagan and Bresler (1983) and Govindaraju et al. (1992) applied the Green-Ampt. infiltration equation in homogeneous unsaturated soil. From their studies it was concluded that water storage is predicting accurately by the Green-Ampt. model under flux-dependent condition.

Govindaraju et al. (1996) used Green-Ampt. model for analysing one-dimensional convective transport in unsaturated soils. The utility of the Green-Ampt. model for homogeneous unsaturated soils is investigated as an alternative to Richards equation. This model, through approximate, provides analytical solution to the flow field. It was found that the flow quantities required for the analytical solution of convective transport are predicted accurately by Green-Ampt. model.

Chu and Marino (2005) developed an infiltration model based on Green-Ampt. equation for heterogeneous soil for variable initial moisture distribution during unsteady rainfall. They have developed an algorithm for determining the ponding condition, simulating infiltration into layered soil profile. Two distinct periods, pre-ponding and post ponding are taken into account. This model tracks the movement of wetting front and checks the status of ponding. The model was also applied to saturated flow condition when wetting front reaches the bottom of the soil profile.

Chen and Young (2006) used the Green-Ampt. equation to measure infiltration in sloping surface. From their analysis they found that infiltration increases with increasing slope angle. The slope effect is not significant for infiltration in ponded depth if the slope is mild to moderate. But the slope effect became more important for low-intensity and short-duration rainfall events, especially as it delayed the time for ponding.

Ma (2010) developed a modified Green-Ampt. model to describe water infiltration process in a 300 cm long and five layered soil column. In their model they had introduced a saturation coefficient to determine the hydraulic conductivity and water content of

wetted zone. They had compare the results of this model with the HYDRUS-1D model and found satisfactory results.

Bateman et.al. (2010) studied the effect of soil infiltration on flat areas flood simulation. In their work they had included the water infiltration as a new element to improve accuracy in the flood simulation. They used Green- Ampt infiltration model for calculating the amount of water infiltrated in to the ground. In the development of the classical Green- Ampt model the surface water depth is neglected. But in their study surface water depth was included as the water depth could be high.

Voller (2011) calculated infiltration in a heterogeneous soil, by using Green-Ampt. model in fractional derivatives form. The result obtained by this model was non-monotonic. In his studies it was postulated that if the length scales of the heterogeneities can be assumed to be power law distributed, then it may be appropriate to model infiltration in heterogeneous soils in terms of fractional derivatives.

2.3.2 Previous works on Richards equation

Brutsaert (1971) developed a fully implicit scheme along with a functional iteration method for the solution of the Richards equation. This model was suitable for predicting infiltration problem in the heterogeneous and anisotropic soil. They had compared the results of this model with the experimental results and found that there was good agreement between these results. The main disadvantage of this model was that it required more work to solve for a time step than the classical implicit scheme.

Perrens and Watson (1977) were used the two-dimensional flow equation for the movement of water in the unsaturated porous material to study an infiltration-redistribution sequence in which the surface flux was spatially nonuniform. A numerical analysis based on a finite difference scheme involving the use of iterative alternating direction implicit techniques was found to describe the two-dimensional flow process satisfactorily.

Celia et al. (1990) developed a numerical model for the solution of unsaturated flow by mass conservative approximation. This approximation is based on the mixed form of Richards equation. It combines benefits inherent in both θ-based and h-based form of the equation. They used Picard iteration method for solution of the governing equation. They

evaluated the water content change over time step directly from the change of pressure head.

Gottardi and Venutelli (1992) used moving finite element (MFE) method for the solution of Richards equation. For an accurate solution of the partial differential equation, using standard finite difference and finite element scheme a fine discretization on space and time is required. To minimise these difficulties, they used MFE method where grid points are moved during computation along the wetting front, so that accuracy can be maintained by using a small number of nodes for simulating cases several meter in depth. They found that the MFE method was faster than FD and FE method. But the main disadvantages of this method are it is not suitable for heterogeneous and layered profile soil. The method is less mass conservative than FD and FE method.

Kirkland et al. (1992) developed two new algorithms for solving Richards equation of variably saturated flow. One-dimensional water content based finite difference method offer improve CPU efficiency in dry heterogeneous soil compare to similar pressure based method. But the usefulness of water content method failed when applied to saturated soil. To remove this difficulty, they developed two new methods which retained the advantage, when applied to a fully saturated condition. In the first method, they defined a new variable for transformed Richards equation which has the characteristic of water content when the soil is unsaturated and of pressure when the soil is at or saturated. In addition to transformed Richards equation method, an improved pressure based method which uses flux updating was presented. The performance of the methods was compared with the mixed form Richards equation and found that the for unsaturated case, the new algorithms were 16 to 59 times faster than the mixed form Richards equation using Pichard iteration. For saturated case, the new algorithms were 6 to 25 times faster than the mixed based algorithm.

Lim and Lee (1993) used Galerkin finite element method for the solution of the one – dimensional, vertical flow of water and mass transport of conservative- nonconservative solute in unsaturated flow. To avoid large mass balance error in h- based Richards equation they used ROMV (restoration of the main variable) concept in discretization step. They had applied this model to sandy soil, and ROMV method showed good mass conservative in water flow analysis.

Pan and Wierenga (1995) presented a new approach to solving Richards equation. They introduced a nonlinearly transformed pressure, P_t, as the dependent variable with the modified Picard method. They compared this method with the φ- based transformed method and h- based modified Picard method and found that this new method offered

Huang et al. (1996) evaluated the performance of different convergence criteria for mixed form Richards equation when modified Picard iteration method is used. They had compared the results in terms of computer processing time (CPU) and number iteration. They derived a nonlinear convergence criteria using tailor series expansion of the water content. The computational efficiency of the new criterion was evaluated against two widely used convergence criteria for different soil types, boundary conditions, initial conditions and layered soils. From the results, they found that new convergence criteria have more CPU efficiency than the other two convergence criteria.

Hari Prasad et al. (2001) developed a numerical model to simulate moisture flow through the unsaturated zone. Richards equation was used for vertical unsaturated flow. They used finite element discretisation in space and the finite difference in time for solution of the governing equation. Sensitivity analysis had been done to analyse the sensitivity of gravity drainage and infiltration process with the variation of unsaturated soli parameter α (measure of capillary fringe thickness) and n (pore size distribution of the soil). The results obtained by the model was validated with already available literature review and found satisfactory results.

Kavetski et al. (2002) developed a noniterative implicit time stepping schemes with adaptive temporal truncation error control for the solution of the pressure form of Richards equation. They had introduced first and second order linearization of adaptive backward Euler/Thomas-Gladwell formulation. Numerical experiments demonstrate that accurate noniterative linearization achieve cost-effective solutions of problems where soils are described by highly nonlinear and nonsmooth constitutive functions. They found that the second-order noniterative scheme was more efficient than the first-order noniterative scheme.

Lu and Zhang (2004) derived the analytical solution of one-dimensional unsaturated flow equation under randomly heterogeneous layered soil column under random boundary conditions. For the first time, they used Kirchhoff transformation for linearization of

steady state unsteady flow equation. This analytical solution was validated via Monte Carlo simulations.

Miller et al. (2006) solved Richards equation using an adaptive method in both space and time. Spatial adaption was based upon a coarse grid and a gradient error indicator using a fixed-order approximation. Temporal adaption was accomplished using variable order, variable step size approximations based upon the backward difference formulas up to fifth order. They had tested the results with the four different one-dimensional problems and found that the proposed method provides a robust and efficient alternative to standard approaches for simulating variably saturated flow in one spatial dimension.

Liang et al. (2007) developed a two-dimensional numerical model and solved the free surface flow and subsurface flow simultaneously. TVD-MacCormack scheme was used to solve the shallow water equation for surface flow, and standard MacCormack scheme was employed to solve the transient Boussinesq equation for unconfined ground water flow.2D shallow water equations were taken as the governing equations of the free surface flow. They assumed that the ground below the surface water is always fully saturated. To define the subsurface flow, they used the 2-D Boussinseq equation.

Weill et al. (2009) developed a model for surface-subsurface flow. A single Richards type equation with domain-dependent parameters was used to describe land surface water, vadose zone and saturated zone water. They had used hybrid finite element formulation to solve this multi-domain Richards equation. They had also used an advective-diffusive transport equation to follow and identify pre-event and event water. The developed model can describe both infiltration excess and saturation excess runoff. They presented validations, verification and application test cases to assess this modelling approach and at the end, they concluded that the model performed well.

Palla et al. (2009) studied unsaturated subsurface water flow in the coarse-grained porous matrix. To analyse the interaction between hydrologic process and green roof installation in the urban environment, it requires improving the understanding of the unsaturated water flow in the coarse-grained porous media. They had applied the SWMS 2D model, based on Richards law and the Van Genuchten-Mualem function to simulate the variably saturated flow within green roof system.

Wu (2010) developed a general numerical algorithm in the context of finite element scheme to solve Richards equation, in which a mass-conservative, modified head based scheme (MHB) was proposed to approximate the governing equation, and mass-lumping techniques were used to keep the numerical simulation stable. He compared the MHB scheme with the MPI scheme in a ponding infiltration example and found that MHB scheme was a little inferior to the MPI scheme in respect of mass balance, but it was superior in convergence character and simplicity.

Mengxi (2010) developed A general numerical algorithm in the context of finite element scheme was developed to solve Richards equation, in which a mass-conservative, modified head based scheme (MHB) was proposed to approximate the governing equation, and mass-lumping techniques were used to keep the numerical simulation stable. He compared the MHB scheme with the MPI scheme in a ponding infiltration example and found that MHB scheme was a little inferior to the MPI scheme in respect of mass balance, but it was superior in convergence character and simplicity.

Casulli and Zanolli (2010) used finite volume method for discretization of mixed form Richards equation. Newton- type algorithm was used for discretization of the Richards equation. They did numerical tests to confirm the efficiency, the robustness, and the usefulness of the proposed algorithm for solving the mixed form of Richards equation under different flow conditions and for any time step size.

Kong et al. (2010) developed a coupled surface and subsurface water flow model based on an unstructured finite volume/ finite difference method. The model domain was divided into a surface water flow layer, and ground water flow layer.

Weill et al. (2011) coupled the surface-subsurface interaction to an existing flow model. In the integrated model same surface routing and mass transport equations were used for both hill slope and channel process, but with different parameterizations for these two cases. For the subsurface an advanced time- splitting procedure was used to solve the advection-dispersion equation for transport, and a standard finite element scheme was used to solve Richards equation for flow. A mass balance-based surface boundary condition was used to resolve surface-subsurface interaction. Surface transport was described by a diffusive wave equation analogous to that used in the flow model, and resolved by the same path-based Muskingum-Cunge scheme, whereas the subsurface

transport equation was solved by a time-splitting technique combining flux limited finite volume and a classical finite element scheme.

2.3.3 Concluding Remark on groundwater model

From the literature review, it is observed that most of the researchers used Richards equation for groundwater movement of the water. Richards equation is a parabolic nonlinear equation which is hard to solve analytically. Researchers have used different numerical method e.g. finite difference, finite element and finite volume methods for the solution of the Richards equation. Again for infiltration into dry soil, finite element method shows oscillatory results even mass is properly conserved (Celia et al. 1990). In this study we are going to study flux exchange between surface water and groundwater. Therefore finite difference method is used for coupling the two processes. Hence Bean and Warming ADI scheme is used for the solution of Saint- Venant equation and ADI scheme is used for the solution of the Richards equation.

Chapter 3

Governing Equation

3. Introduction:

In this chapter, a detailed discussion about the different governing equation for developing the model has been presented. The main objective of the study is to develop a coupled surface-subsurface flow model for a river having the piedmont zone on the bed. There are three main components for developing this coupled model. One is free surface flow model which is described by popular Saint- Venant equation, the second one is the Green-Ampt. infiltration model, which is used to find out the water infiltrated through the piedmont zone and the last one is the subsurface flow model below the river bed which is described by the Richards Equation. The details of these equations have been described in the following sections. Towards the end of the chapter a flowchart related to the coupling of these equations has been given after discussing each equation.

3.1 Governing equation for unsteady free surface flow model

To describe open channel flow, there are basically three equations namely continuity equation, momentum equation and energy equation. The governing equations of gradually varied unsteady free surface flow are a set of nonlinear hyperbolic partial differential equations, which are extensively used to calculate either flow depth and velocity or flow area and discharge in a channel. These equations are named as Saint-Venant equations or shallow water equations. The Saint-Venant equations were first stated in 1871 in a note to the Comptes-Rendus de l'Acad´emie des Sciences de Paris by Adh´emar Barr´e de Saint-Venant, a French engineer. This is one of the most popular models among hydraulic engineers to represent the dynamics of open channel flow. Two sets of equations are used in the shallow water equations namely continuity equation and momentum equation in the form of one dimensional, two dimensional and three dimensional as per field condition with some assumption, which are discussed below.

3.1.1 Assumption for developing governing Equation

Following assumptions are made for derivation of governing equation (Choudhry H.M. 2008)

- The pressure distribution is hydrostatic. This is a valid assumption if the streamline do not have sharp curvature.
- The channel bottom slope is small, i.e., the flow depth measured normal to the channel bottom or measured vertically are approximately the same.
- The flow velocity over the entire channel cross section is uniform.
- The channel is prismatic, i.e. the channel cross section and the channel bottom slope do not change with the distance. The variation in the cross section or bottom slope in a natural channel is generally handled by considering the channel as composed of several prismatic reaches.
- The head loss in unsteady flow may be simulated by using the steady- state resistance laws, such as the Manning or Chezy equation, i.e. head losses for a given velocity during unsteady flow are the same as that of the steady state condition.

The momentum equation consists of terms for the physical processes that govern the flow momentum. These terms are local acceleration term describing the change in momentum due to change in velocity over time, the convective acceleration term representing the change in momentum due to change in velocity along the channel, the pressure force term proportional to the change in the water depth along the channel, the gravity force term proportional to the bed slope S_0, and the frictional force term proportional to the friction slope S_f. The local and convective acceleration terms represent the effect of inertial forces on the flow.

The governing equation of unsteady free surface flow, i.e., the continuity and momentum equations in the conservation form, considering lateral flow, has been used by different investigators (Chow, et al. 1988, Strelkoff 1970, Choudhry H.M. 2008).

$$U_t + E_x + F_y + S = 0$$

$$U = \begin{pmatrix} h \\ uh \\ vh \end{pmatrix} \qquad E = \begin{pmatrix} uh \\ u^2h + \frac{1}{2}gh^2 \\ uvh \end{pmatrix} \qquad F = \begin{pmatrix} vh \\ vuh \\ v^2h + \frac{1}{2}gh^2 \end{pmatrix}$$

$$S = \begin{pmatrix} q \\ -gh\left(s_{0_x} - s_{f_x}\right) - m_{lx} \\ -gh\left(s_{0_y} - s_{f_y}\right) - m_{ly} \end{pmatrix} \qquad s_{f_x} = \frac{N^2 u\sqrt{u^2+v^2}}{R^{4/3}} \qquad s_{f_y} = \frac{N^2 v\sqrt{u^2+v^2}}{R^{4/3}}$$

where h is the water depth, u is the velocity in x direction, v is the velocity in y direction, N is the manning's roughness coefficient, s_{0_x} is the bed slope in x direction s_{0_y} bed slope in y direction, s_{f_x} and s_{f_y} are frictional slope in x and y direction respectively, *R* is the hydraulic radius, q is the lateral out flow or inflow, m_{lx} and m_{ly} momentum loss (dynamic contribution of lateral discharge) in x and y direction respectively.

In presence of piedmont zone, a significant amount of water is infiltrated through the river bed, and the infiltrated amount can be represented by an additional component in the source term. The source term of eq 3.1 can be modified as given below

$$S = \begin{pmatrix} f+q \\ -gh\left(s_{0_x} - s_{f_x}\right) - m_{lx} \\ -gh\left(s_{0_y} - s_{f_y}\right) - m_{ly} \end{pmatrix}$$

where $f = k_0\left[1 + \frac{[\psi(t)+h(t)][\theta_s - \theta_o]}{F_c}\right]$

$m_{lx} = 0.5(f+q)u \qquad m_{ly} = 0.5(f+q)v$

f is the infiltration rate of water infiltrated through the piedmont zone, m_{lx} and m_{ly} momentum loss because of infiltration (dynamic contribution of lateral discharge) in x and y direction respectively. The source term f is calculated from the Green-Ampt equation (eq. 3.2), which is discussed in the following section.

3.2 Governing equation for infiltration model

Large number of infiltration models given by different researchers are available for calculation infiltration in ponded area, Out of these models, the Green-Ampt. model has been widely used by the researchers because of its accuracy and easy way of application (Chu in 1978, Smiles et al. in 1981, Dagan and Bresler in 1983 and Govindaraju et al. in 1992). In the original Green-Ampt. equation, the height of the water depth (ponding depth) is neglected considering the assumption that infiltration rate is more than rate of water supplied. However, to calculate the infiltration rate in a river, this assumption may not be valid. Again, Freyberg et al. (1980) found that the effective suction head in Green-Ampt. equation is a function of time, surface water depth, initial moisture content and soil type. Infiltration rate through the recharge zone is, therefore, calculated by using the following equations,

$$f = k_0\left[1+\frac{[\psi(t)+h(t)][\theta_s-\theta_o]}{F_c}\right] \qquad 3.2$$

$$\psi(t) = \frac{F^*(f^*-k_s)}{(\theta_s-\theta_o)k_s} - h(t) \qquad 3.3$$

where F_c is the cumulative infiltration, $h(t)$ is the water surface height which is a function of time and this time dependent $h(t)$ is obtain from the water depth "h" computed from solution of eq. 3.1; $\psi(t)$ is the time dependent effective suction head; θ_s, θ_o are the saturated and initial soil moisture content respectively; k_s is the saturated hydraulic conductivity. F^* and f^* are obtained from the solution of the Richards equations (Reeder et al. 1980) as followed.

The vertical soil moisture flow can be described by following form of Richard's equation

$$c(\psi)\frac{\partial\psi}{\partial t} = \frac{\partial}{\partial z}\left[k(\psi)\left(\frac{\partial\psi}{\partial z}+1\right)\right] \qquad 3.4$$

where ψ is the suction head, $c(\psi) = d\theta/d\psi$ is the specific moisture capacity, θ is moisture content, $k(\psi)$ is the unsaturated hydraulic conductivity, z is the vertical space

coordinate, t is the time. After calculating the value of ψ, the infiltration rates are determined by applying the Darcy equation to the top layer of the soil column as per the following equation

$$f^* = k_s\left[\frac{h(t)}{Z(t)}+1\right] \qquad 3.5$$

where $h(t)$ is the surface water depth with time and $Z(t)$ is the depth of the saturated zone, k_s is the saturated hydraulic conductivity of the soil at ground surface. f^* is the infiltration rate that used in eq. 3.3.

The water infiltrated through the piedmont zone is calculated by the eq. 3.2. The water infiltrated through the piedmont zone moves as groundwater below the river bed and joins the mainstream at downstream. The flow of this infiltrated water in the sub-surface layers is modelled by using the popular Richards equation and is described in the following section.

3.3 Governing equation for ground water model

Movement of the infiltrated water through the sub-surface layers forms another important aspect of the flow process. Water infiltrated through the piedmont zone moves below the river bed and joins the mainstream at downstream. The most common equation to describe the groundwater movement is Richards equation. Richards equation is expressed mainly in three forms. Pressure based Richard's equation (eq.3.6), water content based Richard's equation (eq.3.7) and mixed form Richard's equation (eq.3.8). Numerical solution of pressure based Richards equation generally yields poor results because of large mass balance errors and erroneous estimation of infiltration depth (Celia et al. 1990). Similarly, water content based method cannot be applied to saturated soil (Krikland et al.1992). On the other hand, numerical solution of mixed form Richards equation can be shown to possess conservative property, so that mass is properly conserved (Celia et al. 1990). This leads to significant improvement of numerical solution performance while requiring no additional effort. Different form of Richards Equations are given below (Celia et al. 1990)

Pressure based Richards equation $$c(\psi)\frac{\partial h}{dt} - \nabla.K(\psi)\nabla\psi - \frac{\partial K(\psi)}{dz} = 0 \qquad 3.6$$

Water content based Richards equation $$\frac{\partial \theta}{dt} - \nabla .D(\theta)\nabla \theta - \frac{\partial K(\psi)}{dz} = 0 \quad 3.7$$

Mixed form Richards equation $$\frac{\partial \theta}{dt} - \nabla .K(\psi)\nabla \psi - \frac{\partial K(\psi)}{dz} = 0 \quad 3.8$$

where $c(\psi)$ is the soil moisture capacity, $k(\psi)$ unsaturated hydraulic conductivity, ψ is the pressure head, $D(\theta)$ is the unsaturated diffusivity and θ is the moisture content.

3.3.1 Necessary soil parameters

Van Genuchten's (1980) model is used to describe the soil properties. The relationship between water content and pressure head (under tension) is given by (Van Genuchten, 1980)

$$S_e = \left[\frac{1}{1+(\alpha h)^n}\right]^m \quad 3.9$$

where α, n and m=1-1/n are the Van Genuchten parameters, whose values depend upon the soil properties. The parameter α is a measure of the first moment of the pore size density function (L^{-1}) and n is an inverse measure of the second moment of the pore size density function. S_e is the effective saturation, given by relationship

$$S_e = \left[\frac{\theta - \theta_r}{\theta_s - \theta_r}\right] \quad 3.10$$

Based on Mualem's (1976) model, the relationship between water content and hydraulic conductivity is given by (Van Genuchten, 1980)

$$k(s_e) = k_s \left\{1 - \left\{1 - s_e^{1/m}\right\}^m\right\}^2 s_e^{1/2} \quad 3.11$$

where k_s is the saturated hydraulic conductivity.

3.3.2 Grid-transformation: Groundwater model

Richards equations are highly nonlinear equations and the analytical solution is not possible except for spatial cases. Finite difference and finite element are the most common numerical method to solve the nonlinear equations. Again, in finite difference

formulation solution are made in grid points. The determination of a proper grid for flow over or through a given geometric shape is extremely important for achieving the solution. The way that such a grid is determined is called grid generation. The solution of governing equation in non-uniform grid is a very difficult task because there is no direct way of solving the governing equation over a non-uniform grid in the context of finite difference method. However, it is possible to transform the non-uniform grid to a uniform rectangular grid with recasting of the governing partial differential equation into rectangular grid. As the flow domain below the river bed is not rectangular, for numerical solution of the Richard's equation, it is necessary to transform the equation to a rectangular domain. Therefore in this study Richards equation has been derived in the grid transformation form by using the following steps (eq. 3.13 to 3.33).

Mixed form of Richards equation can be expressed as given in equation 3.12 (Celia et al. 1990).

$$\frac{\partial \theta}{\partial t} = \frac{\partial}{\partial x}\left(K \frac{\partial \psi}{\partial x} \right) + \frac{\partial}{\partial z}\left(K \frac{\partial \psi}{\partial z} \right) + \frac{\partial K}{\partial z} \qquad 3.12$$

For transformation of this equation from (x,z,t) space to (ξ,η,t) space, we need a transformation for the derivatives, i.e., we need to replace the x and y in the original partial differential equations with corresponding derivatives with respect to ξ and η. For replacing the $\frac{\partial}{\partial x}$ and $\frac{\partial}{\partial y}$ derivatives in terms of $\frac{\partial}{\partial \xi}$ and $\frac{\partial}{\partial \eta}$, following are the expressions used.

$$\frac{\partial}{\partial x}\left(K \frac{\partial \psi}{\partial x} \right) = \frac{\partial K}{\partial x}\frac{\partial \psi}{\partial x} + K \frac{\partial^2 \psi}{\partial x^2} \qquad 3.13$$

$$\frac{\partial K}{\partial x} = \frac{\partial K}{\partial \xi}\frac{\partial \xi}{\partial x} + \frac{\partial K}{\partial \eta}\frac{\partial \eta}{\partial x} \qquad 3.14$$

$$\frac{\partial \psi}{\partial x} = \frac{\partial \psi}{\partial \xi}\frac{\partial \xi}{\partial x} + \frac{\partial \psi}{\partial \eta}\frac{\partial \eta}{\partial x} \qquad 3.15$$

$$\frac{\partial \psi}{\partial x}\frac{\partial K}{\partial x} = \left(\frac{\partial \psi}{\partial \xi}\frac{\partial \xi}{\partial x} + \frac{\partial \psi}{\partial \eta}\frac{\partial \eta}{\partial x} \right)\left(\frac{\partial K}{\partial \xi}\frac{\partial \xi}{\partial x} + \frac{\partial k}{\partial \eta}\frac{\partial \eta}{\partial x} \right)$$

$$= \left[\frac{\partial K}{\partial \xi}\left(\frac{\partial \xi}{\partial x}\right)^2 + \frac{\partial K}{\partial \eta}\frac{\partial \eta}{\partial x}\frac{\partial \xi}{\partial x}\right]\frac{\partial \psi}{\partial \xi} + \left[\frac{\partial K}{\partial \eta}\left(\frac{\partial \eta}{\partial x}\right)^2 + \frac{\partial K}{\partial \xi}\frac{\partial \xi}{\partial x}\frac{\partial \eta}{\partial x}\right]\frac{\partial \psi}{\partial \eta} \quad 3.16$$

$$\frac{\partial}{\partial z}\left(K\frac{\partial \psi}{\partial z}\right) = \frac{\partial K}{\partial z}\frac{\partial \psi}{\partial z} + K\frac{\partial^2 \psi}{\partial z^2} \quad 3.17$$

Figure below shows the transformation from x-z coordinate to ζ and η

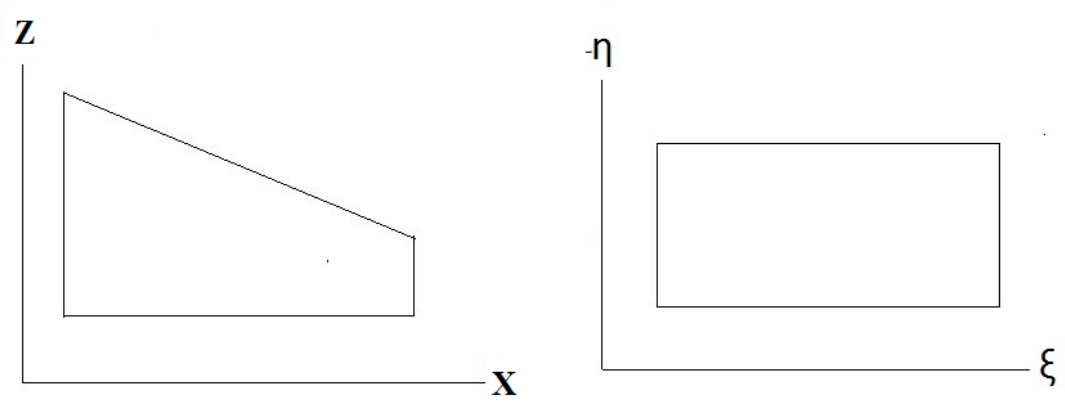

Figure 3.1 Transformation of grid from (x,z) to (ζ,η)

$$\frac{\partial K}{\partial z} = \frac{\partial K}{\partial \xi}\frac{\partial \xi}{\partial z} + \frac{\partial K}{\partial \eta}\frac{\partial \eta}{\partial z} \quad 3.18$$

$$\frac{\partial \psi}{\partial z} = \frac{\partial \psi}{\partial \xi}\frac{\partial \xi}{\partial z} + \frac{\partial \psi}{\partial \eta}\frac{\partial \eta}{\partial z} \quad 3.19$$

$$\frac{\partial \psi}{\partial z}\frac{\partial K}{\partial z} = \left(\frac{\partial \psi}{\partial \xi}\frac{\partial \xi}{\partial z} + \frac{\partial \psi}{\partial \eta}\frac{\partial \eta}{\partial z}\right)\left(\frac{\partial K}{\partial \xi}\frac{\partial \xi}{\partial z} + \frac{\partial K}{\partial \eta}\frac{\partial \eta}{\partial z}\right)$$

$$= \left[\frac{\partial K}{\partial \xi}\left(\frac{\partial \xi}{\partial z}\right)^2 + \frac{\partial K}{\partial \eta}\frac{\partial \eta}{\partial z}\frac{\partial \xi}{\partial z}\right]\frac{\partial \psi}{\partial \xi} + \left[\frac{\partial K}{\partial \eta}\left(\frac{\partial \eta}{\partial z}\right)^2 + \frac{\partial K}{\partial \xi}\frac{\partial \xi}{\partial z}\frac{\partial \eta}{\partial z}\right]\frac{\partial \psi}{\partial \eta} \quad 3.20$$

$$K\left(\frac{\partial^2 \psi}{\partial x^2} + \frac{\partial^2 \psi}{\partial z^2}\right) = K\frac{\partial^2 \psi}{\partial \xi^2}\left[\left(\frac{\partial \xi}{\partial x}\right)^2 + \left(\frac{\partial \xi}{\partial y}\right)^2\right] + K\frac{\partial^2 \psi}{\partial \eta^2}\left[\left(\frac{\partial \eta}{\partial x}\right)^2 + \left(\frac{\partial \eta}{\partial y}\right)^2\right] +$$

$$2K\frac{\partial^2 \psi}{\partial \xi \partial \eta}\left[\left(\frac{\partial \eta}{\partial x}\right)\left(\frac{\partial \xi}{\partial x}\right) + \left(\frac{\partial \eta}{\partial y}\right)\left(\frac{\partial \xi}{\partial y}\right)\right] + K\frac{\partial \psi}{\partial \xi}\left(\frac{\partial^2 \xi}{\partial x^2} + \frac{\partial^2 \xi}{\partial y^2}\right) + K\frac{\partial \psi}{\partial \eta}\left(\frac{\partial^2 \eta}{\partial x^2} + \frac{\partial^2 \eta}{\partial y^2}\right)$$

3.21

$$\frac{\partial K}{\partial z} = \frac{\partial K}{\partial \eta}\frac{\partial \eta}{\partial z} + \frac{\partial K}{\partial \xi}\frac{\partial \xi}{\partial z} \tag{3.22}$$

Now, in the above expressions,

$$a = \left[\frac{\partial K}{\partial \xi}\left(\frac{\partial \xi}{\partial x}\right)^2 + \frac{\partial K}{\partial \eta}\frac{\partial \eta}{\partial x}\frac{\partial \xi}{\partial x}\right] \tag{3.23}$$

$$b = \left[\frac{\partial K}{\partial \eta}\left(\frac{\partial \eta}{\partial x}\right)^2 + \frac{\partial K}{\partial \xi}\frac{\partial \xi}{\partial x}\frac{\partial \eta}{\partial x}\right] \tag{3.24}$$

$$c = K\left[\left(\frac{\partial \xi}{\partial x}\right)^2 + \left(\frac{\partial \xi}{\partial y}\right)^2\right] \tag{3.25}$$

$$d = K\left[\left(\frac{\partial \eta}{\partial x}\right)^2 + \left(\frac{\partial \eta}{\partial y}\right)^2\right] \tag{3.26}$$

$$aa = 2K\left[\left(\frac{\partial \eta}{\partial x}\right)\left(\frac{\partial \xi}{\partial x}\right) + \left(\frac{\partial \eta}{\partial y}\right)\left(\frac{\partial \xi}{\partial y}\right)\right] \tag{3.27}$$

$$bb = K\left(\frac{\partial^2 \xi}{\partial x^2} + \frac{\partial^2 \xi}{\partial y^2}\right) \tag{3.28}$$

$$cc = K\left(\frac{\partial^2 \eta}{\partial x^2} + \frac{\partial^2 \eta}{\partial y^2}\right) \tag{3.29}$$

$$pp = \left[\frac{\partial K}{\partial \xi}\left(\frac{\partial \xi}{\partial z}\right)^2 + \frac{\partial K}{\partial \eta}\frac{\partial \eta}{\partial z}\frac{\partial \xi}{\partial z}\right] \tag{3.30}$$

$$qq = \left[\frac{\partial K}{\partial \eta}\left(\frac{\partial \eta}{\partial z}\right)^2 + \frac{\partial K}{\partial \xi}\frac{\partial \xi}{\partial z}\frac{\partial \eta}{\partial z}\right] \tag{3.31}$$

$$rr = \frac{\partial K}{\partial \eta}\frac{\partial \eta}{\partial z} + \frac{\partial K}{\partial \xi}\frac{\partial \xi}{\partial z} \tag{3.32}$$

Thus, final expression of Richards equation after grid transformation is

$$\frac{\partial \theta}{\partial t} = \left(a + pp + bb\right)\frac{\partial \psi}{\partial \xi} + \left(b + qq + cc\right)\frac{\partial \psi}{\partial \eta} + c\frac{\partial^2 \psi}{\partial \xi^2} + d\frac{\partial^2 \psi}{\partial \eta^2} + aa\frac{\partial^2 \psi}{\partial \xi \partial \eta} + rr \qquad 3.33$$

3.4 Coupling of all the governing equation:

A detailed discussion of the governing equations has been presented in the above sections. Saint- Venant equation has been used to describe the free surface flow in the river; water infiltrated through the piedmont zone has been calculated by the Green-Ampt. infiltration equation, and the movement of this infiltrated water has been described by Richards equation. These three equations are linked via exchange of flux f and water depth h obtained from free surface flow equation, infiltration rate f is calculated by Green Ampt equation and is used as the input flux for the Richards equation. The computed f is used in the free surface model as the source term to compute the new values of flow parameter and the process is repeated. The contribution of ground water to the surface flow is considered from the time when the infiltrated water again emerged as the surface water at a downstream point. A flow chart related to coupling of these equations is presented in fig 3.2.

3.5 Conclusion

In this chapter, the governing equations for the development of the mathematical model considering groundwater recharge zone have been discussed. For developing this model, three governing equations- shallow water equation for unsteady flow, Green-Ampt. infiltration equation for infiltration model and Richard equation for groundwater movement have been considered. As the computational domain, below the river is not of rectangular shape, therefore, Richards equation has been derived for the grid transformation from.

Flow chart for coupled free surface flow- infiltration-subsurface flow model

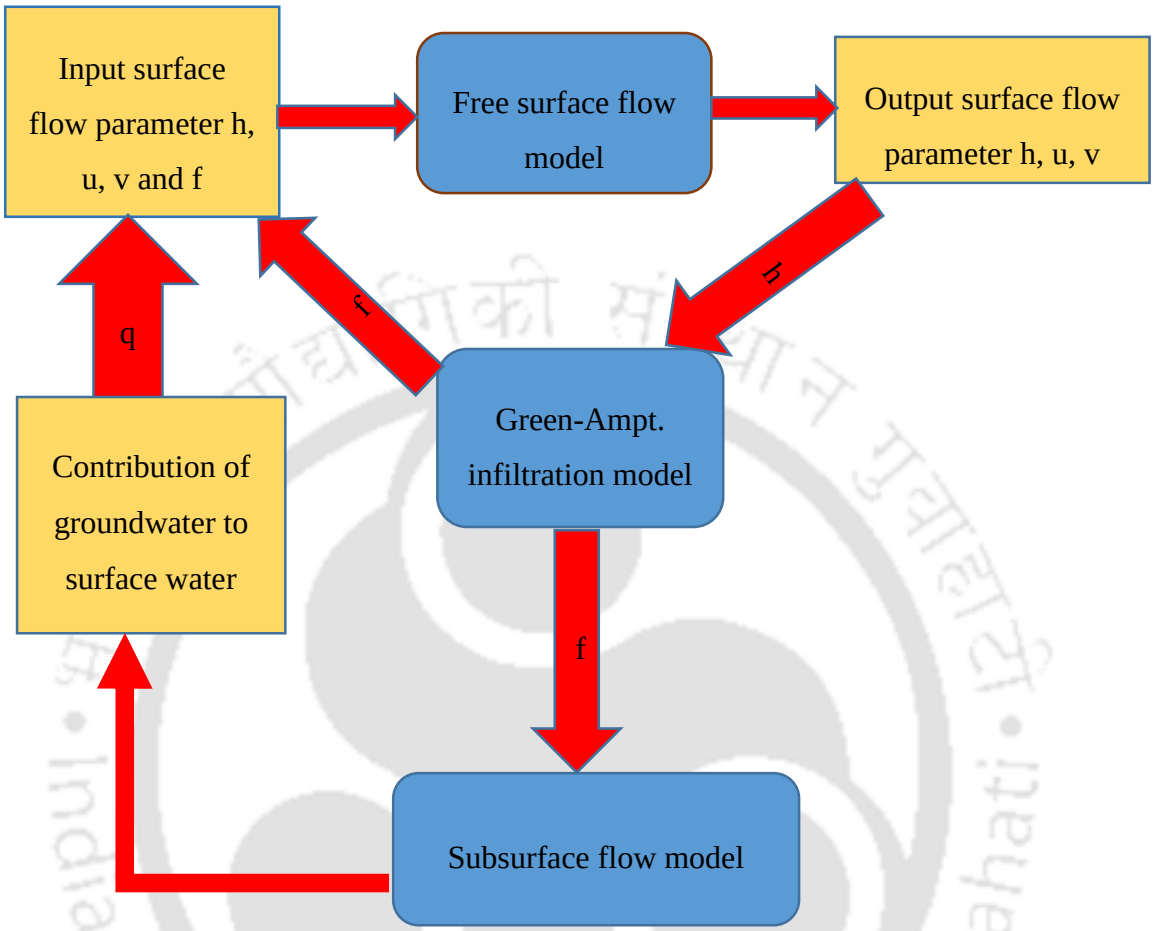

Figure 3.2 flow chart for coupling of all three models

Chapter 4

Solution of Governing Equation

4.1 Introduction

This chapter deals with the solution of the governing equations. The 1-D and 2-D continuity and momentum equations used in this study are a set of hyperbolic equations. These equations are nonlinear partial differential equations, which are not amenable to analytical solution except for very simplified cases. Previously, a numbers of numerical methods have been used by different researchers to approximate the Saint-Venant equation. Characteristic equation, finite difference, finite element and finite volume are the numerical methods used for numerical integration of Saint-Venant equation. Out of all these schemes, finite difference schemes are extensively used by the researchers due to its ease of application and programming and also for giving satisfactory results in different hydrodynamic problems.

Richards equation, which is used to study the moisture content, is a nonlinear parabolic equation and cannot be solved analytically without simplification. Again, simplification gives erroneous results. Hence, it is better to solve the equation numerically. As Richards equation is highly nonlinear, the explicit solutions does not generating true results, unless sufficiently small discretization in time is made for a decided space discretization to maintain stability. So, researchers are using various implicit finite difference methods for the solution of the equation.

In the following section, a detailed discussion about the solution of governing equations is presented. As the nature of the governing equations is different e.g. Saint- Venant equation is hyperbolic and Richards equation is parabolic in nature, therefore, same numerical scheme may not be suitable in respect of accuracy and computational time. Each of the governing equations is therefore solved separately using numerical scheme that is suitable for its solution, and thereafter necessary parameters from one model are used as the input for the other model. A flow chart regarding coupling of these model was discussed in previous chapter.

4.2 Numerical formulation of free surface flow model by finite difference method

In Saint-Venant as well as in some other non-linear partial difference equations, among all the numerical methods, finite difference methods have been extensively used by the investigators. Finite difference schemes are of two types- explicit scheme and implicit scheme. In finite difference scheme for solving partial differential equation, the calculations are performed on a grid, placed over x-y-t plane. The x- y-t grid is a network of point defined by taking the distance increments of length Δx and Δy, and the time increments of duration Δt. The x and y directions are designated by the subscripts i and j respectively and the t direction is designated by the subscript k. Flow variable at known time level is denoted by subscript k and that in unknown time level by k+1. A detailed sketch about the space and time discretization of the finite difference method is shown in fig 4.1

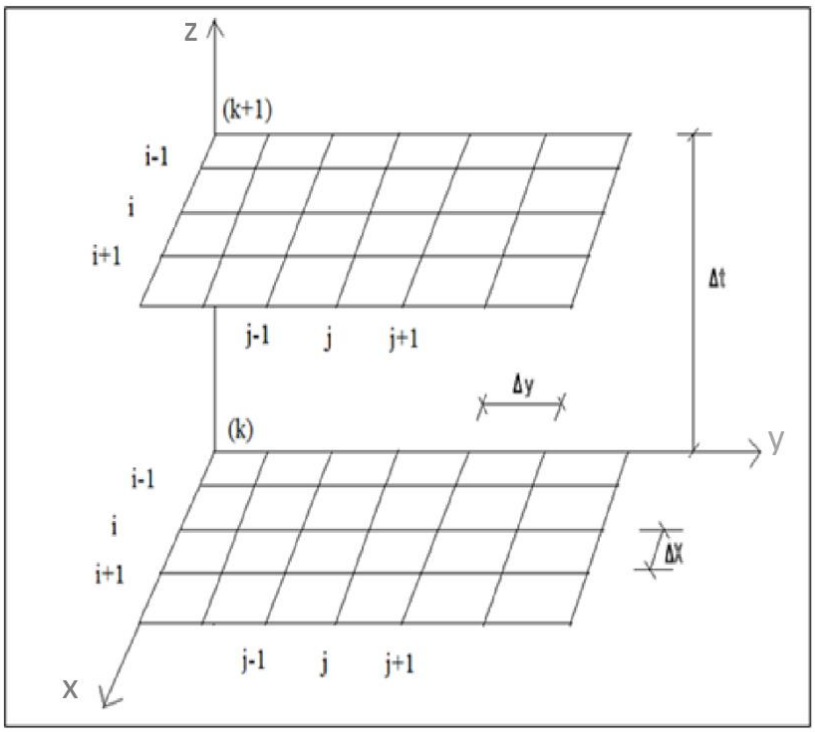

Figure 4.1 Finite difference Method

Though the explicit schemes are relatively simple to set up and program, the main disadvantage of explicit schemes is time step limit, i.e. for the explicit approach, once the Δx is chosen, Δt is not an independent and arbitrary choice; rather Δt is restricted to be equal to or less than a certain value prescribed by the stability criterion. In many cases,

very small time step is maintained for stability resulting large computer running time to complete the calculation over a given time interval. However, for the implicit scheme, one can go for much larger time step than that for the explicit scheme. Therefore, use of implicit scheme reduces the time step in comparison to the explicit scheme.

4.2.1 Beam and Warming implicit scheme

In the implicit finite-difference schemes, the spatial partial derivatives and the coefficient are replaced in terms of the values at unknown time level. Beam and Warming (1976) developed them for the solution of hyperbolic system in conservation-law form and they have been used in computational fluid dynamics. The scheme is non-iterative, which results in considerable saving in computation time, spatially in multidimensional problem. This scheme is an implicit scheme, which is second order accurate in time and can be made second or fourth order accurate in space.

Later, various researchers e.g. Molls et al. (1995), Molls and Zhao (2000), Kassem and Chaudhry (2005) and Kalita et.al (2014) applied this scheme for the solution of unsteady free surface flow problem and found satisfactory results.

4.2.1.1 Formulation of 1-D Saint-Venant equation with Beam and Warming implicit scheme

Beam and Warming scheme used in this study is described below (Chaudhry, 2008)

$$\left[I + \frac{\Delta t}{2}\left(\frac{\partial P}{\partial x} + B \right)^{k} \right] \Delta_t U^{k+1} = -\Delta t \left(\frac{\partial E}{\partial x} + S \right)^{k} \qquad 4.1$$

where I is the identity matrix, P and B are the Jacobians of E and S respectively and given as

$$P = \begin{pmatrix} 0 & 1 \\ gD - u^2 & 2u \end{pmatrix} \qquad B = \begin{pmatrix} 0 & 0 \\ \left(-gS_0 - 1.33gn^2u|u|\right)/R^{1.33} & gn^2|u|/R^{1.33} \end{pmatrix} \qquad 4.2$$

For correct signal transmission, the matrix P and E may be split as

$$P = P^+ + P^-,\ E = E^+ + E^- \qquad 4.3$$

where $P^+ = MD^+M^{-1}$; $P^- = MD^-M^{-1}$; $E_x^+ = P^+U_x$; $E_x^- = P^-U_x$

$D = \begin{pmatrix} u+c & 0 \\ 0 & u-c \end{pmatrix}$ is the diagonal matrix of Eigen values of P and

$$M = \begin{pmatrix} 1/(2c) & -1/(2c) \\ (u+c)/(2c) & -(u-c)/(2c) \end{pmatrix} \quad 4.4$$

Substituting the values of eq. (4.3) into eq. (4.1)

$$\left[I + \frac{\Delta t}{2} \left\{ \frac{\partial}{\partial x} \left(P^{+} + P^{-} \right) + B \right\}^{k} \right] \Delta_t U^{k+1} = -\Delta t \left[\frac{\partial}{\partial x} \left(E^{+} + E^{-} \right) + S \right]^{k} \quad 4.5$$

Finite Difference form of equation (4.5) may be written as

$$\left[I + \frac{1}{2} \frac{\Delta t}{\Delta x} \left\{ \left(\nabla_x P^{+} + \Delta_x P^{-} \right) + \frac{\Delta t}{2} B_i \right\}^{k} \right] \Delta_t U^{k+1} = -\frac{\Delta t}{\Delta x} \left[P_i^{+} \nabla_x U + P_i^{-} \Delta_x U \right]^{k} - \Delta t S_i^{k} \quad 4.6$$

where, $\nabla_x P^{+} = P_i^{+} - P_{i-1}^{+}$ and $\Delta_x P^{-} = P_{i+1}^{-} - P_i^{-}$.

The left-hand side of eq. (4.6) constitutes the block tridiagonal system for each time step which is solved by using Thomas algorithm.

4.2.1.2 Formulation of 2-D Saint- Venant equation with Beam and Warming implicit scheme

2-D Saint- Venant equation from eq 3.1

$$U_t + E_x + F_y + S = 0$$

The system of eq. 3.1 may be solved by using time-difference approximations of the general form

$$U^{k+1} = U^{k} - \Delta t \left[\frac{\gamma}{1+\mu} \left(\frac{\partial U}{\partial t} \right)^{k+1} + \frac{1-\gamma}{1+\mu} \left(\frac{\partial U}{\partial t} \right)^{k} + \frac{\mu}{1+\mu} \left(\frac{\partial U}{\partial t} \right)^{k-1} \right] \quad 4.7$$

In which γ and μ are the parameters leading to a variety of scheme. Substituting for $\frac{\partial U}{\partial t}$ in terms of source and flux terms E, F, S yields

$$U^{k+1} = U^k - \Delta t\left[\frac{\gamma}{1+\mu}\left(\frac{\partial E}{\partial x}+\frac{\partial F}{\partial y}+s\right)^{k+1}+\frac{1-\gamma}{1+\mu}\left(\frac{\partial E}{\partial x}+\frac{\partial F}{\partial y}+s\right)^{k}\right]+\frac{\mu\Delta t}{1+\mu}\left(\frac{\partial U}{\partial t}\right)^{k-1} \qquad 4.8$$

Using local Taylor series expansion for E, F, S yields

$$E^{k+1} = E^k + A^k\left(U^{k+1}-U^k\right) \quad F^{k+1} = F^k + BB^k\left(U^{k+1}-U^k\right) \quad S^{k+1} = S^k + Q^k\left(U^{k+1}-U^k\right) \qquad 4.9$$

Where A, BB and Q are the jacobian of E, F and S respectively

$$A = \frac{\partial E}{\partial U} \qquad BB = \frac{\partial F}{\partial U} \qquad Q = \frac{\partial S}{\partial U} \qquad 4.10$$

Putting the values eq. 4.9 and eq. 4.10 in eq. 4.7

$$U^{k+1} = U^k - \left[\begin{array}{l}\frac{\gamma}{1+\mu}\left(\frac{\partial}{\partial x}A^kU^{k+1}+\frac{\partial}{\partial y}B^kU^{k+1}+Q^kU^{k+1}\right)\\ -\frac{\gamma}{1+\mu}\left(\frac{\partial}{\partial x}A^kU^{k}+\frac{\partial}{\partial y}B^kU^{k}+Q^kU^{k}\right)+\frac{1}{1+\mu}\left(\frac{\partial E}{\partial x}+\frac{\partial F}{\partial y}+S\right)^k\end{array}\right]+\Delta t\frac{\mu}{1+\mu}\left(\frac{\partial U}{\partial t}\right)^{k-1}$$

Transposing the dependent variable at advanced time level to the left hand side of this equation yields a linear system for U^{k+1}

$$\left[I+\Delta t\frac{\gamma}{1+\mu}\left(\frac{\partial}{\partial x}A^k+\frac{\partial}{\partial y}B^k+Q^k\right)\right]U^{k+1}$$

$$=\left[I+\Delta t\frac{\gamma}{1+\mu}\left(\frac{\partial}{\partial x}A^k+\frac{\partial}{\partial y}B^k+Q^k\right)\right]U^k - \Delta t\frac{1}{1+\mu}\left(\frac{\partial E}{\partial x}+\frac{\partial F}{\partial y}+S\right)^k+\Delta t\frac{\mu}{1+\mu}\left(\frac{\partial U}{\partial t}\right)^{k-1} \qquad 4.11$$

where, I is the identity matrix. By using forward difference operator $\Delta_t U^{k+1} = U^{k+1} - U^k$ eq. 4.7 becomes

$$\left[I+\Delta t\frac{\gamma}{1+\mu}\left(\frac{\partial}{\partial x}A^k+\frac{\partial}{\partial y}B^k+Q^k\right)\right]\Delta_t U^{k+1} = -\Delta t\frac{1}{1+\mu}\left(\frac{\partial E}{\partial x}+\frac{\partial F}{\partial y}+S\right)^k+\frac{\mu}{1+\mu}\Delta_t U^k$$

4.12

The above algorithm is said to be in delta form, the flow variable, U, exist only in increments of U between two time levels. The principal advantage of this formulation is the computational efficiency due to reduction in number of terms.

$U_{i,j}^{k+1}$ is obtained by adding $\Delta_t U^k$ to $U_{i,j}^{k}$ values for the last time step values. The flow variables obtained from this sequence are in the form h, uh and vh. The primitive flow variables h, u and v are then obtained by solving the following equations

$$h_{i,j}^{k+1} = h_{i,j}^{k} + \Delta_t h_{i,j}^{k+1}$$

$$u_{i,j}^{k+1} = \frac{(uh)_{i,j}^{k} + \Delta_t (uh)_{i,j}^{k+1}}{h_{i,j}^{k+1}}$$

$$v_{i,j}^{k+1} = \frac{(vh)_{i,j}^{k} + \Delta_t (vh)_{i,j}^{k+1}}{h_{i,j}^{k+1}}$$

4.2.2 Artificial viscosity

The solution obtained by a finite- difference scheme has a dissipative error if the leading term of the truncation errors in the scheme has even derivatives and the solution has dispersive errors if the leading term has odd derivatives. The dispersive errors usually produce oscillations in the computed results in the vicinity of steep wave fronts. These oscillations are purely due to numerical errors and have nothing to do with the physical phenomenon being simulated. To smooth these oscillations, the artificial viscosity is added to the scheme. Artificial viscosity model is used in the Beam and Warming scheme by adding the following equation to the RHS of eq. 4.12

$$Av = CT\left[\left(L_{i,j+1}^{k+1} - 2L_{i,j}^{k+1} + L_{i,j-1}^{k+1}\right) + \left(L_{i+1,j}^{k+1} - 2L_{i,j}^{k+1} + L_{i-1,j}^{k+1}\right)\right]$$

For one dimensional flow the following term is added to the RHS of the eq. 4.6

$$Av = CT\left[\left(L_{i+1}^{k+1} - 2L_{i,j}^{k+1} + L_{i-1}^{k+1}\right)\right]$$

In this case, *CT* is the regulating coefficient in the order of (0-0.4)

4.3 Numerical solution of Richards equation

Richards equations are highly nonlinear equation and analytical solution is not possible except for special cases. Finite difference and finite element are the most common numerical methods to solve nonlinear equation. For infiltration into dry soil, finite element method shows oscillatory solution. Different researchers showed that explicit scheme is not suitable to solve Richards equation and from the literature, it is observed that different implicit schemes were used by the investigator (Perrens and Watson 1977, Celia et al. 1990, Lim and Lee 1993, Hanks and Bowers1962). It is found from the literature that Alternate Direction Implicit (ADI) scheme was used by different researchers to solve one dimensional Richards equation and 2-D pressure based Richards equation (Cooley 1971, Parissopoulos and Wheater 1988, Perrens and Watson 1977, Weeks et al. 2004) and yield satisfactory results. In this model this scheme is applied to solve the 2-D mixed form Richards equation.

4.3.1 Formulation of 2-D Richards equation by Alternate Direction Implicit scheme

The numerical discretization of this equation by finite difference method leads to a nonlinear set of equation. Gottardi and Venutelli (1993) derived the finite difference approximation of 1-D Richards equation with the help of ADI scheme. Researchers (Cooley in 1971, Weeks et al. in 2004, Clement et al. in 1994, H, An et al. in 2011) have used Iterative Alternate Direction Implicit (IADI) scheme for solution of 2-D and 3-D Richards equation. This scheme is time consuming because of its iterative nature. To reduce computational time, non-iterative Alternate Direction Implicit scheme (ADI) which has been used by different researchers (Anderson 1995, LeVeque in 2005, Paceman and Rachford 1955, Strang 1968) to solve other parabolic equation is used in this study to solve 2-D Richards equation and the step involved in deriving the 2- D Richards equation by ADI scheme is discussed below. Finite difference discretization of Richards equation is

$$\frac{\theta_{i,j}^{k+1,m+1}-\theta_{i,j}^{n}}{\Delta t}=\frac{K_{i-1/2,j}^{k+1,m+1/2}}{(\Delta z)^2}\left(\psi_{i-1,j}^{k+1,m+1/2}-\psi_{i,j}^{k+1,m+1/2}\right)+\frac{K_{i+1/2}^{k+1,m+1/2}}{(\Delta z)^2}\left(\psi_{i+1,j}^{k+1,m+1/2}-\psi_{i,j}^{k+1,m+1/2}\right)$$

$$+\frac{K_{i,j-1/2}^{k+1,m+1/2}}{(\Delta x)^2}\left(\psi_{i,j-1}^{k+1,m+1}-\psi_{i,j}^{k+1,m+1}\right)+\frac{K_{i,j+1/2}^{k+1,m+1/2}}{(\Delta x)^2}\left(\psi_{i,j+1}^{k+1,m+1}-\psi_{i,j}^{k+1,m+1}\right)-\frac{K_{i+1/2,j}^{k+1,m+1/2}-K_{i-1/2,j}^{k+1,m+1/2}}{\Delta z} \quad 4.3.1$$

$$\theta_{i,j}^{k+1,m+1} = \theta_{i,j}^{k+1,m} + \frac{d\theta}{dh}\left(\psi_{i,j}^{k+1,m+1} - \psi_{i,j}^{k+1,m}\right) + 0(\delta^2) \qquad 4.3.2$$

$$\frac{d\theta}{dh} = c \text{ and } \delta_{i,j}^{k+1,m} = \left(\psi_{i,j}^{k+1,m+1} - \psi_{i,j}^{k+1,m}\right)$$

Substituting the value of eq.4.3.2 into eq.4.3.1, it results

$$\left(\frac{1}{\Delta t}c_{i,j}^{k+1,m}\right)\delta_{i,j}^{k+1,m} + \frac{\theta_{i,j}^{k+1,m} - \theta_{i,j}^{k}}{\Delta t} = \frac{K_{i-1/2,j}^{k+1,m}}{(\Delta z)^2}\left(\psi_{i-1,j}^{k+1,m+1} - \psi_{i,j}^{k+1,m+1}\right) + \frac{K_{i+1/2}^{k+1,m}}{(\Delta z)^2}\left(\psi_{i+1,j}^{k+1,m+1} - \psi_{i,j}^{k+1,m+1}\right)$$
$$+ \frac{K_{i,j-1/2}^{k+1,m}}{(\Delta x)^2}\left(\psi_{i,j-1}^{k+1,m+1} - \psi_{i,j}^{k+1,m+1}\right) + \frac{K_{i,j+1/2}^{k+1,m}}{(\Delta x)^2}\left(\psi_{i,j+1}^{k+1,m+1} - \psi_{i,j}^{k+1,m+1}\right) - \frac{K_{i+1/2,j}^{k+1,m} - K_{i-1/2,j}^{k+1,m}}{\Delta z} \qquad 4.3.3$$

The coefficient matrix generated from above equation is pentadiagonal. The solution procedure for the pentadiagonal system of equation is very time-consuming. To overcome this difficulty, the alternate direction implicit method or ADI method is used. This algorithm produces two sets of tridiagonal simultaneous equations to be solved in sequence, which is shown in eq. 4.3.3(ii) and eq. 4.3.3(iv).

$$\left(\frac{1}{\Delta t}c_{i,j}^{k+1,m}\right)\delta_{i,j}^{k+1,m+1/2} + \frac{K_{i,j-1/2}^{k+1,m}}{(\Delta x)^2}\left(\delta_{i,j-1}^{k+1,m+1/2} - \delta_{i,j}^{k+1,m+1/2}\right) + \frac{K_{i,j+1/2}^{k+1,m}}{(\Delta x)^2}\left(\delta_{i,j+1}^{k+1,m+1/2} - \delta_{i,j}^{k+1,m+1/2}\right)$$
$$= \frac{K_{i-1/2,j}^{k+1,m}}{(\Delta z)^2}\left(\psi_{i-1,j}^{k+1,m} - \psi_{i,j}^{k+1,m}\right) + \frac{K_{i+1/2,j}^{k+1,m}}{(\Delta z)^2}\left(\psi_{i+1,j}^{k+1,m} - \psi_{i,j}^{k+1,m}\right) + \frac{K_{i,j-1/2}^{k+1,m}}{(\Delta x)^2}\left(\psi_{i,j-1}^{k+1,m} - \psi_{i,j}^{k+1,m}\right) \qquad 4.3.3(i)$$
$$+ \frac{K_{i,j+1/2}^{k+1,m}}{(\Delta x)^2}\left(\psi_{i,j+1}^{k+1,m} - \psi_{i,j}^{k+1,m}\right) - \frac{\theta_{i,j}^{k+1,m} - \theta_{i,j}^{k}}{\Delta t} - \frac{K_{i+1/2,j}^{k+1,m} - K_{i-1/2,j}^{k+1,m}}{\Delta z}$$

$$\alpha\alpha_{i,j}^{k+1,m}\delta_{i,j-1}^{k+1,m+1/2} + \beta_{i,j}^{k+1,m}\delta_{i,j}^{k+1,m+1/2} + \gamma\gamma_{i,j}^{k+1,m}\delta_{i,j+1}^{k+1,m+1/2} = RR_{i,j}^{k+1,m} \qquad 4.3.3(ii)$$

where

$$\alpha\alpha_{i,j}^{k+1,m} = \frac{K_{i-1/2,j}^{k+1,m}}{(\Delta z)^2}$$

$$\beta_{i,j}^{k+1,m} = \frac{1}{\Delta t} c_{i,j}^{k+1,m} - \frac{K_{i-1/2,j}^{k+1,m}}{(\Delta z)^2} - \frac{K_{i+1/2,j}^{k+1,m}}{(\Delta z)^2}$$

$$\gamma\gamma_{i,j}^{k+1,m} = \frac{K_{i+1/2,j}^{k+1,m}}{(\Delta z)^2}$$

$$RR_{i,j}^{k+1,m} = \frac{K_{i-1/2,j}^{k+1,m}}{(\Delta z)^2}\left(\psi_{i-1,j}^{k+1,m} - \psi_{i,j}^{k+1,m}\right) + \frac{K_{i+1/2,j}^{k+1,m}}{(\Delta z)^2}\left(\psi_{i+1,j}^{k+1,m} - \psi_{i,j}^{k+1,m}\right) + \frac{K_{i,j-1/2}^{k+1,m}}{(\Delta x)^2}\left(\psi_{i,j-1}^{k+1,m} - \psi_{i,j}^{k+1,m}\right)$$

$$+ \frac{K_{i,j+1/2}^{k+1,m}}{(\Delta x)^2}\left(\psi_{i,j+1}^{k+1,m} - \psi_{i,j}^{k+1,m}\right) - \frac{\theta_{i,j}^{k+1,m} - \theta_{i,j}^{k}}{\Delta t} - \frac{K_{i+1/2,j}^{k+1,m} - K_{i-1/2,j}^{k+1,m}}{\Delta z}$$

$$\left(\frac{1}{\Delta t} c_{i,j}^{k+1,m+1/2}\right)\delta_{i,j}^{k+1,m+1} + \frac{K_{i-1/2,j}^{k+1,m+1/2}}{(\Delta z)^2}\left(\delta_{i-1,j}^{k+1,m+1} - \delta_{i,j}^{k+1,m+1}\right) + \frac{K_{i+1/2}^{k+1,m+1/2}}{(\Delta z)^2}\left(\delta_{i+1,j}^{k+1,m+1} - \delta_{i,j}^{k+1,m+1}\right)$$

$$= \frac{K_{i-1/2,j}^{k+1,m+1/2}}{(\Delta z)^2}\left(\psi_{i-1,j}^{k+1,m+1/2} - \psi_{i,j}^{k+1,m+1/2}\right) + \frac{K_{i+1/2}^{k+1,m+1/2}}{(\Delta z)^2}\left(\psi_{i+1,j}^{k+1,m+1/2} - \psi_{i,j}^{k+1,m+1/2}\right)$$

$$+ \frac{K_{i,j-1/2}^{k+1,m+1/2}}{(\Delta x)^2}\left(\psi_{i,j-1}^{k+1,m+1/2} - \psi_{i,j}^{k+1,m+1/2}\right) + \frac{K_{i,j+1/2}^{k+1,m+1/2}}{(\Delta x)^2}\left(\psi_{i,j+1}^{k+1,m+1/2} - \psi_{i,j}^{k+1,m+1/2}\right)$$

$$- \frac{\theta_{i,j}^{k+1,m+1/2} - \theta_{i,j}^{n}}{\Delta t} - \frac{K_{i+1/2,j}^{k+1,m+1/2} - K_{i-1/2,j}^{k+1,m+1/2}}{\Delta z} \qquad 4.3.3(iii)$$

$$\alpha\alpha_{i,j}^{k+1,m}\delta_{i-1,j}^{k+1,m+1} + \beta_{i,j}^{k+1,m+1/2}\delta_{i,j}^{k+1,m+1} + \gamma\gamma_{i,j}^{k+1,m+1/2}\delta_{i+1,j}^{k+1,m+1} = RR_{i,j}^{k+1,m+1/2} \qquad 4.3.3\ (iv)$$

$$\alpha\alpha_{i,j}^{k+1,m+1/2} = \frac{K_{i-1/2,j}^{k+1,m+1/2}}{(\Delta z)^2}$$

$$\beta_{i,j}^{k+1,m+1/2} = \frac{1}{\Delta t} c_{i,j}^{k+1,m+1/2} - \frac{K_{i-1/2,j}^{k+1,m+1/2}}{(\Delta z)^2} - \frac{K_{i+1/2,j}^{k+1,m+1/2}}{(\Delta z)^2}$$

$$\gamma\gamma_{i,j}^{k+1,m+1/2} = \frac{K_{i+1/2,j}^{k+1,m+1/2}}{(\Delta z)^2}$$

$$RR_{i,j}^{k+1,m+1/2} = \frac{K_{i-1/2,j}^{k+1,m+1/2}}{(\Delta z)^2}\left(\psi_{i-1,j}^{k+1,m+1/2} - \psi_{i,j}^{k+1,m+1/2}\right) + \frac{K_{i+1/2}^{k+1,m+1/2}}{(\Delta z)^2}\left(\psi_{i+1,j}^{k+1,m+1/2} - \psi_{i,j}^{k+1,m+1/2}\right) + \frac{K_{i,j-1/2}^{k+1,m+1/2}}{(\Delta x)^2}\left(\psi_{i,j-1}^{k+1,m+1/2} - \psi_{i,j}^{k+1,m+1/2}\right)$$
$$+ \frac{K_{i,j+1/2}^{k+1,m+1/2}}{(\Delta x)^2}\left(\psi_{i,j+1}^{k+1,m+1/2} - \psi_{i,j}^{k+1,m+1/2}\right) - \frac{\theta_{i,j}^{k+1,m+1/2} - \theta_{i,j}^{k}}{\Delta t} - \frac{K_{i+1/2,j}^{k+1,m+1/2} - K_{i-1/2,j}^{k+1,m+1/2}}{\Delta z}$$

where $\delta_{i,j}^{n+1,m+1} = h_{i,j}^{n+1,m+1} - h_{i,j}^{n+1,m}$

The solution procedure starts with the solution of the tridiagonal system (Eq. 4.3.3 (ii)).The formulation of eq. 4.3.3(ii) is implicit in the x-direction and explicit in the z-direction; thus the solution at this stage is referred to as x sweep. Solving the tridiagonal system of eq. 4.3.3 (ii) provides the necessary data for right-hand side of eq. 4.3.3 (iv) to solve the tridiagonal system of eq. 4.3.3 (iv). In this equation, the finite difference equation is implicit in the z-direction and explicit in the x-direction and it is referred as the z sweep.

4.4 Conclusion

In this chapter, we have discussed the solution of the governing equation. The governing equations are nonlinear in nature and therefore exact solutions are very difficult if not impossible. Therefore, numerical methods are used for the solution of the governing equations. The equations are first solved separately with different numerical methods which are suitable. Beam and Warming implicit finite difference scheme has been applied for solution of the shallow water equation coupled with Green-Ampt. infiltration equation. This method is not time-consuming like other implicit methods as it does not involve iteration process. Again, for the solution of the Richards equation, ADI scheme is used. Therefore, in this chapter, a brief discussion about the formulation of the Beam and Warming scheme for Saint-Venant equation and the ADI scheme for Richards equation are presented and based on this discussion, numerical forms to be used in this study are confirmed.

Chapter 5

Model Development and Validation

5.1 Introduction

This chapter contains the development of coupled surface–subsurface flow model considering piedmont zone in the river bed. The model was first developed by using the governing equations, discussed in chapter 3 and solution of the governing equations were made as per the numerical method discussed in the chapter 4. The boundary conditions and the initial conditions used for developing the model are discussed in this section**.** After development of the individual models, they are linked via exchange of flux and details of the same is discussed in this chapter. Model validation is presented towards end of this chapter.

5.2 Development of free surface flow model

5.2.1 Initial condition

A two-dimensional unsteady flow model is developed considering the infiltration zone in the river bed. The assumptions of the governing equations are considered during the development of the model. In the development of mathematical model one needs to clearly state all those sensible assumptions, which are essential for model implementation in a real river and yet provide useful result. The channel with piedmont zone has been considered as straight one with mild slope. To obtain the flow profile at time t=0, i.e. just at the beginning of the unsteady flow, a steady gradually varied flow profile is computed for the initial steady state discharge and is used as the initial condition.

5.2.2 Boundary condition

For the solution of the governing equations in grid system by using a numerical method, it is important to know the values of the independent parameters at the boundary of the domain. Boundary conditions are necessary to define the interaction of the site-specific model with entire flow system.

Commonly, three types of boundary conditions are encountered in the solution of partial differential equations, namely, Dirichlet boundary conditions, Neumann boundary conditions and Robin boundary conditions. Numerical form of Saint-Venant equation can be solved in the interior grid points only. It is not possible to solve at the boundaries without using the boundary conditions. Therefore, two boundary conditions are required to calculate the flow parameters at the boundaries. One is upstream boundary condition and other is downstream boundary condition. An additional boundary condition known as intermediate boundary condition will also be required if we consider the lateral outflow and inflow of water in the main stream.

5.2.2.1 Upstream boundary Condition

The discharge hydrograph as shown in fig 5.1 has been taken as the upstream boundary condition for the hypothetical river reach. The discharge hydrograph shown in the figure is the total discharge of the river w.r.t time which is distributed equally in each upstream grid, as the cross section of the river is considered rectangular and effect of side friction on discharge variation across the channel is neglected.

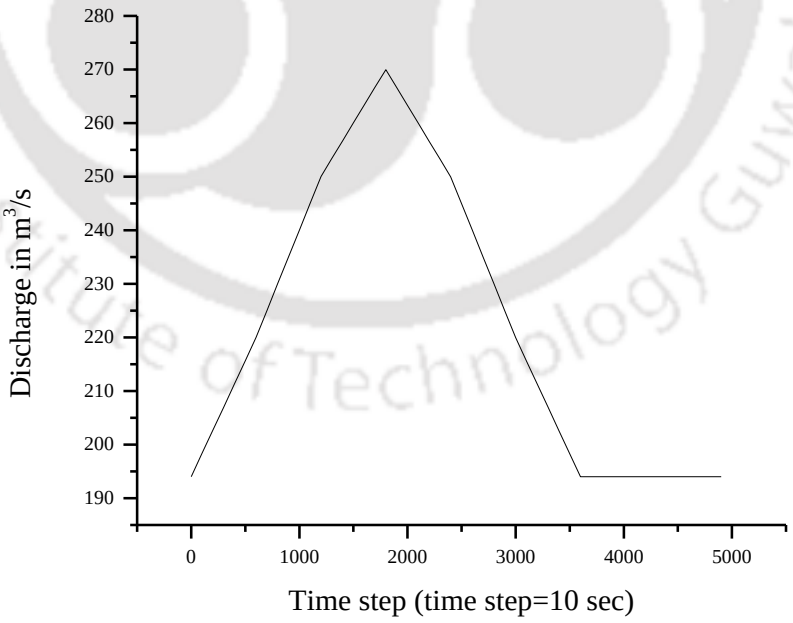

Figure 5.1 Upstream boundary condition

5.2.2.2 Downstream boundary condition

To calculate the flow parameters at the downstream boundary, we have used two equations the positive characteristic equation [Eq. 5.1] and the Manning's equation [Eq. 5.2]

$$u_{i,j-1}^{k} + 2C_{i,j-1}^{k} = u_{i,j-1}^{k+1} + 2C_{i,j-1}^{k+1}, \qquad \text{For } \frac{dx}{dt} = u + C \qquad 5.1$$

$$u = \frac{1}{N} y^{\frac{2}{3}} s_f^{\frac{2}{3}} \qquad 5.2$$

where, $u_{i,j}^{k}$ is the velocity at (i,j)th grid in space and kth grid in time. $C_{i,j}^{k}$ is the celerity at (i,j)th grid in space and kth grid in time. Celerity C is computed by using expression for rectangular channel as $C = \sqrt{gy}$, where g is the acceleration due to gravity and y is the flow depth.

In case of availability of water level at any control section at downstream, the downstream boundary condition can be replaced by flow depth at that control section.

Extrapolation technique

The unknown flow variables at the downstream boundary can also be evaluated by extrapolation from the interior domain (Anderson et. al 1984). The extrapolation may be considered as first order or second order as given below,

For first order extrapolation, value of any variable (f) at 'n' node will be,

$$f(n) = f(n-1) \qquad 5.3$$

Similarly, using second order extrapolation,

$$f(n) = 2\,f(n-1) - f(n-2)$$

5.2.2.3 Intermediate boundary condition

Once the flow reaches the piedmont zone, the flow process changes. Therefore, an intermediate boundary condition was introduced at the upstream of the piedmont zone.

This intermediate boundary condition is solved by the positive characteristic equation and manning's equation as discussed earlier in case of downstream boundary condition.

5.2.2.4 Reflective boundary condition

For 2-D flow, one more boundary condition is required which is known as solid boundary having no flow through it. The solid banks are simulated as free slip boundaries (Klonidis and Soulis 2001). The values of h and u are extrapolated from the interior domain. For enabling no cross flow through the boundaries, v value is set to zero. The reflective boundary condition is implemented by creating dummy cell at the end of the surface, as shown in fig 5.2. The direction of normal velocity component is altered here to have zero resultant velocity at the solid wall.

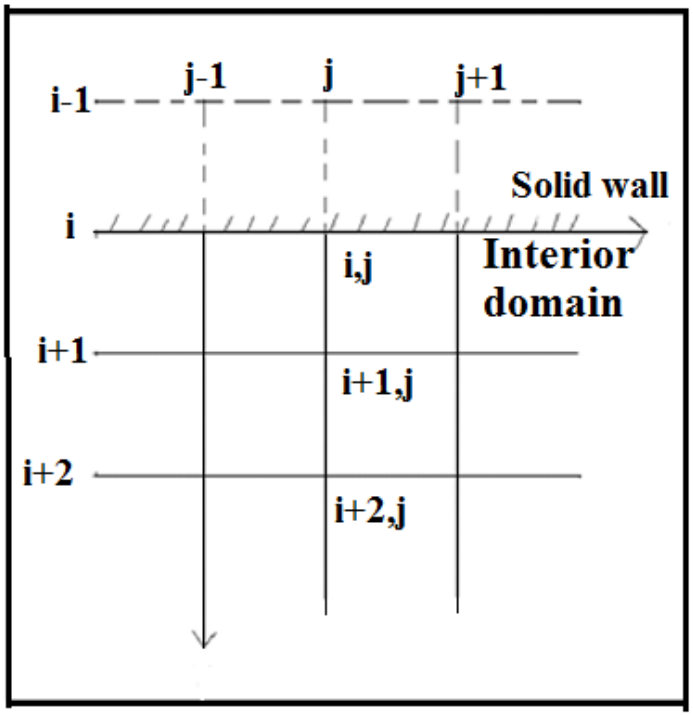

Figure 5.2 Reflective boundary condition

The value of the flow variable at dummy cell is given by,

$$h(i-1, j, k) = h(i+1, j, k)$$

$$u(i-1, j, k) = u(i+1, j, k)$$

$$v(i-1, j, k) = -v(i+1, j, k)$$

5.3 Development of groundwater model

This study aims to develop a surface–subsurface flow model considering the groundwater recharge zone on the river bed. As the piedmont zone is developed at the foot of a hill, therefore an assumption is made that water infiltrated through the recharge zone moves along the river only. The amount of water, which is infiltrated through the piedmont zone, is calculated with the help of Green- Ampt infiltration model. This water moves as groundwater below the river bed and it is described by well-known Richards equation. Therefore, after developing the free surface flow model along with infiltration model, a groundwater model is developed and linked with the surface water model to describe the flow condition as discussed earlier in section 3.4 of chapter 3. Details of the groundwater model are discussed below:

5.3.1 Boundary condition

The boundary condition for groundwater model is shown in fig 5.3. Dirichlet and Neumann type of boundaries are considered. As shown in the figure below, a time-dependent flux Q(t) (Neumann boundary) is applied over the length of 200 m and the remaining river bed is considered to have neither infiltration nor evaporation losses i.e. no flow boundary is applied (Dirichlet boundary). Again, no flow boundaries are applied on the upstream side and the groundwater table is considered at the bottom. Fig 5.4 below shows the detail of the boundary conditions.

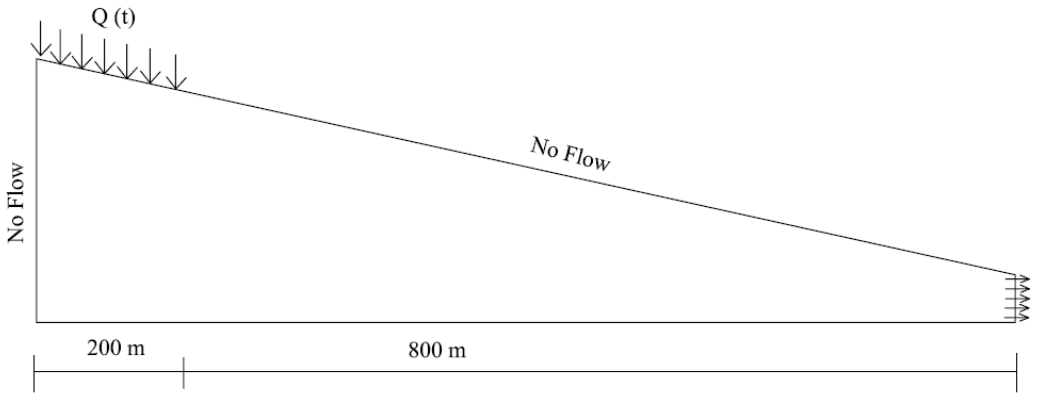

Figure 5.3 Boundary condition for groundwater model

5.4 Coupling of unsteady free surface flow model with groundwater model

After developing the above two models, they are linked through exchange of flux between them. Water infiltrated through the piedmont zone which is calculated from Green-Ampt. infiltration model, is considered as the input flux for groundwater model. This infiltrated water moves as groundwater below the river bed and after some time it again joins the mainstream at downstream of the river. Infiltration rate (f) is calculated from eq. 3.2 and is used as the input flux for Richards equation in the infiltrated area. Unsteady flow model with piedmont zone is run simultaneously with the groundwater flow model until it reaches a steady state with constant infiltration rate. Beyond this point the groundwater model is run with the constant infiltration rate as the input flux. Surface water model is again activated when the groundwater starts to contribute the mainstream at far downstream. This approach has helped in reducing computational time and has made the computation faster.

5.5 Validation of the model

Utilizing field data and laboratory data available at different sources, the model is validated in two parts. One part deals with the unsteady flow model considering the infiltration through river bed and the other part deals with the groundwater movement of the infiltrated water.

5.5.1 Validation of free surface flow model with piedmont zone

Because of economic constraints and other difficulties of installation, sufficient numbers of gauging stations are not available in most of the tributaries of Brahmaputra Basin. Therefore, the proposed model has been validated using published field data of Trout Creek River (Niswonger et.al 2005). Trout Creek is a mountain front stream that drains the north-west flank of Battle Mountain near Valmy, Nevada. It is a high gradient river with a very low depth of flow. Mountain front streams may not follow same hydraulic conductivity throughout the river because of decrease of sediment size. In general hydraulic conductivity decreases downstream in mountain front stream. However, near the piedmont zone the hydraulic conductivity do not increase because of poorly sorted debris flow deposits acting like a sieve to infiltrating water. Three values of hydraulic conductivity have been used for the model as per Table 5.1 (Niswonger et al. 2005). The coupled free surface flow -infiltration model is used to calculate the flow parameters e.g.

discharge, water surface elevation in the river reach of length 11.7 km. Discharge hydrograph (Fig 5.4) measured above Marrigold Mine (Niswonger et al. 2005) is used as the upstream boundary condition. A uniform flow of 0.046 m^3/s and 0.13 m^3/s is used as an initial condition for the year of 2000 and 2004 respectively. Parameter values used in the Green-Ampt. model for calculating water infiltration through the river bed is shown in Table 5.2. Values of flow parameters at downstream boundary are calculated by using the characteristic equations as described in eq. 5.1 and eq. 5.2. Model results were observed to be in good agreement with the observed field data (Fig 5.5).

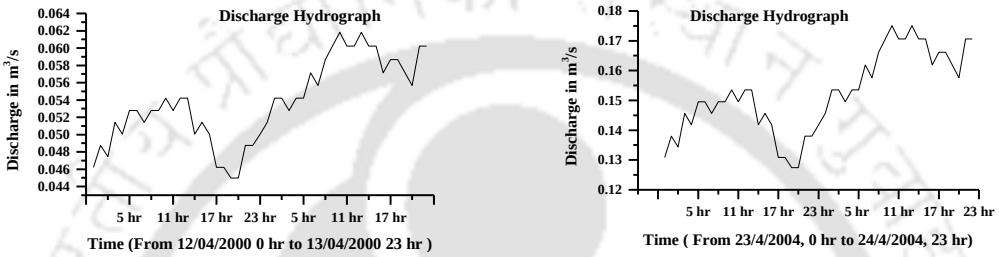

Figure 5.4 Upstream boundary condition (a) For the date of 13/04/2000 (b) For the date of 24/03/2004

Table 5.1 Variation of hydraulic conductivity with distance

Distance of the river in km from upstream of the river	Hydraulic conductivity in m/s
5.88 km	0.000005
3.22 km	0.000007
2.1 km	0.00001

Table 5.2 Parameters used in Green-Ampt. Model

Parameter	Values
Hydraulic conductivity	As per table 1
Initial water content	0.072
Saturated water content	0.036

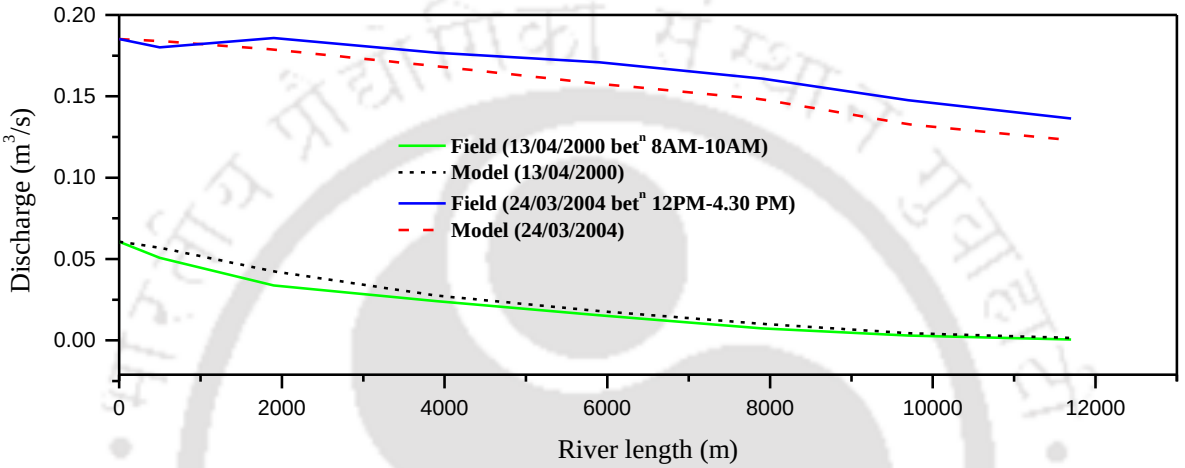

Figure 5.5 Comparison of model data with field data

5.5.2 Validation of the groundwater model

The groundwater model is validated with the experimental data of Vaculin et al. (1979). This example is selected to verify the performance of the groundwater model. The flow condition of the given problem is two-dimensional, transient, variably saturated flow. The flow domain consisted of a rectangular soil slab, 6.00 m × 2.00 m, with an initial horizontal water table located at a height of 0.65 m. At the soil surface, a constant flux of q = 3.55 $mday^{-1}$ was applied over a width of 1.00 m in the centre. The remaining soil surface was covered to prevent evaporation losses, because of the symmetry, only one side (here the right side) of the flow domain needs to be modelled. As illustrated in fig. 5.6, the modelled portion of the flow domain is 3.00 m × 2.00 m, with no-flow boundaries on the bottom and on the left side (accounting for the symmetry). At the soil surface, the constant flux of 3.55 $mday^{-1}$ is applied over the left 0.50 m of the top of the modelled domain. The remaining soil surface at the top is a no-flow boundary. The water level on the right face of the block is maintained at 0.65 m. As this problem has a steady-state solution (both experimental (Vauclin et al., 1979) and numerical) without the

development of a seepage face, a no-flow boundary is used above the water table on the right side of the domain.

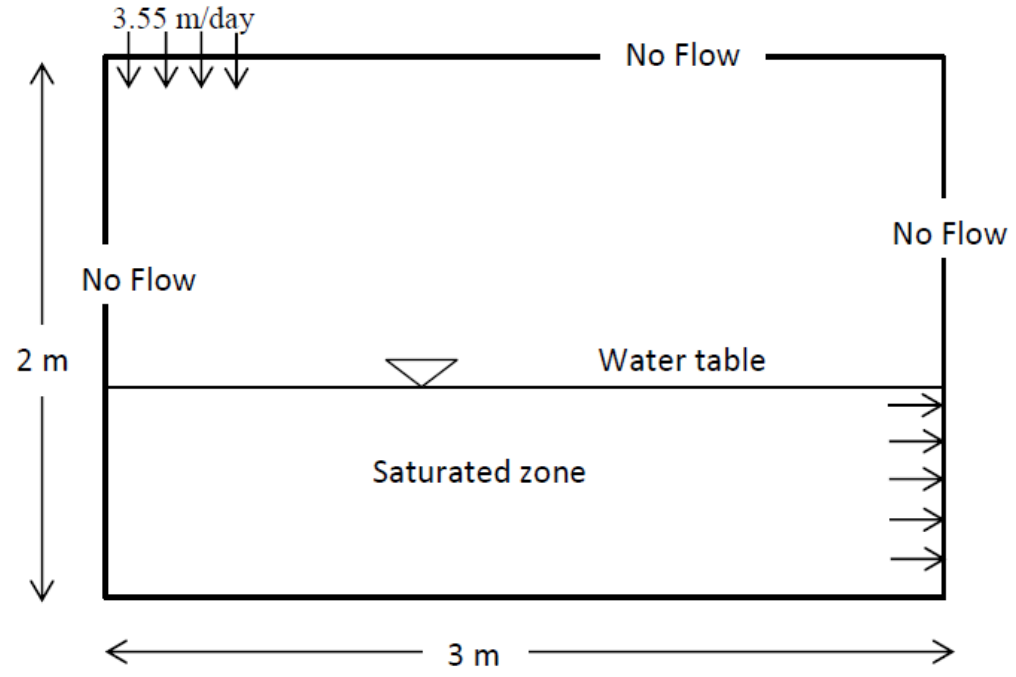

Figure 5.6 Detailed of Vauclin et al. model

From Vauclin et al. (1979), the soil properties used in the model are a saturated hydraulic conductivity of 8.40 $mday^{-1}$, a porosity of $\eta = \theta_s = 0.30$, and a residual saturation of $\theta_r = 0.01$. The Van Genuchten (1980) model is fitted to the water retention and the relative hydraulic conductivity data given by Vauclin et al. (1979); the estimated values for the soil properties are $\alpha = 3.3\ m^{-1}$ and $n = 4.1$.

Specific storage may be neglected for this problem because changes in storage are facilitated by the filling of pores, which overshadows the effects of compressibility for the vertical extent of this flow domain; hence, the specific storage coefficient is set to zero. The nodal spacing in the x and z directions are $\Delta x = 0.10$ m and $\Delta z = 0.05$ m, respectively. The soil system is assumed to be initially at hydrostatic equilibrium with respect to the water table throughout the flow domain. Transient positions of the water table are compared with the experimental results presented by Vauclin et al. (1979) in fig. 5.7, which indicates that there is an excellent agreement between the transient water-table positions predicted by the algorithm and those observed.

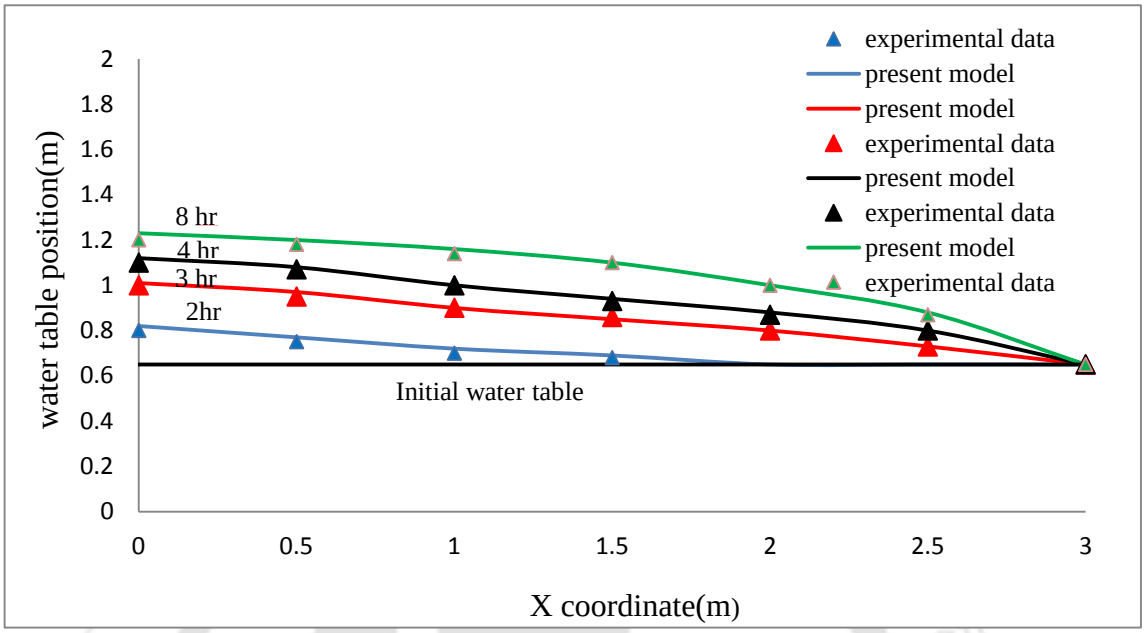

Figure 5.7 Comparison between Vauclin et al. experimental data and present model

5.6 Conclusion

In this chapter, a detailed discussion about the model development and its validation are discussed. The assumptions that are made in the governing equation are also maintained in the development of the model. Different types of boundary conditions are applied for development of the model. As the field data and experimental data are not available for coupled model (surface water- infiltration- groundwater model) the developed model is validated in two parts. First part considers the unsteady flow with piedmont zone is validated with field data of Trout Creek River and the second part where groundwater simulation considered is validated with Vaculin et al. experimental data. From the comparison of the results it has been found that there is good agreement between them

Chapter 6

Model Application

6.1 Introduction

The coupled model developed in chapter 5, i.e., the coupled surface-subsurface flow model with piedmont zone in the river bed can be represented as given below:

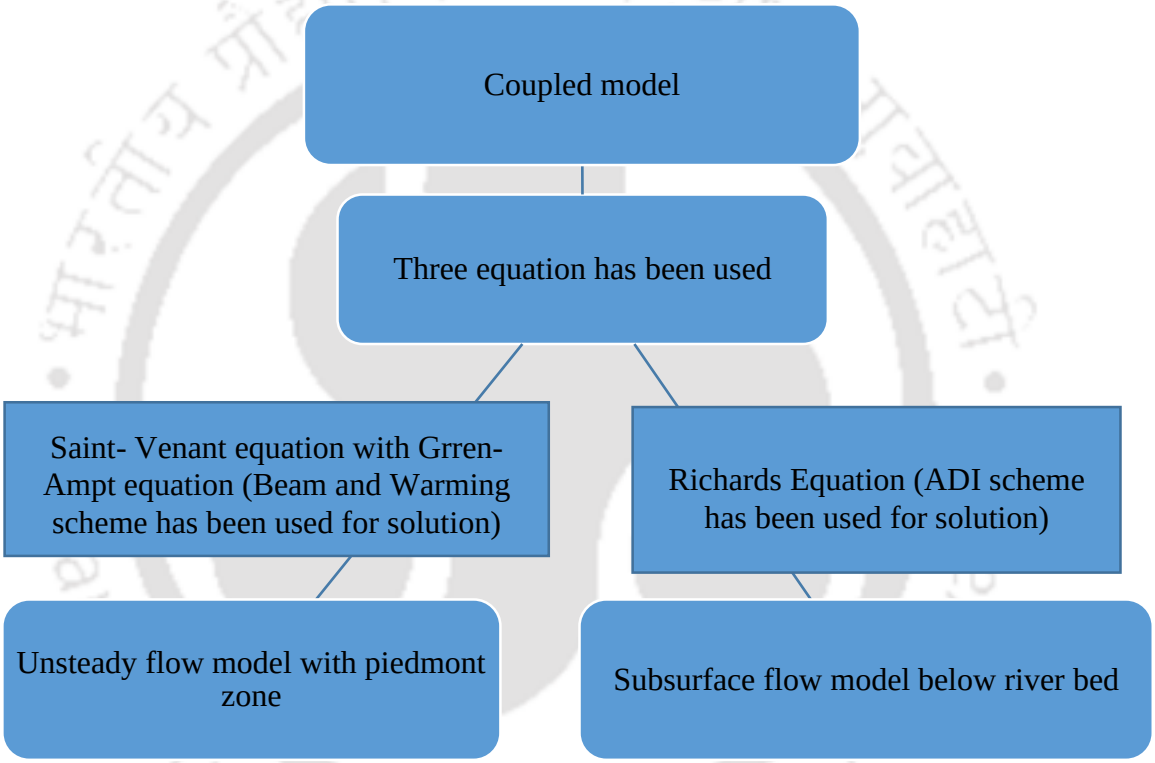

Figure 6: Flow chart of the developed model

From the above figure it is cleared that model is developed in two components i.e. one component is unsteady flow model with piedmont zone in the river bed and other is subsurface flow model.

Unsteady flow with piedmont zone is described by Saint-Venant equation and Green-Ampt equation. The two equations are

$$U_t + E_x + F_y + S = 0$$

$$U = \begin{pmatrix} h \\ uh \\ vh \end{pmatrix} \qquad E = \begin{pmatrix} uh \\ u^2h + \frac{1}{2}gh^2 \\ uvh \end{pmatrix} \qquad F = \begin{pmatrix} vh \\ vuh \\ v^2h + \frac{1}{2}gh^2 \end{pmatrix}$$

$$S = \begin{pmatrix} f + q \\ -gh\left(s_{0_x} - s_{f_x}\right) - m_{lx} \\ -gh\left(s_{0_y} - s_{f_y}\right) - m_{ly} \end{pmatrix} \qquad s_{f_x} = \frac{N^2 u\sqrt{u^2+v^2}}{R^{4/3}} \qquad s_{f_y} = \frac{N^2 v\sqrt{u^2+v^2}}{R^{4/3}}$$

where, $f = k_0\left[1 + \frac{[\psi(t) + h(t)][\theta_s - \theta_o]}{F_c}\right]$ is the Green-Ampt equation

$$m_{lx} = 0.5(f + q)u \qquad m_{ly} = 0.5(f + q)v$$

Subsurface flow below the river bed is described by Richards equation

$$\frac{\partial\theta}{dt} - \nabla.K(\psi)\nabla\psi - \frac{\partial K(\psi)}{dz} = 0$$

Details of all these governing equations are already discussed in chapter 3(Governing equation). These equations are nonlinear and analytical solutions are not available without simplification. Therefore the above equations are solved numerically and details of numerical solution of the above equations are discussed in chapter 4 (Numerical solution of governing equation)

The model developed through numerical simulation of above equations is first applied to a hypothetical case. To visualize the effect of piedmont zone on surface flow, the model result obtained for flow depth, river discharge and water surface elevation with the consideration of piedmont zone and without consideration of piedmont zone are compared and presented in this chapter.

For convenience of model application input data required are tabulated below

Table: 6.1 Input data required to run the model

Classification of Parameters	Parameters
Hydrological Parameter	Upstream boundary condition, Initial condition, Hydraulic conductivity of the piedmont zone, Downstream boundary condition,
Topographical Parameter	Bathymetry of the river, C/S area of the river, width of the river, Length of the riverbed slope, area of piedmont zone, location of piedmont zone
Hydrodynamic Parameters	Manning's roughness coefficient

As the flow in the Himalayan Rivers like rivers of Brahmaputra Basin may range from very high discharge in the monsoon to a very low discharge in the non-monsoon period, possible effect of such varying discharge is also investigated by running the model for high and low discharge.

To ascertain applicability of the model in different situations, developed coupled model is applied to a hypothetical river reach for following variations in its subsurface layers.

a) Piedmont zone with homogeneous subsurface soil formation.

b) Piedmont zone with layered subsurface soil formation with following cases

I. with increasing hydraulic conductivity from top most layer to bottom most layer
II. with decreasing hydraulic conductivity from top most layer to bottom most layer
III. Arbitrarily varying hydraulic conductivity in different layer.

To examine effect of different involved soil parameters such as hydraulic conductivity and capillary fringe on different flow variables, a sensitivity analysis for these parameters is carried out in a systematic manner.

After ascertaining its applicability in different situations and having an understanding about the sensitive parameters, the model is applied to a 2nd order tributary of Brahmaputra River having a piedmont zone in it.

6.2 Model application on hypothetical case

The coupled two-dimensional surface-subsurface flow model with piedmont zone in the river bed is applied to a hypothetical case. The length of the hypothetical channel considered is 2.00 km and of width 200m. A piedmont zone of area 200m × 200m is considered at a distance of 1.00 km from the u/s through which water is infiltrated. This infiltrated water moves as groundwater and joins the river at downstream. Three different slopes are considered in the river reach. The lengths of the reaches are 1.00km, 500 m and 500 m for upper, middle and lower reaches respectively. Correspondingly, their slopes are 1:2000, 1:3000 and 1:2500. The flow hydrograph shown in chapter-5 (fig. 5.1) is used as the upstream boundary.

6.3 Results obtained from hypothetical case

Results obtained from hypothetical cases are discussed below. The coupled surface-subsurface flow model with piedmont zone, developed in chapter-5, has been used to study the effect of presence of piedmont zone on different flow variable e.g. water surface elevation, depth hydrograph, discharge are discussed in details in this section. The flow behaviour of infiltrated water in subsurface is also discussed in details in this section with the help of groundwater component of the model developed in the previous chapter.

6.3.1 Water surface elevation

Spatio-temporal variation of water surface elevation is discussed in this section. Fig 6.1 (a) shows the 2-D plot water surface elevation for two different cases-1) without considering piedmont zone and 2) with considering piedmont zone. For proper visualisation in fig 6.1 (a), centre line of water surface elevation is plotted in fig 6.1(b).

From this figure, we have noticed that because of the presence of piedmont zone, water surface elevation downstream of the piedmont zone decreases. This happens because a significant amount of water is infiltrated through the permeable zone and moves as groundwater. The fig 6.1 (c) shows the centre line of water surface profile at different time steps. Plotting of centre line profile is preferred, as the difference among the different time dependent water surfaces is not visible clearly in 2D plot. This plot basically shows the transition phase of the water surface profile when the flood hydrograph travel through the channel. From this figure, it is seen that water surface rises up to a time step of 2000 and then decreases and remains constant at time step 5000. The figure thus shows that the river reaches a steady state after elapse of 5000 time step. Figure 6.1(d) represents the water surface elevation for different values of hydraulic conductivity. Compression of the graph reveals that the water surface elevation at the downstream of the recharge zone decreases with increase in the value of hydraulic conductivity ‘k’.

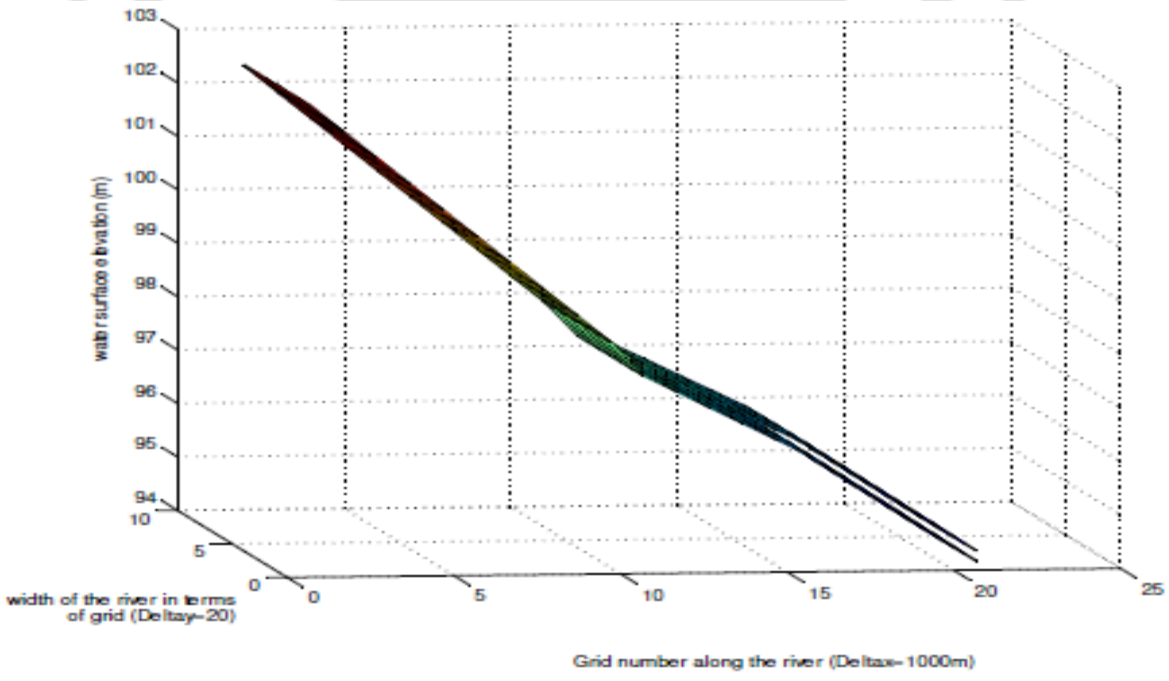

Figure 6.1(a) 2-D plot of water surface elevation for two different cases

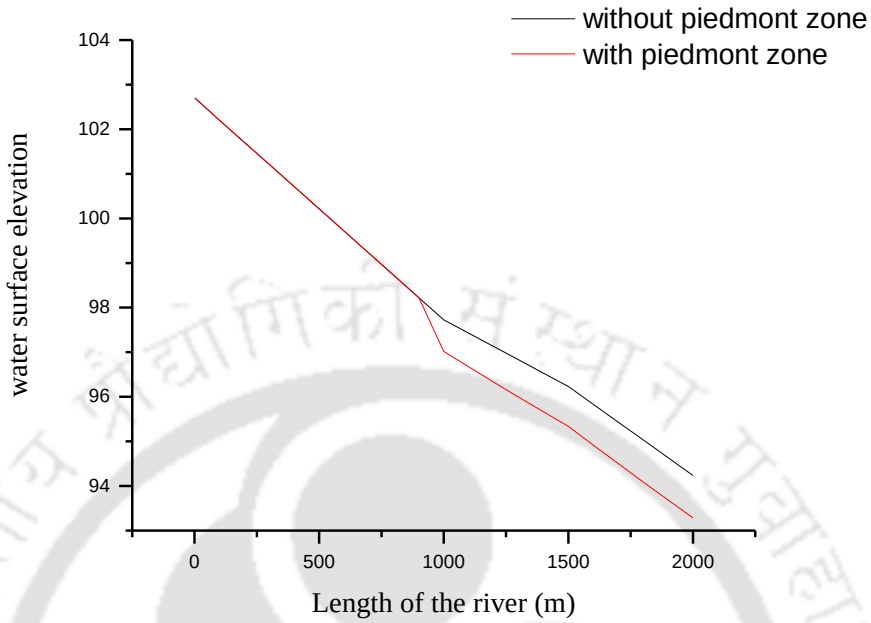

Figure 6.1 (b) Water surface elevation for two different case

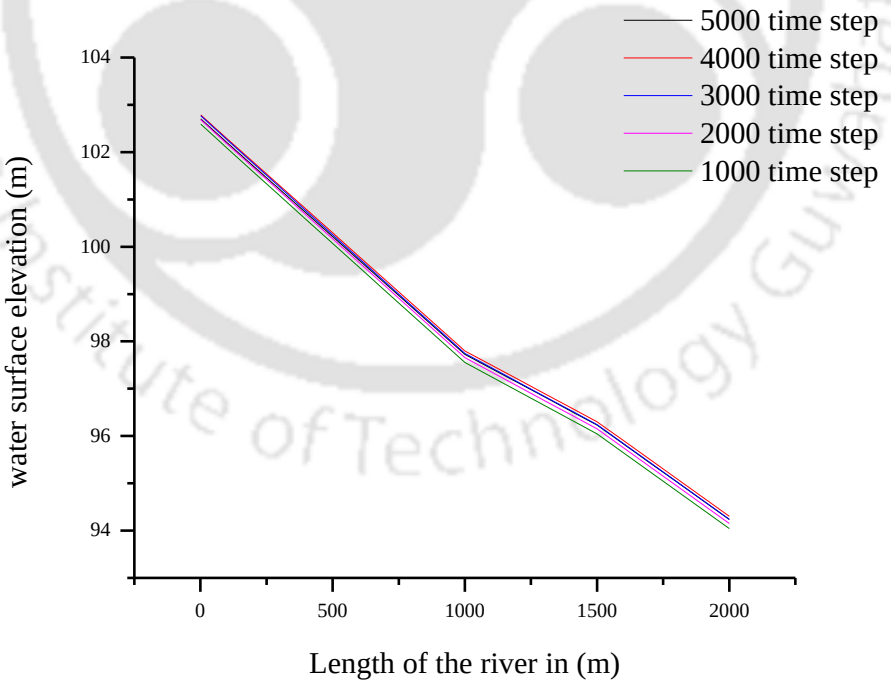

Figure 6.1 (c) Water surface elevation at different time step

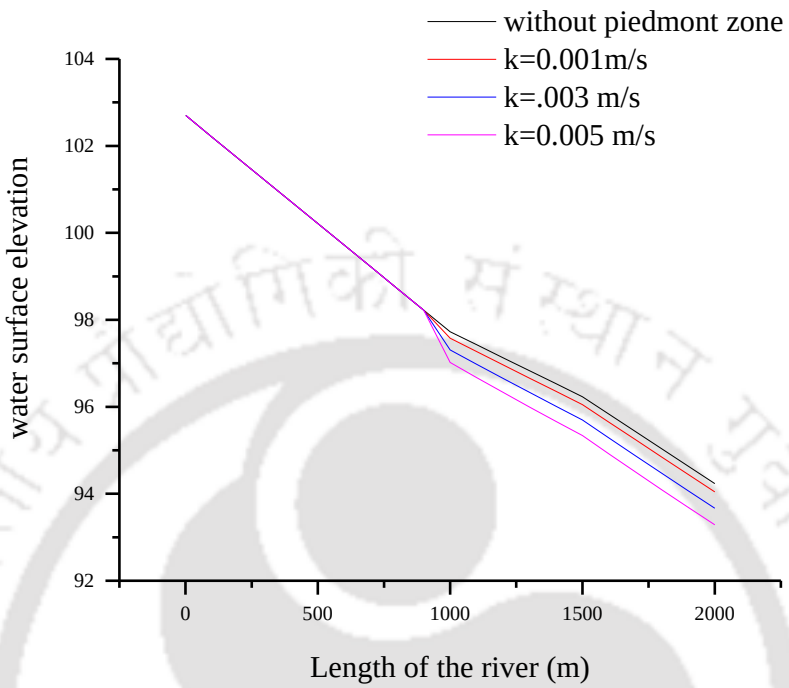

Figure 6.1 (d) water surface elevation for different values of hydraulic conductivity

6.3.2 Depth hydrograph

This section presents depth hydrograph for the centreline for different conditions. Fig 6.2 (a) shows the depth hydrograph with piedmont zone and without piedmont zone. From this figure, we have seen that because of the presence of piedmont zone peak of the depth hydrograph decreases. The percentage decrease of depth hydrograph due to the presence of piedmont zone is approximately 1.5% of hydrograph without piedmont zone. Fig 6.2 (b) describes the depth hydrograph for different K values of piedmont zone.

6.3.3 Discharge hydrograph

In this segment, we are discussing the effect of discharge hydrograph with hydraulic conductivity. Fig 6.3 (a) shows the discharge hydrograph 1) considering piedmont zone and 2) ignoring the effect of piedmont zone together for better visual comparison at 1.3 km section. From these figures, it is seen that due to the presence of recharge zone in the

river, reduction in peak discharge is in the order of 2 m^3/s, which is approximately 7% of the peak flow without considering recharge zone. Fig 6.3 (b) shows the discharge hydrograph corresponding to 3 different values of hydraulic conductivity. From this figure, it is revealed that with the increase in hydraulic conductivity peak of the discharge hydrograph decreases.

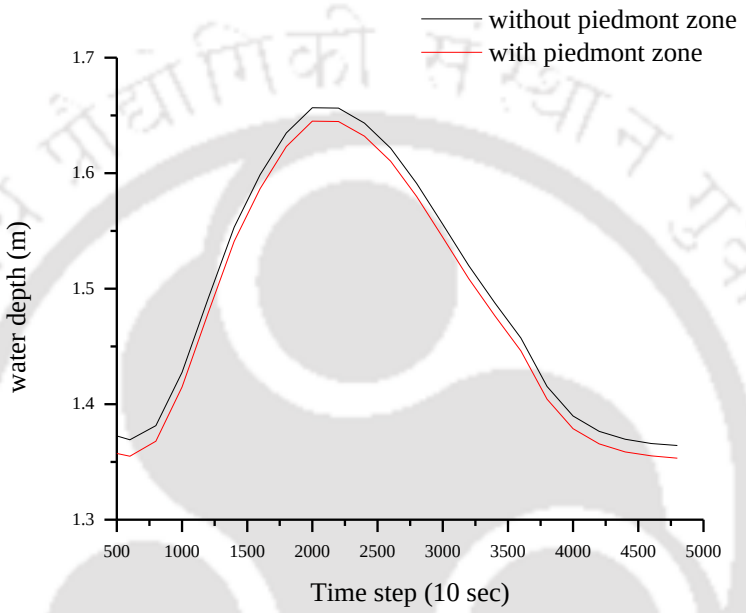

Figure 6.2 (a) Depth hydrograph for two different case

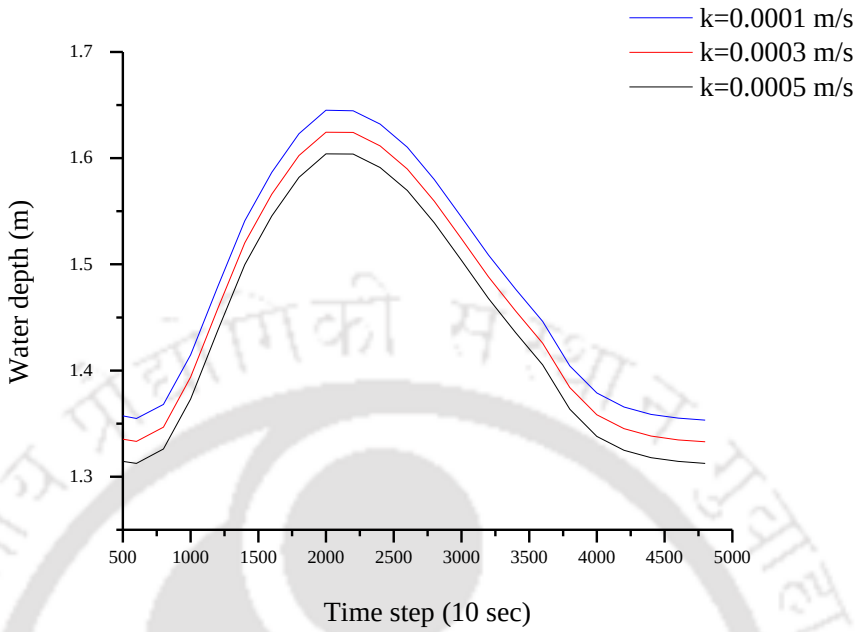

Figure 6.2 (b) Depth hydrograph at different values of k

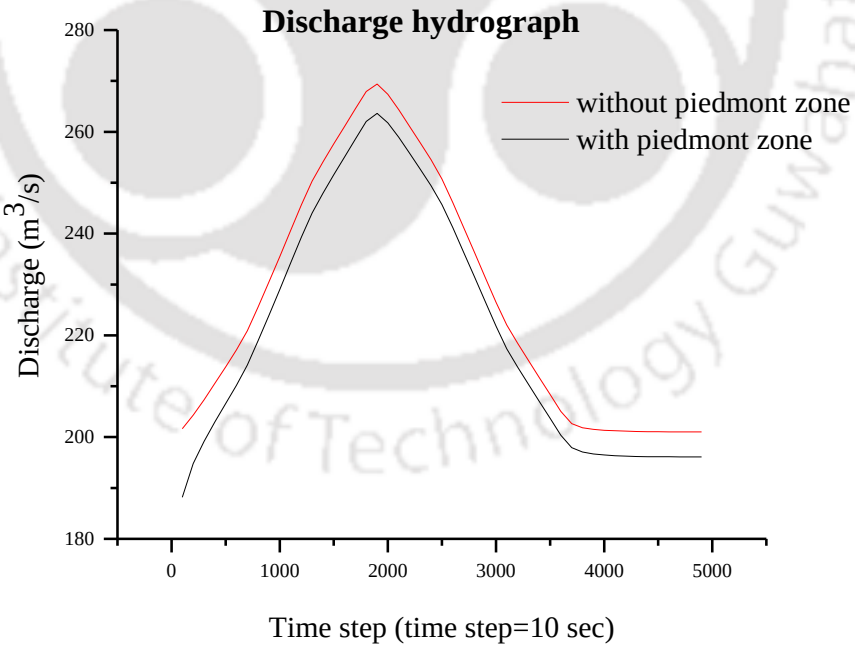

Figure 6.3 (a) Discharge hydrograph for two different situations

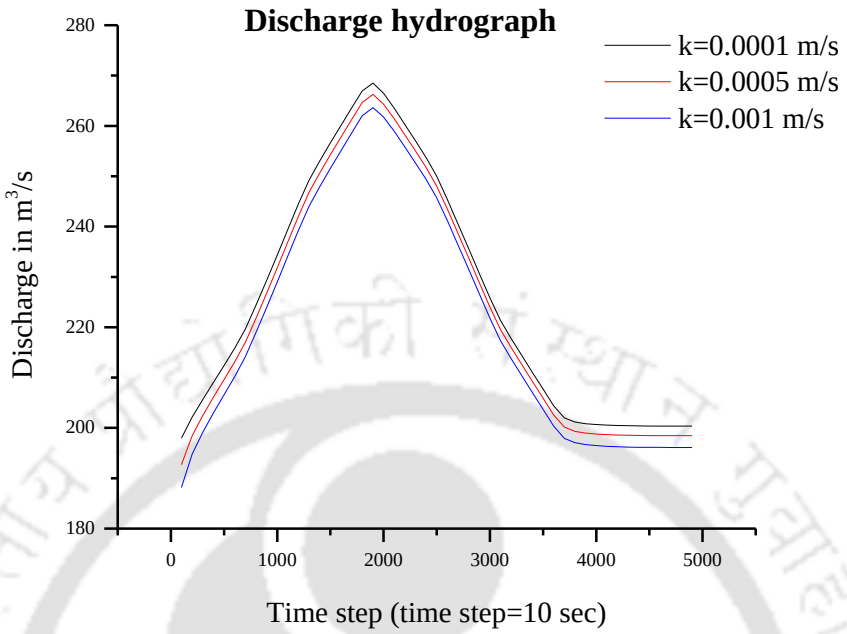

Figure 6.3 (b) Discharge hydrograph for different values of k

6.3.4 Infiltration

In this section, a detailed discussion of the infiltration is made. Fig 6.4(a) presents rate of the infiltration with different values of hydraulic conductivity at the centre line. These graphs describe the infiltration rate with three different values of hydraulic conductivity. This figure, shows dependency of infiltration rate on the hydraulic conductivity

6.3.5 Rise of ground water table for homogeneous soil

Fig 6.5 describes the rise of centre line of the groundwater table below the channel bed at different time step starting from 5hr to 150hr. From this figure, it is seen that with the increase of time, water table rises. At 150hr upstream water rises to a height of 2.25m and at the downstream, it starts to rise. Here hydraulic conductivity is taken as 0.0005 m/s. The length of the flow domain below the river is 1000m, and depth is 4 m at upstream boundary, and 0.4 m at downstream boundary i.e. the shape of the flow field below the river bed is trapezoidal.

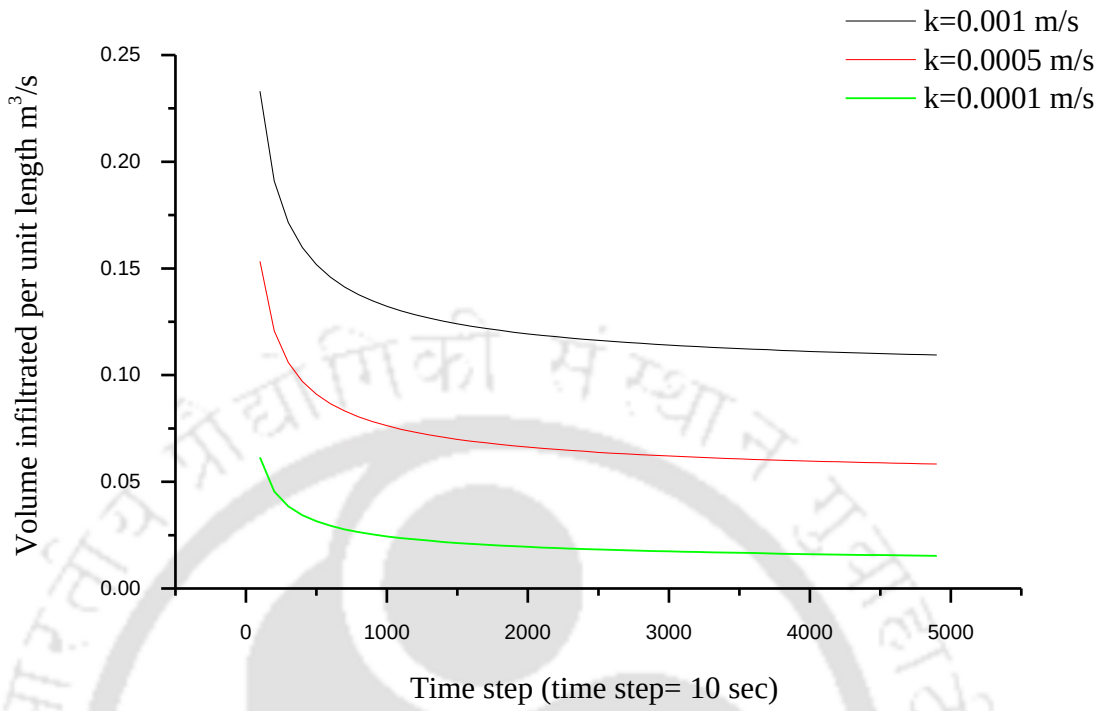

Figure 6.4 Volume infiltrated per unit length

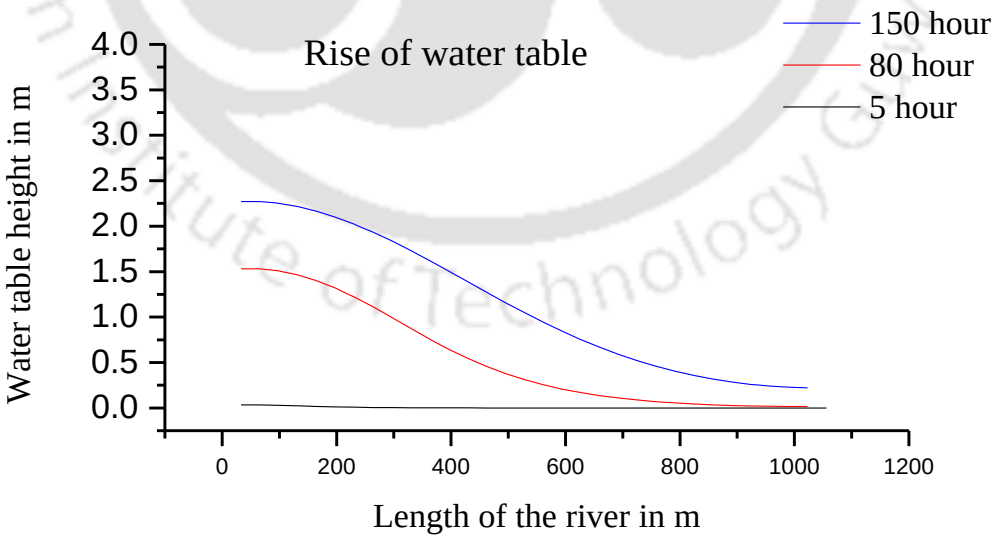

Figure 6.5 Rise of water table

6.3.6 Rise of water table for layered soil

Model has been tested for different layered soil formation which are shown below

Case 1

Decreasing hydraulic conductivity from top layer to bottom layer.

Layered soil with following hydraulic conductivity	
k=10.5 m/day	1m
k=7.5 m/day	1m
k=5.5 m/day	1m
k=4.5 m/day	1m

Case 2

Increasing hydraulic conductivity from top to bottom layer

Layered soil with following hydraulic conductivity	
k=4.5 m/day	1m
k=5.5 m/day	1m
k=7.5 m/day	1m
k=10.5 m/day	1m

Case 3

Mixed form hydraulic conductivity from top to bottom layer

Layered soil with following hydraulic conductivity	
k=5.5 m/day	1m
k=10.5 m/day	1m
k=4.5 m/day	1m
k=7.5 m/day	1m

Fig 6.6 (a) shows rise of water table for different types of soil formation in 5 hour. In this figure difference among the water tables is not visible. Therefore in fig 6.6 (b) water tables have been shown in reduced scale where difference in water tables is clearly visible. From this figure we have seen that rise of water table is more if a soil has case 1 type of soil formation and minimum for case 2 type of soil formation. Fig 6.6 (c) and fig 6.6 (d) represent the water table height at 100 and 150 hours. From these figures it can be concluded that rise of water table is more if soil has case 1 formation, i.e. if a soil has hydraulic conductivity highest at the top layer and decreasing continuously to the bottom most layer.

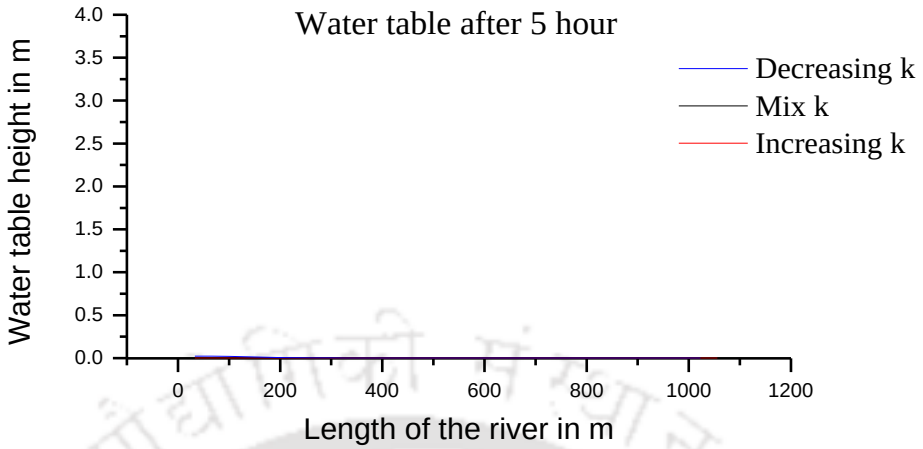

Figure 6.6. (a) Comparison of water table after 5 hour

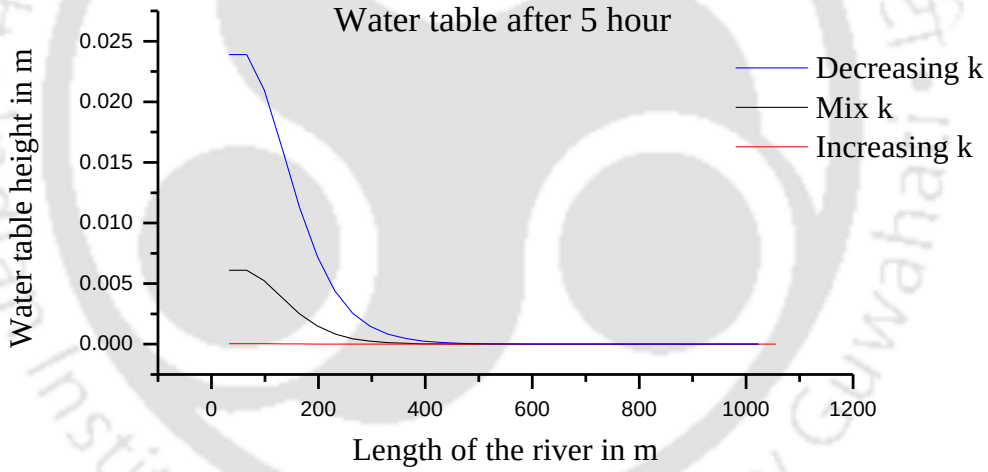

Figure 6.6. (b) Comparison of water table after 5 hour (In reduced scale)

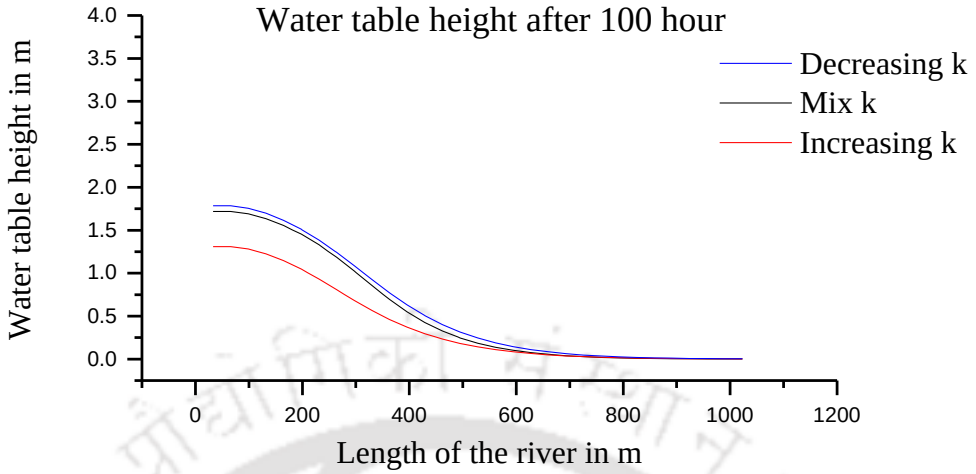

Figure 6.6. (c) Comparison of water table after 100 hour

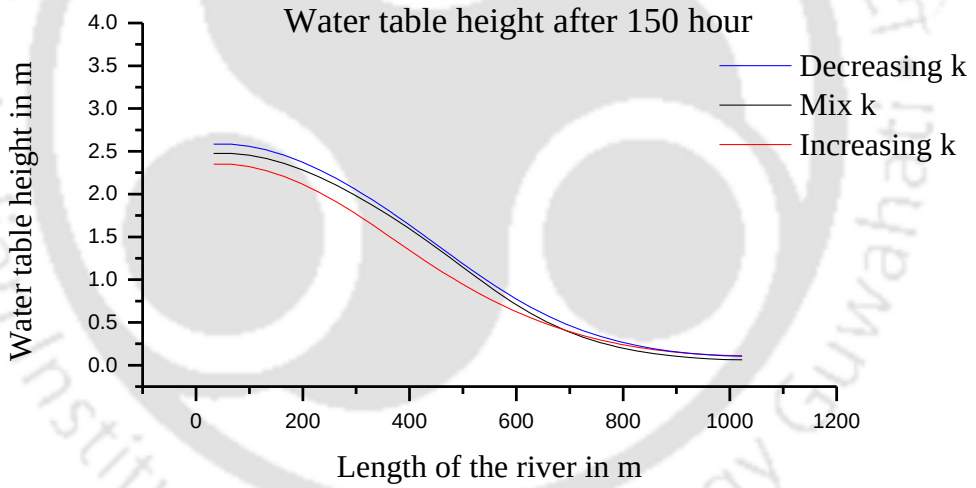

Figure 6.6. (d) Comparison of water table after 150 hour

6.3.7 Velocity Vector:

Fig 6.7 (a) represents the velocity vector of groundwater movement at 6hr. Because the length of the flow domain is 1000 m and depth is 4 m in upstream end and 0.4 m in downstream end it is difficult to visualise the dimension and direction of velocity vectors. Fig 6.7 (b) accounts for the same velocity vectors in a transformed grid. In this computational domain, it is observed that flow direction is downward i.e. because of infiltration through the piedmont zone water moves from upward to downward. Because

of the open boundary at the downstream, the flow direction in that region is outward. Fig 6.7 (c) shows the velocity vector at 12hr. From this figure it is seen that water continues to moves downwards from the river bed and from the bottom, water table starts to move upwards as indicated by the velocity vectors. Fig 6.7 (d) shows the velocity vector at 102hr. From this figure, it is seen that as the times run water moves from top to bottom and because of that water table rises. Again as the downstream boundary is open water flows out from this end.

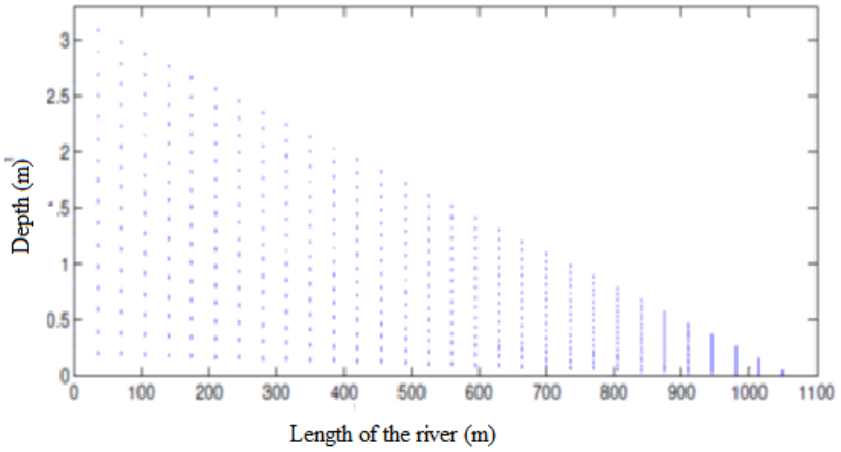

Figure 6.7 (a) Velocity vector at 6hr

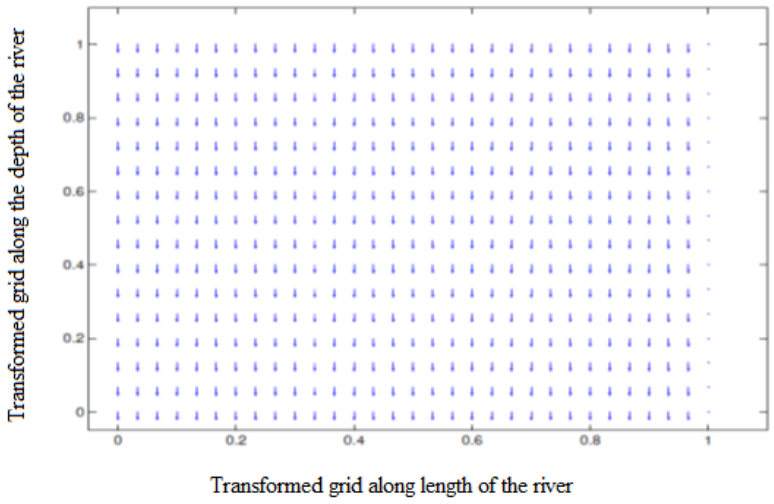

Figure 6.7 (b) Velocity vector at 6hr (Transformed grid)

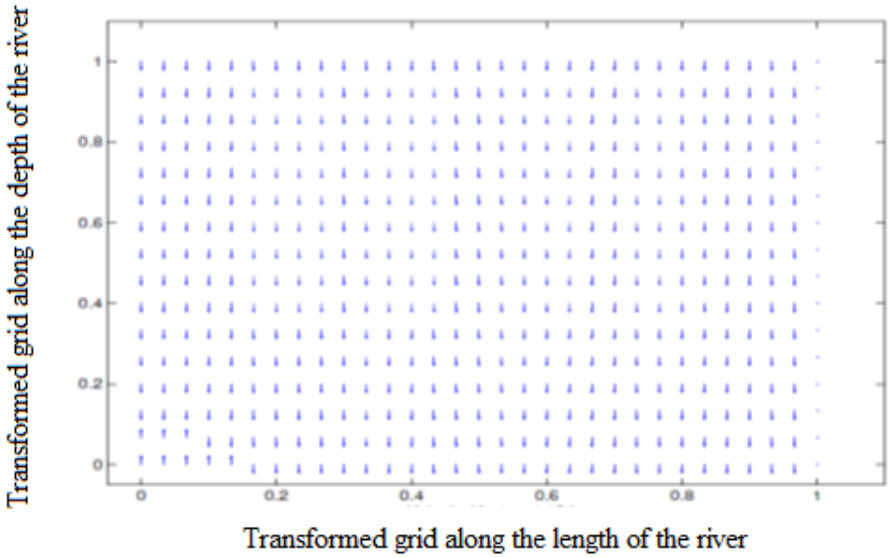

Figure 6.7 (c) Velocity vector at 12hr

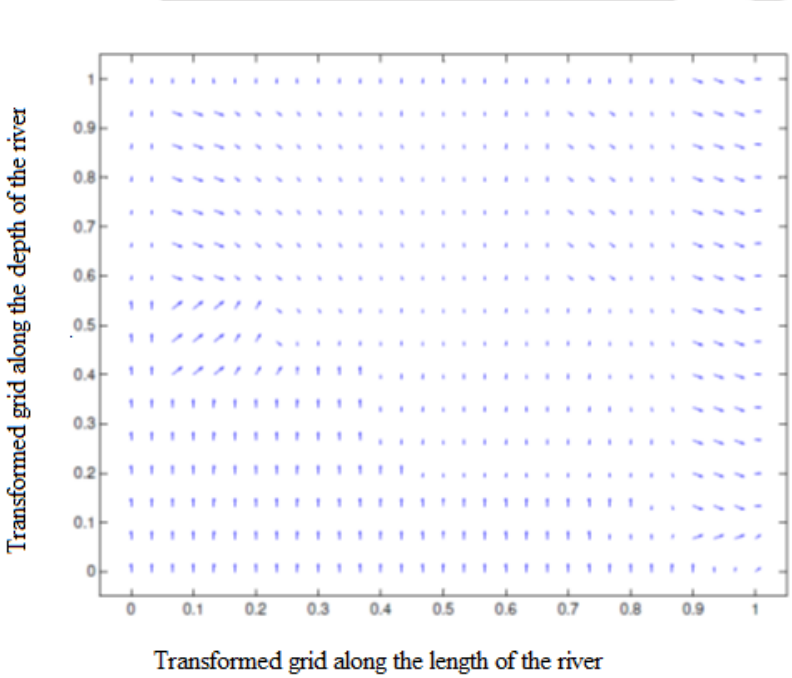

Figure 6.7 (d) Velocity vector at 102hr

6.3.8 Contribution of groundwater to mainstream

Fig 6.8 shows the contribution of groundwater to stream flow. From this figure, it is revealed that after 102hr groundwater starts contributing to the mainstream. Because of this contribution the stream flow increases by maximum 5.5%.

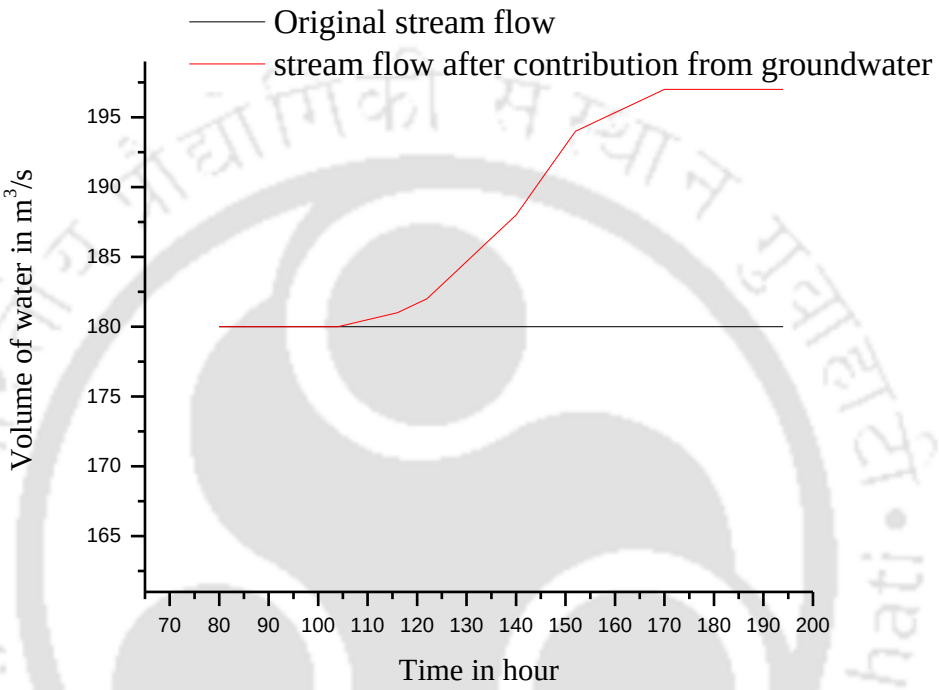

Figure 6.8 Contribution from Groundwater to Stream flow

6.3.9 Sensitivity analysis of hydraulic conductivity

Fig 6.9 (a) and 6.9 (b) show the sensitivity of peak depth and peak discharge to hydraulic conductivity. The central value of hydraulic conductivity is taken as 0.0005 m/sec, which is a logical value for sand-gravel mixture, which is commonly found in a river bed of such permeable river. From these figures, it is observed that during the period of low discharge, for a variation of ±100% in the value of hydraulic conductivity peak depth and peak discharge varies within a range of ±5.0% and ±0.5% respectively. Similarly During the high flow period, for the same variation in hydraulic conductivity, percentage changes of peak depth and peak discharge range between ± 7.0% and ±4.2 % respectively.

From fig 6.9 (c), it is observed that effect of hydraulic conductivity is significant on volume change. For low discharge river with an increase in the value of hydraulic

conductivity from an initial impermeable status, the channel flow volume decreases at a much higher rate and then decreases gradually with a uniform rate beyond k=0.0002. For higher discharge river decrease in channel flow volume is also high up to a value of k=0.0005, the rate of percentage change in flow volume remain high and then it drops gradually to a steady flat rate.

In fig 6.4 (d) describes a sensitivity analysis between percentage change of infiltration rate and percentage change of hydraulic conductivity. Here sensitivity analysis is carried out for three different k values k=0.001, 0.0005 and 0.0001 where k=0.0005 is taken as the central value. From this figure, it is seen that rate change of infiltration rate is ± 60% where hydraulic conductivity changes over a rate of ±100%

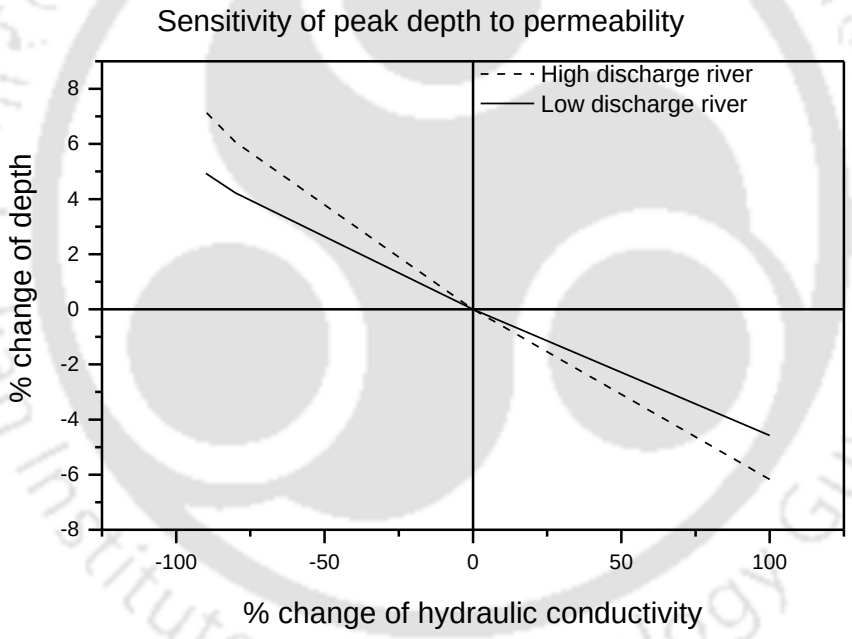

Figure 6.9 (a) Sensitivity analysis of peak depth to permeability

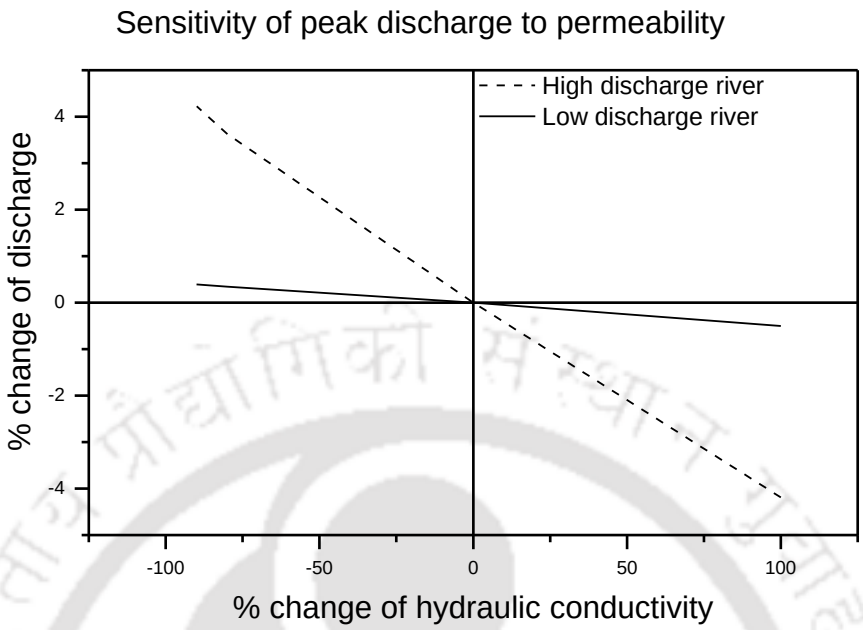

Figure 6.9 (b) Sensitivity analysis of peak discharge to permeability

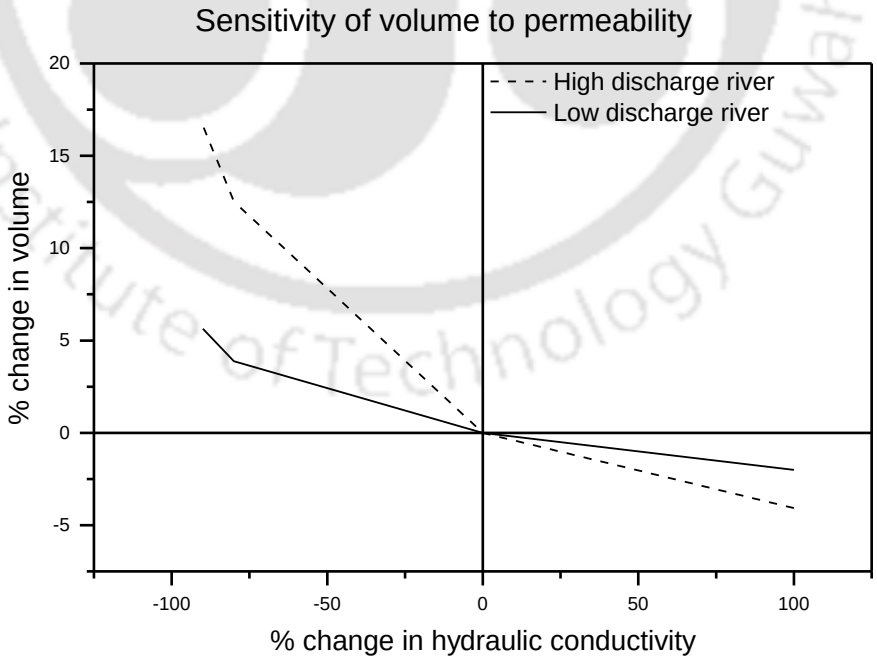

Figure 6.9 (c) Sensitivity analysis of volume to permeability

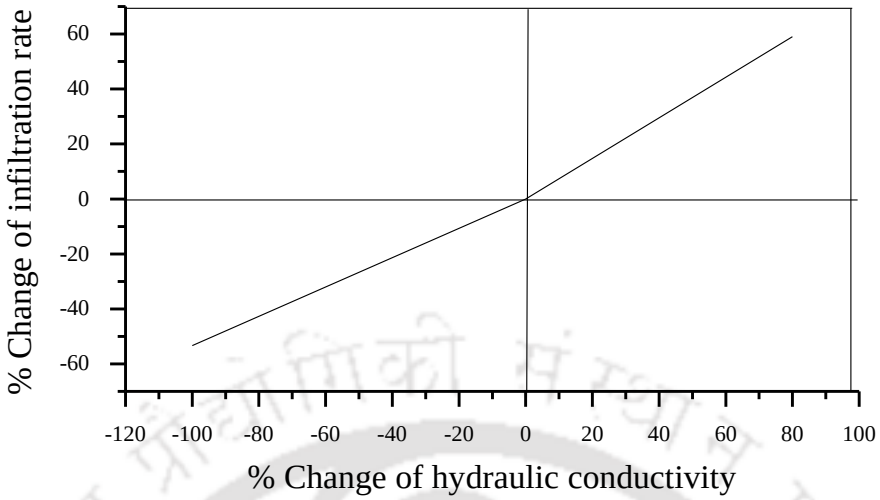

Figure 6.9 (d) Sensitivity analysis of infiltration to permeability

6.3.10 Sensitivity analysis of capillary fringe thickness (α)

Capillary fringe represents the zone immediately above the groundwater table. The Van Genuchten parameter α is a measure of capillary fringe thickness. This parameter has a significant influence on moisture movement through the unsaturated zone. From this figure it is seen that if the capillary fringe is more, the rise of water table is less, i.e. if soil has higher size of capillary fringe then the water table rises slowly. Taking 2.3 as the central value when size of the capillary fringe is decrease to 1.3 i.e. 43%, the rise of water increases by 0.14 m at upstream and 0.5m at downstream. Similarly if the capillary fringe size increase to 3.3 i.e. 43% the rise of water table decreases by 0.05 m at upstream and 0.09 m at downstream.

6.4 Field application of the model

The developed model is applied to a 2nd order tributary of Brahmaputra River which originates from Bhutan and such piedmont zone was reported by Goswami et al. in 1996 in the foot hill area of this river located in India. From the sensitivity analysis of hydraulic conductivity it is noticed that precise estimation of hydraulic conductivity is necessary to get proper results. Therefore double ring infiltrometer test was performed on the field to estimate the hydraulic conductivity accurately.

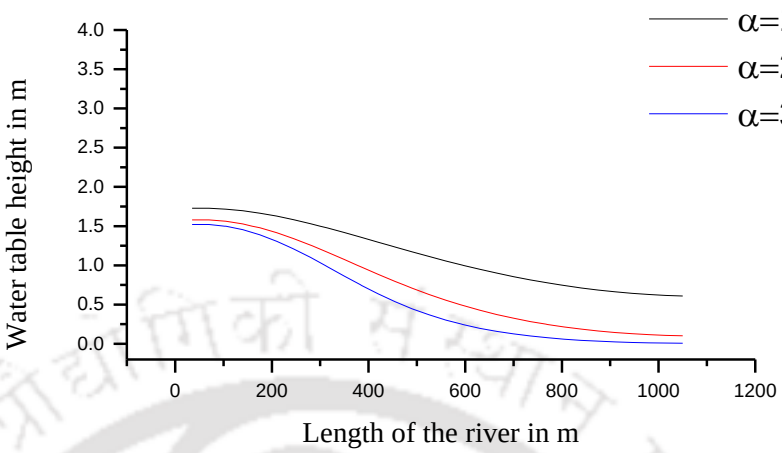

Figure 6.10 Water table height for different values of α

The geographical location of the river is between $26^0 50' 35'' N$ and $92^0 02' 16'' E$. The river is situated in Amjuli village, Udalguri District in Assam. The width of the river is 30m. Double ring infiltrometer test was conducted in 3 locations of the river to calculate infiltration characteristics of the river. Fig 6.12 shows the location of the river where the developed model is applied.

Well located near the river is found to be have water level at a depth of 100ft. Local people also confirmed that in most of the nearby well the water table in the rainy season remain in the similar depth. Therefore groundwater table is considered at a depth of 30m. In absence of detail geological data the subsurface soil profile of the piedmont zone is considered as homogeneous with average permeability characteristic. To generate the input hydrograph for this river, IDF curve generated for Lamabari Tea Estate, Assam has been used which is the nearest place where rainfall data are recorded. Details of input hydrograph are discussed in section 6.4.2.

6.4.1 Double ring infiltrometer test

The double ring infiltrometer is a simple instrument used for determining water infiltration of the soil. The rings are partially inserted into the soil and filled with water, after which the speed of infiltration is measured. This rate becomes constant when the saturated infiltration rate for the particular soil has been reached. The double ring limits the lateral spread of water after infiltration. The standard double ring infiltrometer set

consists of two pairs of inner and outer rings, a driving plate, an impact- absorbing hammer, measuring bridges and measuring rods with floats. The purpose of the outer ring is to have the infiltrating water act as a buffer zone against infiltrating water straining away sideways from the inner ring. The photographs below (fig 6.12(a)-6.12(d)) show field test carried out in the site where the developed model has been applied.

Double ring infiltrometer test results

Table 6.2 Double ring infiltrometer field test results.

Sl No	Test 1		Test 2		Test 3	
	Time (S)	Water Depth (cm)	Time (S)	Water Depth (cm)	Time (S)	Water Depth (cm)
1	0	20	0	18	0	18
2	117	19	114	17	107	17
3	284	18	290	16	272	16
4	473	17	516	15	463	15
5	608	16	754	14	680	14
6	865	15	1010	13	919	13
7	1093	14	1280	12	1200	12
8	1333	13	1554	11	1410	11
9	1590	12	1861	10	1640	10
10	1855	11	2170	9	1890	9
11	2130	10	2490	8	2170	8
12	2428	9	2860	7	2465	7
13	2728	8	3250	6	2764	6
14	3028	7	3655	5	3067	5
15	3330	6	4060	4	3374	4
16	3633	5	4480	3	3682	3
17	3936	4	4930	2	3991	2
18	4240	3	5430	1	4300	1
19	4545	2				
20	4850	1				

Figure 6.11 Application of model to this area

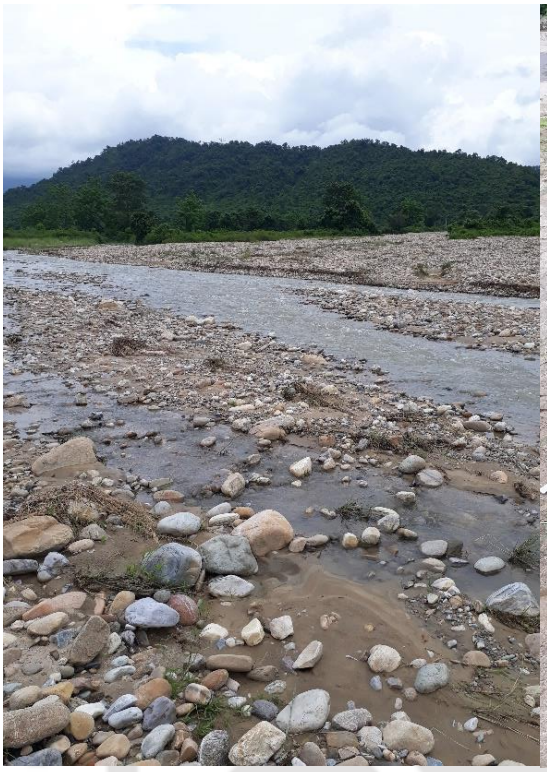

Figure 6.12 (a) Tributary where the developed model is applied

Figure 6.12 (b) Installation of double ring infiltrometer

Figure 6.12 (c) Double ring infiltrometer test

Figure 6.12 (d) Double ring infiltrometer test

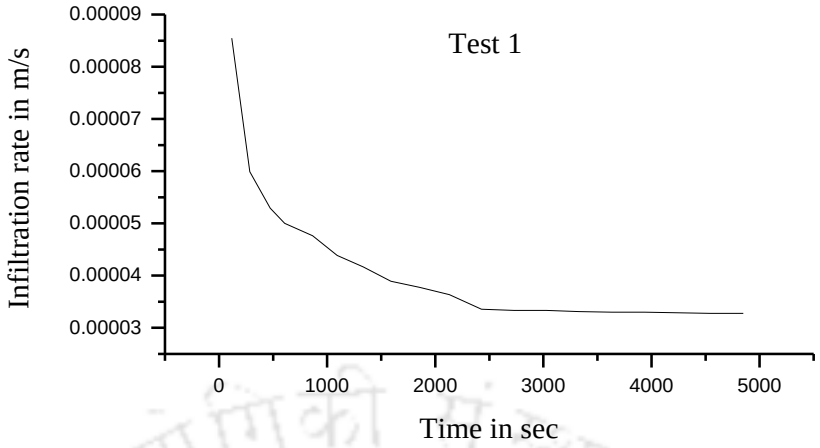

Figure 6.13 (a) Graph of infiltration rate vs time

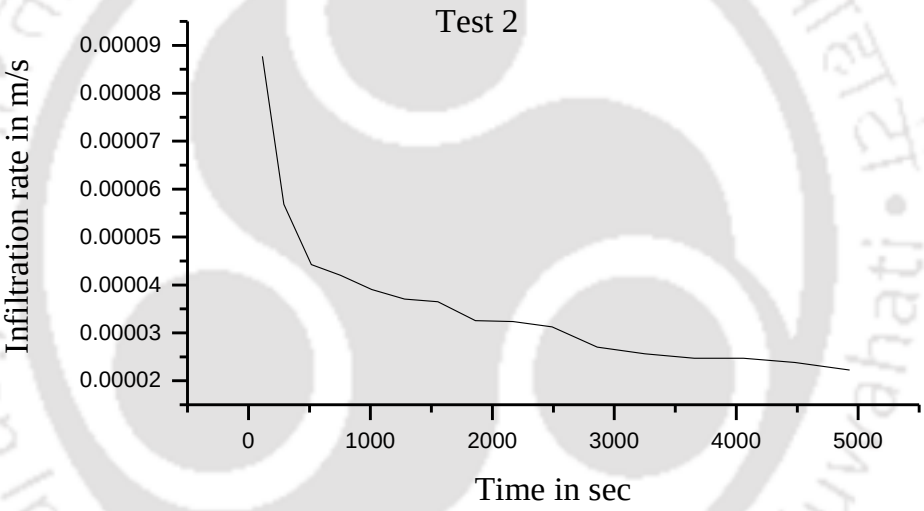

Figure 6.13 (b) Graph of infiltration rate vs time

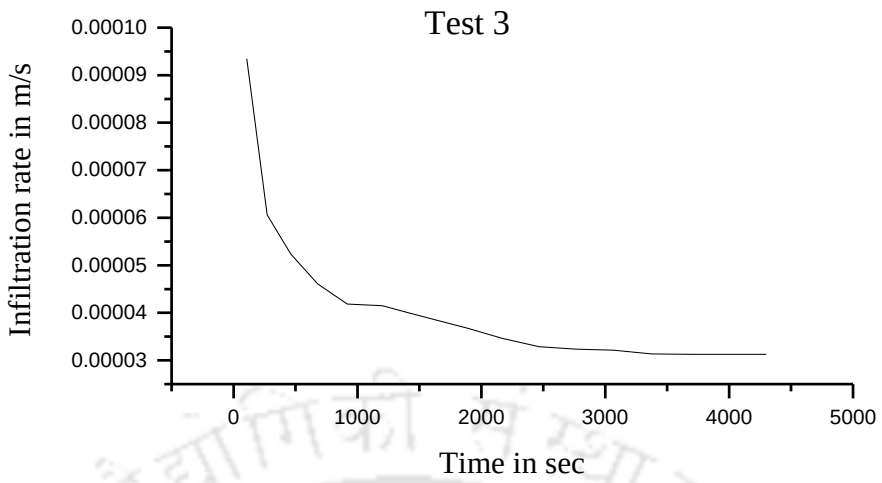

Figure 6.13 (c) Graph of infiltration rate vs time

Fig 6.13(a), 6.13(b) and 6.13(c) show the infiltration rate for field test. From this figures it is observed that for test 1 and test 3 constant rate of infiltration achieved around 3500 sec and rate of infiltration is 3.5×10^{-5}. i.e. soil become saturated after 3500 sec. But for test 2 constant rate of infiltration is not occurred during the infiltration test. Again when saturation occurred rate of infiltration becomes equal to the saturated hydraulic conductivity. Therefore when this model is applied to this field condition we have used 3.4×10^{-5} m/s as the saturated hydraulic conductivity.

6.4.2 Input hydrograph

For determining the flow characteristics and to design hydraulic structure it is necessary to determine maximum flow hydrograph. A number of methods have been used to calculate the maximum value of the flood runoff hydrograph. The rational method developed by Kuichling (1889) is a simple technique for estimating a design discharge from a small watershed. Application of the rational method is based on a simple formula that relates runoff producing potential of the watershed, the average intensity of rainfall for a particular length of time (the time of concentration), and the watershed drainage area. The formula is

$$Q_p = C_p I_p A_p$$

where, Q_p = Maximum flood hydrograph (L^3/T)

C_p = Run off Coefficient (Unit less)

I_p = Intensity of rainfall (L/T)

A_p = Area of watershed (L^2)

To calculate the maximum flood discharge by rational formula it is necessary to calculate rainfall intensity and area of watershed.

Design rainfall intensity

As the IMD weather stations are located at a far distance from the study area, rainfall data of Lamabari Tea Estate, located at a distance of 25 km from the study area is used to generate the IDF (intensity- duration- frequency) curve (fig 6.14). Data of this tea estate has been used to calculate the design rainfall intensity. The design rainfall intensity was computed for different return periods to generate scenarios of high and low discharge.

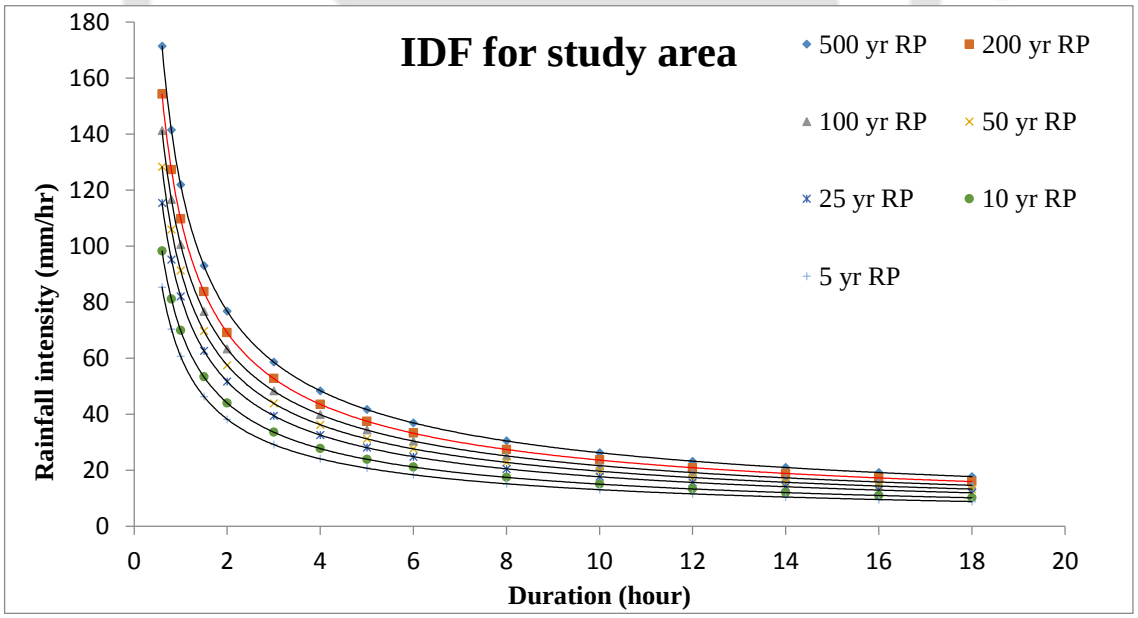

Figure 6.14 IDF curve used for rainfall intensity

Table 6.3: Parameter of IDF curve for different return periods

Return Period (Year)	Parameter 'aa'	Parameter 'bb'	R-Square value
500	121.91	0.667	1
200	109.73	0.667	1
100	100.52	0.667	1
50	82.093	0.667	1
25	91.307	0.667	1
10	69.914	0.667	1
5	60.701	0.667	1

The general form of these curves were given by an empirical formula, $I_p = aa \times T_0^{-bb}$.

For 200 years return period aa= 109.73 and bb=0.667 and for 10 years return period aa= 69.14 and bb=0.667. T_0 is the duration of rainfall.

Watershed area

Watershed delineation has been carried out by using ARC- SWAT interface of SWAT model. The watershed area and the other watershed attributes like length of the longest flow channel (L_c), slope of the longest flow channel (S_c), which are used in calculation of time of concentration are obtained from the attribute table of delineated watershed.

Time of concentration, which is define as the time taken by a water particle to flow from furthest point of watershed to the watershed outlet, is calculated by Williams formula (Fang et al. 2008) (SI unit), which is given as

$$T_c(\text{min}) = 0.057948 L_c A_p^{-0.1} S_c^{-0.2}$$

Following details has been found by delineating the watershed.

Length of the longest flow channel (L_c) = 4325.865389 m

Area of watershed (A_p) = 272.48438 hec= 272.48438 × 10^4 m^2

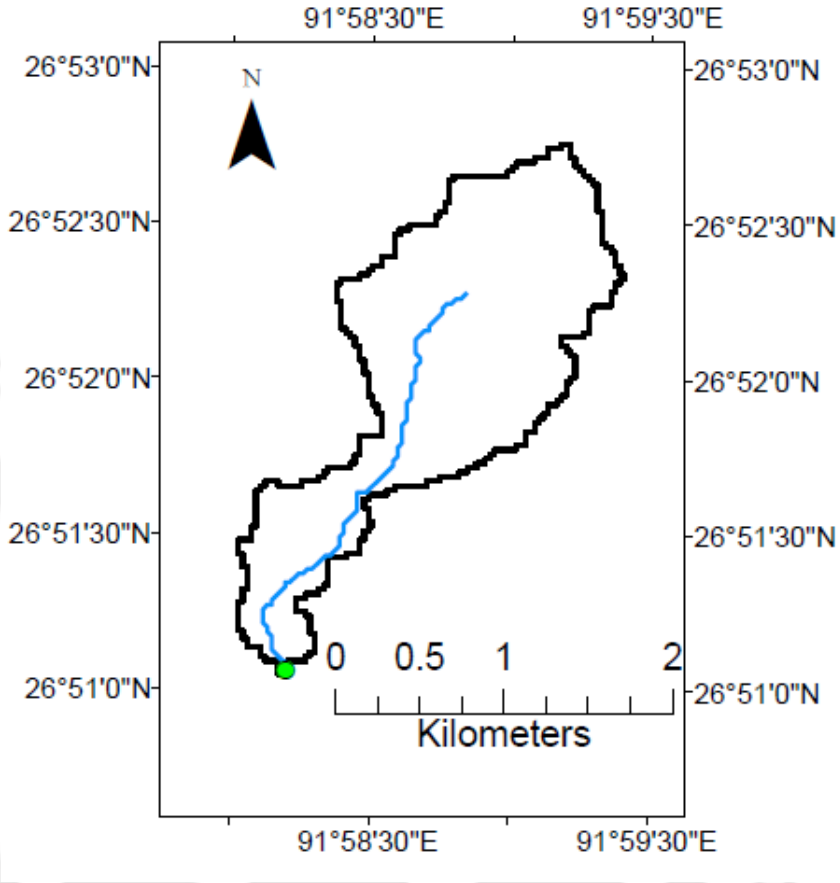

Figure 6.15 Study watershed

Slope of the longest flow channel (S_c) = 8.345151 % = 0.083

Time of concentration (T_c) = 93.70 min = 1.56 hr

Generation of input hydrograph

Intensity of rainfall (200 years return period) I_p= 81.56 mm/ hr

Intensity of rainfall (10 year return period) I_p= 51.39 mm/hr

Peak Discharge $Q_p = C_p I_p A_p$

For 200 year return period = 0.75 × 81.56 mm/hr × 2724843 m^2 = 46 m^3/s

For 10 year return period= 0.75 × 51.39 mm/hr × 2724843 m^2 = 29 m^3/s

Basin lag time tp = $C_t \times (L \times L_{ca})^{0.3}$= 0.65 × $(4.3 \times 4.2)^{0.3}$=1.54 hr

Standard duration of effective rainfall (t_r)= tp/5.5= 1.54/5.5= 0.28 hr

Based on the above parameters, approximate triangular input hydrographs (fig 6.16 (a) and fig 6.16(b)) for two different return periods are generated.

The developed model has been run for these two hydrographs.

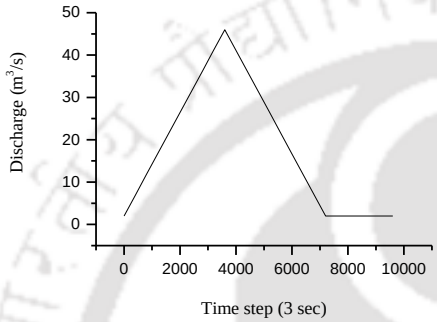

Figure: 6.16 (a)Upstream Hydrograph for 200 year return period

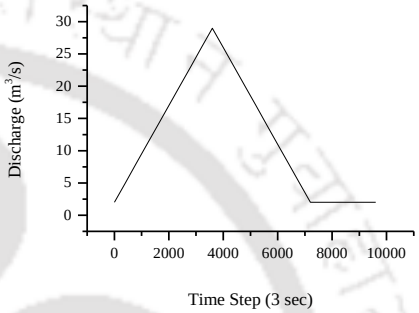

Figure: 6.16 (b)Upstream Hydrograph for 10 year return period

6.4.3 Results from field application

This section shows the results obtained from application of the developed model in the field. Results include the water surface elevation, depth hydrograph and discharge hydrograph. These results are plotted for with considering piedmont zone and without considering piedmont zone for better visualization of piedmont zone on flow variable

Water surface elevation

Fig 6.17 (a) shows the 2D water surface elevation after 3000 sec for 200 years return period. From this figure it is seen that because of the presence piedmont zone the water surface elevation d/s of the piedmont zone decreases. For better visualization the centre line of water surface elevation is plotted in fig 6.17 (b) and 6.17 (c) for 200 years and 10 years return periods. From these figures it is noticed that because of presence of piedmont zone, water surface elevation decreases by19 cm at downstream point for both the returns period.

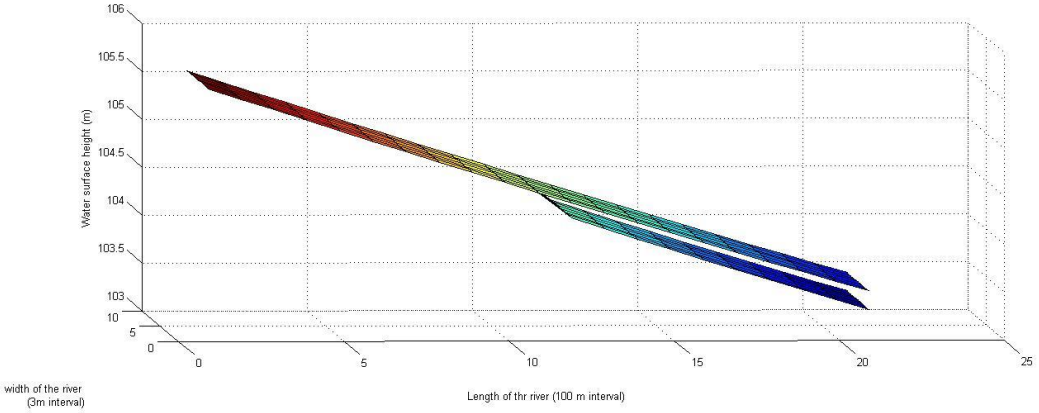

Fig 6.17 (a) 2-D plot of water surface elevation for 200 years return period

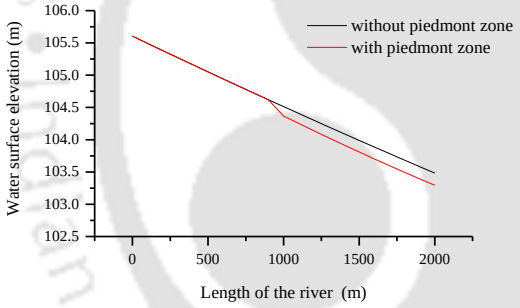

Figure 6.17 (b) water surface elevation for 200 years return period

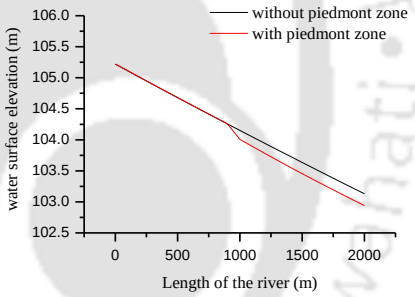

Figure 6.17 (c) water surface elevation for 10 years return period

Figure 6.17 Water surface elevation

Depth hydrograph

Fig 6.18 (a) and 6.18 (b) show depth hydrograph at 1.3 km section for two cases-i) with piedmont zone and ii) without piedmont zone. From the comparison of these two figures it is observed that because of presence of piedmont zone peak of the depth hydrograph decreases by 13% and 10% for 200 years and 10 years return period respectively.

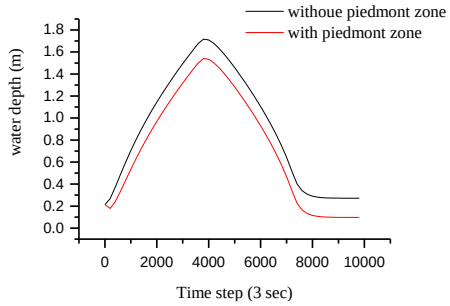

Fig 6.18 (a) Depth hydrograph for 200 year return period

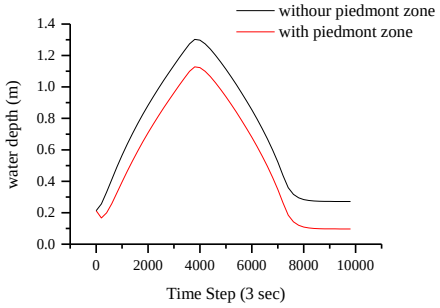

Fig 6.18 (b) Depth hydrograph for 10 year return period

Discharge hydrograph

For better visualization of effect of piedmont zone, discharge hydrograph considering piedmont zone and discharge hydrograph without considering piedmont zone are plotted together on fig 6.19 (a) and 6.19 (b) for the return period 10 years and 200 years respectively. From this figure it is seen that peak of the discharge hydrograph decreases by 9.49 % and 6.47% for the return period 10 years and 200 years respectively because of presence of piedmont zone.

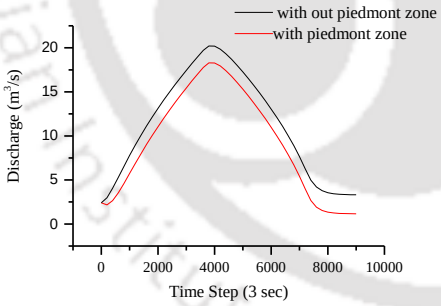

Figure 6.19 (a) Discharge hydrograph for 10 years return period

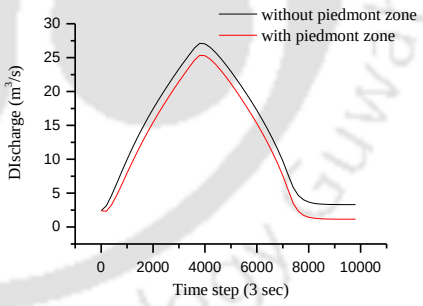

Figure 6.19 (b) Discharge hydrograph for 200 years return period

6.5 conclusion

In this chapter, a discussion about the application of the model is done. First, the model is applied to a hypothetical river reach where a piedmont zone of 200m × 200m is considered. From the results, it is noticed that piedmont zone has a significant effect on

various flow parameters. Following this, a detailed discussion about the groundwater movement of infiltrated water through the piedmont zone is discussed. The results obtained from the sensitivity analysis of peak depth, peak discharge and flow volume to hydraulic conductivity showed that hydraulic conductivity has some effects on these flow parameters, and cannot be ignored since these values can considerably influence the design of downstream hydraulic structures. A field study is done by applying the developed model to a 2nd order tributary of Brahmaputra River, where such piedmont zones exist. Double ring infiltrometer test was performed on the field to determine the infiltration characteristics of the river. From the field study it was found that the river is highly permeable in nature. It was found that river sometime does not even flow on the downstream of the piedmont zone during the winter period. In summer also, when there is no rain for a period of 15 days in the catchment, then very little amount of flow appears in the downstream of the piedmont zone. This indicates the high permeable characteristics of the river. Although the model has the capability of handling non uniform subsurface layer, in absence of detail subsurface bore log data, the hydraulic conductivity of the subsurface layer below the river is considered as uniform and result presented therefore has this limitation.

Chapter 7

Conclusion, Discussion and Scope of Future Study

7.1 Introduction:

Although a brief conclusion has already been presented in each of the previous chapters, a comprehensive overall discussion and general conclusion on all the works performed under this study have been given in this chapter.

7.2 Conclusion and discussion

From the literature review, it has been seen that coupled surface-subsurface water model has been a topic of interest among the researchers from last three decades. For free surface flow model, though researchers have widely used Saint- Venant equation, most of the researchers, to reduce complexity, has carried out the free surface flow modelling neglecting the infiltration zone in the river bed. From practical point of view such study can provide acceptable result if infiltration from the river bed is negligible. On the other hand, it is extremely important to consider the existence of piedmont zone in the computational domain if such a zone exits in the river, as a significant amount of water infiltrates to the ground through it.

Review of the literature concluded that shallow water equation, which consists of continuity and momentum equations, are of nonlinear form and cannot be solved analytically without simplification. However, with the help of numerical schemes, nonlinear equations are solved without simplifications. Finite difference, finite element and finite volume are the three most important categories of numerical methods for the solution of the nonlinear equations. Finite element and finite volume methods are generally used for the solution of the governing equations in complex geometry. However, these methods are complicated to implement. For the solution of the Saint-Venant equation, finite difference and finite element methods do not make much difference in results. Thus most of the scholars used finite difference methods due to its ease of application and programming and found satisfactory results in different

hydrodynamic problems. Finite difference methods are divided into two categories, explicit and implicit finite difference scheme. Though the explicit schemes are relatively simple to set up and program, the main disadvantage of explicit schemes is time step limit. For implicit scheme, one can go for much larger time step then explicit scheme. Therefore use of implicit scheme reduces the time step compared to the explicit scheme. Beam and Warming (1976) developed a non-iterative implicit scheme for hyperbolic systems in conservative form and this scheme has been successfully applied in this study.

Water infiltrated through the piedmont zone moves below the river bed and joins the mainstream at downstream. Researchers have widely used Richards equation to study the groundwater movement. Richards equation can be categorised in three forms: pressure based, water content based and mixed form. Out of these, mixed form of Richards equation can be applied for all soil formation because pressure based Richards equation shows large mass balance error and water content based Richards equation cannot be used in dry soil. Richards equation is also parabolic nonlinear equation which is hard to solve analytically without simplification. From the literature it is seen that researchers had widely used finite difference and finite element scheme for the solution of the same.

From the literature review, we have seen that researchers are paying interest in developing coupled groundwater surface water model. However, no literature has been found regarding the consideration of piedmont zone in the computation of unsteady free surface flow model. So development of a coupled model for flow simulation in a river, where piedmont zone exists in the computational domain of unsteady free surface flow, is uniqueness of this study. The model is developed using Saint- Venant equation along with the Green-Ampt. equation. Richards equation is coupled with the free surface flow model by the flux exchange and is used to study movement of infiltrated water through the unsaturated and saturated subsurface layers.

The developed model is validated with two parts. First part, which included unsteady free surface flow model with piedmont zone, is validated with the field data of Trout Creek River and the second part validated with the Vaculin et al. model results. From the validation of the model it is found that there is good agreement between them and they can be used to develop a coupled model.

After validation of the model, it is applied to hypothetical river reach where such piedmont zone is considered in the computational domain.

For deriving better understanding about impact of having the piedmont zone in the computational domain, the model is run for two conditions 1) considering piedmont zone in the computational domain. 2) Without taking into account piedmont zone. Results for water surface elevation, depth hydrograph and discharge hydrograph are obtained for both the cases. The significant change in results indicates the effect of piedmont zone in the computational results. From the results, it is seen that percentage change in peak depth, and peak discharge is 5% and 7% respectively. The model was also run for three different soil formations namely increasing hydraulic conductivity from top to bottom layer, decreasing hydraulic conductivity from top to bottom and mixed form of hydraulic conductivity. Results obtained from different soil formation revealed that rise of the water table is more if the soil has hydraulic conductivity highest at the top and decreases to bottom chronologically. From the plotting of velocity vector, it is seen that flow direction at the bottom is reversed i.e. water table starts to rise at 12 hours. Water infiltrated through the piedmont zone moves through the subsurface and joins the main stream at 102 hours. Because of this contribution, the mainstream volume is increased by 5.5% at downstream of the point where ground water starts contributing to the river flow.

To know the effect of some important physical soil parameters like hydraulic conductivity and capillary fringe in flow variables a sensitivity analysis of these parameters is done in this study. From the sensitivity analysis of hydraulic conductivity, it is seen that during the low flood period, for a variation of ±100% in the value of hydraulic conductivity taking k=0.0005 m/s as the central value, peak depth and peak discharge varies within a range of ±5.0% and ±0.5% respectively. Similarly During the high flow period, for the same variation in hydraulic conductivity, percentage changes of peak depth and peak discharge range between ± 7.0% and ±4.2 % respectively. Effect of hydraulic conductivity is also noticeable in change in flow volume and infiltration rate. For a variation of 100% in hydraulic conductivity, the infiltration rate changes over 60%. From the sensitivity analysis of capillary fringe, it is noticed that rise of water table is

significant with the size of capillary fringe i.e. smaller the size of the capillary fringe more is the rise of the water table.

After details analysis of the model in hypothetical cases, model is applied to a tributary of Brahmaputra River where such piedmont zone is reported (Goswami et al.1996). The 2nd order tributary considered in this study originates from Bhutan. To know infiltration characteristics of the river, double ring infiltrometer test is conducted in the field. With the help of double ring infiltrometer, hydraulic conductivity is calculated at the surface (upto 20 cm depth from the surface) of the soil. Well located near the river is found to have water level at a depth of 30m. Local people also confirmed that in most of the nearby well the water table in the rainy season remain in the similar depth. Therefore groundwater table is considered at a depth of 30m. In absence of detail geological data the subsurface soil profile of the piedmont zone is considered as homogeneous with average permeability characteristic. For obtaining design rainfall intensity of the study area, IDF curve generated by using precipitation data of a tea garden located 25Km away from the study area has been used. As the primary focus of the field application is to establish model applicability in the actual field, model is implemented with the above input information, some error due to data inadequacy may be there though.

7.3 Scope of future study

The governing equations of free surface flow used in this study has some inherent assumptions, and, in true sense, are valid in in a channel having small bed slope and where there is no sharp vertical or horizontal curvature. In spite of these assumptions, numerical solution of these equations gives acceptable result, as these assumptions become still valid within small grid size. In future some modification can be made in the governing equations itself so that the model can be applied to a high gradient sharp curvature river.

Though the numerical methods presented in this study has successfully solved the governing equations in different situations, a comparison of different numerical methods can also be done to study the efficiency of different numerical scheme in handling the problem under consideration.

Results obtained from different subsurface soil formation concluded that unsaturated flow depends upon the subsurface soil layer. In our field application we have consider the soil profile below the river bed as homogeneous. In reality subsurface soil layer may not be homogeneous. So in future detail subsurface soil investigation can be carried out for application of the model in the field with more reliability.

References

1. Abbott, M. B. and Basco, D. R. (1990). “Computational Fluid Dynamic, John Wiley, New York, NY.
2. Akanbi, A., and Katopodes, N. (1988). "Model for flood propagation on initially dry land." J. Hydraul. Eng., 114(7), 689-706.
3. Akbari, G. and Firoozi, B. (2010). “Implicit and explicit numerical solution of Saint-Venant’s equations for simulating flood wave in natural rivers.” Proc.5th National Cong. Civ. Eng., Ferdowsi University of Mashhad, Iran
4. Alhan, C. M. K. and Madina, M. A. (2006). “Kinematic and Diffusion Waves: Analytical and Numerical Solutions to Overland and Channel Flow.” J. Hydraul. Eng. 133(2), 217–228.
5. Anderson, J. D. (1995) “ Computational Fluid Dynamics.” McGRAW- HILL International Edition.
6. Barr´e de Saint-Venant A (1871) Th´eorie du mouvement non-permanent des eaux avec applicationaux crues des rivi`eres et `a l’introduction des mar´ees dans leur lit. Comptes rendus Acad Sci Paris 73:148–154, 237–240.
7. Bateman, Allen. Medina, Vicente. and Velasco, David (2010) “Soil infiltration effect in flat areas floods simulations.” XVIII International Conference on Water Resources, CIMNE, Barcelona.
8. Beam, R.M., Warming, R.F. (1976) “An implicit finite difference algorithm for hyperbolic systems in conservation law form.” J. Comput. Phys. 22, 87–110.
9. Bellos, C. V., and Sakkas, J. G. (1987). “1-D dam-break flood-wave propagation on dry bed.” J. Hydraul. Eng. 113(12), 1510–1524.
10. Bellos, C. V., Soulis, J. V., and Sakkas, J. G. (1991). “Computation of two dimensional dam break induced flows.” Adv. Water Resour. 14(1), 31-41.
11. Bellos, V. and Hrissanthou, V. (2011). “Numerical simulation of Dam break flood wave.” European Water. 33, 45-53
12. Bhallamudi, S. M., and Chaudhry, M. H. (1992). “Computation of flows in open channel transitions.” J. Hydraul. Res., 30(1). 77-93.

13. Blade, E., Valentin, M. G., Juny, M. S., and Dolz, J. (2008). "Preserving steady-State in one dimensional finite-volume computations of river flow." J. Hydraul. Eng., 134(9), 1343-1347.
14. Bradford, S. F. and Katopodes, N. D. (2001). "Finite volume model for non level basin irrigation." J. Irrig. Drain. Eng., 127(4), 216-223.
15. Casulli, V. and Zanolli, P. (2010) "A nested Newton-type algorithm for finite volume methods solving Richards equation in mixed form." SIAM J. Sci. Comput. 32 (4), 2255-2273.
16. Celia, M. A., Bouloutas, T. E. and Zarba, R. L. (1990) "A General Mass-Conservation Numerical Solution for the Unsaturated Flow Equation." Water Resour. Res. 26 (7), 1483-1496.
17. Chaga, Patricia and Souza, Raimundo (2005). "Solution of Saint- Venant's equation to study flood in Rivers, through numerical Methods." Hydrology Days. 205-210.
18. Chaudhry, M. H. (1987). " Applied Hydraulic Transient." 2nd edn. Van Nostrand Reinhold, Newyork, NY.
19. Chaudhry, M. H. (2008). "Open channel flow." 2nd edn. Prentice-Hall Inc, Englewood Cliffs.
20. Chen, J., Steffler, P. M., and Hicks, F. E. (2007). "Conservative formulation for natural open channels and finite-element implementation." J. Hydraul. Eng., 133(9), 1064-1073.
21. Childs, E.C., Bybordi, M. (1969) "The vertical movement of water in stratified porous material. 1. Infiltration." Water Resour. Res. 5(2), 446–459.
22. Chow, V. T. (1959). " Open-Channel Hydraulics." McGraw-Hill, New York, NY.
23. Chu, S.T. (1978) "Infiltration during an unsteady rain." Water Resour. Res. 14 (3), 461–466.
24. Clement, T.P., Wise, W.R. and Molz, F.J. (1994) "A physically based, two-dimensional, finite difference algorithm for modelling variably saturated flow." J. Hydrol. 161, 69–91.
25. Cooley, R.L. (1971) "A finite difference method for unsteady flow in variably saturated porous media: application to a single pumping well." Water Resour. Res. 7, 1607–1625.

26. Craya, A. (1946). " Calcul graphique des regimes variables dans les canaux" La Houille Blanche no.1, 79-138, no.2, 117-130.
27. Cunge, J. A., Holly, F. M. and Verwey, A. (1980). "Practical Aspects of Computational River Hydraulics." Pitman, London.
28. Dagan, G. and Bresler, E. (1983) "Unsaturated flow in spatially variable fields, 1. Derivation of models of infiltration and redistribution." Water Resour. Res. 19(2), 413-420.
29. Delis, A.I., Skeels, C.P., and Ryrie, S.C. (2001). "Implicit high-resolution methods for modelling one-dimensional open channel flow", J. Hydraul. Res. 38(5), 369-382.
30. Dennis, A. Lyn and Peter Goodwin (1987). "Stability of a general Preissmann Scheme." J. Hydraul. Engg. 113, 16-28.
31. Dressler, R. F. (1952), "Hydraulic resistance effect upon the dam-break functions." J. Res. of the National Bureau of Standards, 49(3), 217-225.
32. Fennema, R. J. and Chaudhry, M. H. (1986). "Explicit numerical schemes for unsteady free surface flows with shocks." Water Resour. Res., 22(13), 1923-1930.
33. Fennema, R. J. and Chaudhry, M. H. (1990). "Explicit methods for 2-D transient free surface flows." J. hydraul. Engg. 116(8),1013-1024.
34. Fennema, R. J., and Chaudhry, M. H. (1989). "Implicit methods for two dimensional unsteady free-surface flows," J. Hydraul. Res., 27(3), 321-332.
35. French, R. H. (1985). "Open channel Hydraulics." Mcgraw-Hill, Newyork, NY.
36. Freyberg, D.L., Reeder, J.W., Franzini, J.B., Remson, I. (1980). "Application of the Green-Ampt. model to infiltration under time-dependent surface water depth." Water Resour. Res., 16, 3, 517–528.
37. Ghostine, R., Mignot, E., Abdallah, M., Lawniczak, F., Vazquez, J., Mose, R., and Gregoire, C. (2010). "Discontinuous Galerkin finite-element method for simulation of flood in crossroads." J. Hydraul. Eng., 136(8), 474-482.
38. Goswami, D.C., Goswami, I.D., Duarah, B.P., Deka, P.P. (1996) "Geomorphological mapping of Assam using satellite remote sensing techniques. Indian J. Geomorph." 1, 2, 225– 235.

39. Goswami, P. K. and Yhokha, A. (2010) “Geomorphic evolution of the Piedmont Zone of the Ganga Plain, India: a study based on remote sensing, GIS and field investigation.” Int J Remote Sens., 31, 5349-5364.
40. Gottardi, G. and Venutelli (1992) “Moving Finite Element Model for One-Dimensional Infiltration in Unsaturated Soil.” Water Resour. Res. 28 (12), 3259-3267.
41. Gottardi, G. and Venutelli, M. (1993) “Richards: computer program for the numerical simulation of one-dimensional infiltration into unsaturated soil.” Comput and Geosci 19(9), 1239-1266.
42. Govindaraju, R.S., Or, D., Kavvas, M.L., Rolston, D.E. and Biggar, J. (1992) “Error analyses of simplified unsaturated flow models under large uncertainty in hydraulic properties.” Water Resour. Res. 28(11), 2913-2924.
43. Green, W.H. and Ampt, G. (1911) “Studies on soil physics, 1. The flow of air and water through soils.” J. Agric. Sci. 4(1), 1-24.
44. Gunaratnam, D. J., and Perkins, F. E. (1970) "Numerical Solution of Unsteady Flow in Open Channel” Report No. 127, Hydrodynamic Laboratory, MTT.
45. Hachum, A.Y., Alfaro, J.F. (1980) “Rain infiltration into layered soils: prediction.” J. Irrig. Drain. Div. 106, 311–319.
46. Hanks, R. J. and S. A. Bowers (1962). “Numerical solution of the moisture flow equation for infiltration into layered soils.” Soil Sci. Soc. Proc., 26, 530-534.
47. Hari Prasad, K. S., Mohan Kumar, M. S. and Sekhar, M. (2001) “Modelling flow through unsaturated zones: Sensitivity to unsaturated soil properties.” Sadhana. 26 (6), 517-528.
48. Hicks, F. E., and Steffler, P. M. (1992). “Characteristic dissipative Galerkin scheme for open channel flow.” J. Hydraul. Eng., 118(2), 337-352.
49. Houghton, D. D., and Kasahara, A. (1967). “Nonlinear shallow fluid flow over an isolated ridge.” NCAR Rep. No. 259a, National Center for Atmospheric Research, Boulder, Colorado.
50. Huang, J., and Charles, C. S. (1985). “Stability of dynamic flood routing schemes.” J. Hydraul. Eng., 111(12), 1497-1505. J. Hydrol. 178, 69-91.
51. Huang, K., Mohanty, B. P. and Van Genuchten, M. Th. (1996) “A new convergence criterion for the modified Picard iteration method to solve the variably saturated flow equation.” J. Hydrol.178, 69-91.

52. Hyunuk, A., Ichikawa, Y., Tachikawa, Y. and Shiiba, M. (2014) "A new Iterative Alternating Direction Implicit (IADI) algorithm for multi-dimensional saturated–unsaturated flow." J. Hydrol.408, 127-139.
53. Isaacson, E., Stoker, J. J. and Troesch, B. A. (1954). "Numerical Solution of Flood Prediction and River Regulation Problem (Ohio-Mississippi Floods)." Report II, Inst. Math. Sci. Rept. IMM-NYU-205, New York University.
54. Jin, M. and Fread, D.L. (1997). "Dynamic flood routing with explicit and implicit numerical solution scheme." J. hydraul. Engg. 123(3), 166-173.
55. Kalita, H. M. and Sarma A.K. and Bhattacharjya, R. K. (2014) "Evaluation of Optical River Training Work using GA Based Link Simulation Optimization Approach." Water Resour Manag, 28, 2077-2092.
56. Kalita, H.M and Sarma A.K. (2012) "Efficiency and performances of finite difference schemes in the solution of Saint Venant's equation." International journal of civil and structural engineering, IPA, Volume 2 (3), 941-949.
57. Kassem, A.A., Chaudhry, M.H. (2005) "Effect of bed armouring on bed topography of channel bends." J. Hydrol. Eng., 131, 12, 1136–1140.
58. Katopodes, N. D. (1984). "A dissipative Galerkin scheme for open-channel Flow." J. Hydraul. Eng. 110(4), 450-466.
59. Kavetski, D., Binning, P. and Sloan, S. W. (2002). "Noniterative time stepping schemes with adaptive truncation error control for the solution of Richards equation." Water Resour. Res. 38 (10), 1211
60. Khan, A. A. (2000). "Modeling flow over an initially dry bed." J. Hydraul. Res. 38(5), 383–388.
61. Kirkland, M.R., Hills, R.G. and Wierenga, P.J. (1992) "Algorithms for solving Richards equation for variably saturated soil." Water Resour. Res. 28 (8), 2049-2058.
62. Kong, J., Xin, P., Song, Z. Y. and Li, Ling (2010) "A new model for coupling surface and subsurface water flows: With an application to a lagoon." J. Hydrol., 390,116-120.
63. Kuiry, S.N., Sen, D. and Bates, P.D. (2010) "Coupled 1D–Quasi-2D Flood Inundation Model with Unstructured Grids." J. Hydraul. Eng. 136(8), 493-506.
64. Lai, Y. G. (2010). "Two-Dimensional Depth-Averaged Flow Modeling with an Unstructured Hybrid Mesh." J. Hydraul. Eng. 136(9), 12-23.

65. Lax, P.D. (1954). “Weak solution of nonlinear hyperbolic partial differential equation and their numerical computation.” Comm. Pure Appl. Math. 7, 159-163.
66. LeVeque, R.J. (2005) “Finite Difference Methods for Differential Equations.” University of Washington, Seattle.
67. Li Chen and Michael H. Young (2006) “Green-Ampt. infiltration model for sloping surfaces.” Water Resour. Res. 42, W07420.
68. Liang, D., Falconer, R. A. and Lin, B. (2007) “Coupling surface and subsurface flows in a depth averaged flood wave model.” J. Hydrol. 337, 147-158.
69. Liggett, J. A. and Cunge, J. A. (1975). “Numerical Method of solution of unsteady flow equations” in unsteady open channel flow, Mahmood, K. and Yevjevuch, V. (eds) Water Resources Publications, Fort Collins.
70. Lim, S. C. and Lee, K.J. (1993) “A mass conservative numerical solution of vertical water flow and mass transport equation in unsaturated porous media.” Ann. Nucl. Energy. 20, 91-99.
71. Lu, Z. and Zhang, D. (2004) “Analytical solutions to steady state unsaturated flow in layered, randomly heterogeneous soils via Kirchhoff transformation.” Adv. Water Resour. 27, 775-784.
72. Lui, F., Feyan, j., Berlamont, j. (1992) **“**computation method for regulating unsteady flow in open channels”, J. Irrig. Drain Eng.118, 674-689.
73. M. R.Kirkland and R. G. Hints (1992) “Algorithm for solving Richards equation for variably saturated soil.” Water Resour. Res. 28 (9), 2049-2058
74. Macchione, F. and Morelli, M. A. (2003) “Practical aspects in comparing shock-capturing schemes for dam break problems.” J. Hydraul. Eng., 129(3), 187-195.
75. Massau, J. (1889) “ L’integration graphique and Appendice au memories ur I’integration graphique” Assoc. des Ingenieeurs sortis des Ecoles Speciales de Gand, Belgium, Annales vol. 12, 185-444.
76. Miller, C.T., Abhishek, C. and Farthing, M.W. (2006) “A spatially and temporally adaptive solution of Richards equation.” Adv. Water Resour. 29, 525-545.
77. Miller, S., and Chaudhry, M. H. (1989) “Dam-break flows in curved channel.” J. Hydraul. Eng., 115(11), 1465-1478.

78. Mingham, C. G., and Causon, D. M. (1998) "High-resolution finite-volume method for shallow water flows." J. Hydraul. Eng., 124(6), 601-614.
79. Molls, T., Chaudhry, M.H., Khan, K.W. (1995) "Numerical simulation of two-dimensional flow near a spur-dike." Adv. Water Resour. 18 (4) 221–236.
80. Molls, T., Zhao, G. (2000) "Depth-averaged simulation of supercritical flow in channel with wavy sidewall." J. Hydraul. Eng. ASCE, 126, 6, 437–445.
81. Mousseau, V.A., Knoll, D.A., and Reisner, J.M. (2002) "An Implicit Nonlinearly Consistent Method for the Two-Dimensional Shallow-Water Equations with Coriolis Force", American Meteorological Society. 2611-2625.
82. Navarro, P. G., Alcrudo, F., and Saviron, J. M. (1992) "1-D open-channel flow simulation using Tvd-Mccormack scheme." J. Hydraul. Eng., 118(10), 1359–1372.
83. Niswonger, R.G., Prudic, D.E., Pohll, G., Constantz, J. (2005) "Incorporate seepage losses into the unsteady stream flow equations for simulation intermittent flow along mountain front streams." Water Resour. Res., 41, W06006.
84. Palla, A., Gnecco, I. and Lanza, L. G. (2009) "Unsaturated 2D modelling of subsurface water flow in the coarse-grained porous matrix of a green roof." J. Hydrol. 379,193-204.
85. Pan, L and Wierenga, P. J. (1995) "A transformed pressure head-based approach to solve Richards equation for variably saturated soils." Water Resour. Res. 31 (4), 925-931.
86. Parissopoulos, G.A., Wheater, H.S. (1988) "On numerical errors associated with the iterative alternating direction implicit (IADI) finite difference solution of the two dimensional transient saturated-unsaturated flow(Richards) equation." Hydrol Process 2, 187–201.
87. Patowary, S. and Sarma, A.K. (2016). "Safe IDF curves from daily rainfall data for Guwahati city." WRF-05, Proceedings of national conference on water Resources and flood management with special reference to flood modelling, SBNIT, Gujrat.
88. Paul. G. Samuels and Caroline P. Skeels (1990). "Stability limits for Preissmann's scheme." J. Hydraul. Eng. 116(8), 997-1012.

89. Peaceman, D.W. and Rachford, H.H. (1955) “The Numerical Solution of Parabolic and Elliptic Differential Equations.” SIAM J Appl Math, 3(1), 28-41
90. Perrens, S. J. and Watson, K. K. (1977) “Numerical analysis of two-dimensional infiltration and redistribution.” Water Resour. Res. 13 (4), 781-790.
91. Preissmann A (1961) Propagation des intumescences dans les canaux et rivi`eres. In: 1er Congr`es de l’Association Franc¸aise de Calcul, Grenoble, France, pp 433–442.
92. Price, R. K. (1974) "Comparison of Four Numerical Methods for Flood Routing," Journal of the Hydraulics Division, ASCE, Vol. 100, No. HY7.
93. R.S. Govindaraju, M.L. Kavvas, S.E. Jones and D.E. Rolston (1995) “Use of Green-Ampt. model for analyzing one-dimensional convective transport in unsaturated soils.” J. Hydrol. 178, 337-350.
94. Rahman, M., and Chaudhry, M.H. (1998) “Simulation of dam- break flow with grid adaptation” Adv. Water Resour. 21,309-1708.
95. Rashid, R. S. and Chaudhry M. H. (1995) “Flood routing in channels with flood plains”, J. Hydrol.. 171, 75-91.
96. Rossell, R. P., and Ting, F. C. K. (2013). “Hydraulic and contraction scour analysis of a meandering Channel: James River bridges near Mitchell, South Dakota.” J. Hydraul. Eng., 139(12), 1286-1296.
97. Saikia, M. D. (2007). “Simulation of dam break hydraulics in natural flood plain topography." PhD thesis, Civ. Eng. Dept., Indian Institute of Technology Guwahati, Assam, India.
98. Saikia, M. D. and Sarma, A. K. (2006). “Analysis for adopting logical channel section for 1D dam break analysis in natural channels.” ARPN J. Eng. Applied Sci., 1(2), 46-54.
99. Sarma A.K. and Das M.M. (2003) “Analytical Solution of Flood-Wave Resulting from Dike Failure, Journal of Water and Maritime Engineering, ICE.” 156, 41-45.
100. Schwanenberg, D., and Harms, M. (2004). “Discontinuous Galerkin finite-element method for transcritical two-dimensional shallow water flows.” J. Hydraul. Eng., 130(5), 412-421.

101. Sharp, J. J., and Moore, E. (1976). "Analysis of unsteady flow in open channels." *Int.* J. Math. Educ. Sci. Technol., 7(4), 377-393.
102. Shukla, U. K. and Bora, D. S. (2003). "Geomorphology and sedimentology of Piedmont zone, Ganga Plain, India." Current Science. 84(8), 1034-1040.
103. Singh, J., Altinakar, M. S. and Ding, Y. (2011). "Two-dimensional numerical modeling of dam-break flows over natural terrain using a central explicit scheme." Adv. Water Resour. 34, 1366-1375.
104. Siviglia, A., Nobile, G., and Colombini, M. (2008). "Quasi-conservative formulation of the one dimensional Saint-Venant–Exner model." J. Hydraul. Eng., 134(10), 1521-1526.
105. Smiles, D.E., Perroux, K.M., Zegeli n, S.J. and Raats, P.A.C. (1981) "Hydrodynamic dispersion during constant rate absorption of water by soil." Soil SCI. Soc. Am. J., 45, 453-458.
106. Soleymani, M. and Delphi, M. (2012). "Comparison of flood routing models (Case Study: Maroon River, Iran)." J. World Applied Sci., 16 (5), 769-775.
107. Stecca, G., Siviglia, A. and Blom, A. (2016) "An accurate numerical solution to the Saint-Venant-Hirano model for mixed-sediment morphodynamics in rivers." Adv. Water Resour. 93, 39-61.
108. Stoker, J. A. (1957). "Water Wave." Wiley (Interscience), Newyork, NY.
109. Strang, G. (1968) On the Construction and Comparison of Difference Schemes. SIAM J. Numer. Anal. 5, 506-517.
110. Strelkoff, T., 1970. Numerical solution of Saint-Venant equations. J. Hydraul. Eng., 96, 223–252.
111. Szymkiewicz. (1995) "Numerical stability of implicit four-point scheme applied to inverse linear flow routing" J. Hydrol. 176, 13-23.
112. Trikha, A. K. (1977) "Variable Time Steps for Simulating Transient Liquid Flow by Method of Characteristics," Journal of Fluids Engineering, ASME.
113. Van Genuchten, M. Th. (1980) "A closed-form equation for predicting the hydraulic conductivity of unsaturated soils." Soil Sci. Soc. Am. 44, 892–898.
114. Vauclin, M., D. Khanji, and G. Vachaud (1979) Experimental and numerical study of a transient, two-dimensional unsaturated-saturated water table recharge problem water Resour. Res., 15, 1089-1101.
115. Vaughan R. Voller (2011) "On a fractional derivative form of the Green–Ampt infiltration model." Adv. Water Resour. 34, 257-262.

116. Weeks, S.W., Sander, G.C., Braddock, R.D., Matthews, C.J. (2004) "Saturated and unsaturated water flow in inclined porous media." Environ Model Assess. 9 (2), 91–102.

117. Weill, S., Mouche, E. and Patin, J. (2009) "A generalized Richards equation for surface/subsurface flow modelling." J. Hydrol. 366, 9-20.

118. Willem F. Brutsaert (1971) "A Functional iteration Technique for Solving the Richards Equation Applied to Two-Dimensional Infiltration Problems." Water Resour. Res. 7 (6), 1583-1596.

119. Wu, MA. (2010) "finite-element algorithm for modeling variably saturated flows." J. Hydrol., 394, 315-323.

120. Wu, W. (2004) "Depth-averaged two-dimensional numerical modeling of unsteady flow and nonuniform sediment transport in open channels." J. Hydraul. Eng., 130(10), 1013-1024.

121. Xuefeng Chu and Miguel A. Marin (2005) "Determination of ponding condition and infiltration into layered soils under unsteady rainfall." J. Hydrol. 313, 195-207.

122. Ying, X., Khan, A.A. and Wang, S. S. Y. (2004) "Upwind Conservative Scheme for the Saint Venant Equations." J.Hydraul. Eng., 130(10), 977-987.

123. Zarrati, A. R., Tamai, N., and Jin, Y. C. (2005). "Mathematical modeling of meandering channels with a generalized depth averaged model." J. Hydraul. Eng., 131(6), 467-475.

124. Zhang, S., Xu, D., Li, Y., and Bai, M. (2013). "One-Dimensional Coupled Model of Surface Water Flow and Solute Transport for Basin Fertigation." J. Irrig. Drain Eng., 139(3), 181–192.

125. Zhao, D. H., Shen, H. W., Tabios, G. Q., Lai, J. S., and Tan, W. Y. (1994). "Finite volume two dimensional unsteady flow model for river basins." J. Hydraul. Eng., 120(7), 863-883.

Paper Presented and Published

1) Patowary, S. and Sarma, A. K. (2017) "A modified hydrodynamic model for routing unsteady flow in a river having piedmont zone." J. Hydrol. Hydromech. 65 (1), 60-67.

2) Patowary S. and Sarma A.K. (2012) "Hydrodynamic flood routing considering piedmont zone." International Journal of Civil and Structural Engineering 3 (3), 464 – 474.
3) Patowary S. and Sarma A.K. (2012) "Two dimensional numerical model for urban drainage system." Urban hydrology, Watershed Management and Socio-Economic Aspects, Water Science and Technology Library, Springer 73, 163-173.

Paper under review

1) Patowary, S. and Sarma, A. K. (2018) "A 2-D coupled surface and sub-surface flow model for river flow simulation with piedmont zone." Submitted to Water Resources Management.